Technical Report Documentation Page

1. REPORT No.
CA-DOT-TL-6666-1-74-18

2. GOVERNMENT ACCESSION No.

3. RECIPIENT'S CATALOG No.

4. TITLE AND SUBTITLE
Dynamic Fracture Toughness Determination By The Instrumented Charpy Impact Test

5. REPORT DATE
June 1974

6. PERFORMING ORGANIZATION

7. AUTHOR(S)
Smith, Roger D.; Jonas, Paul g.

8. PERFORMING ORGANIZATION REPORT No.
CA-DOT-TL-6666-1-74-18

9. PERFORMING ORGANIZATION NAME AND ADDRESS
Transportation Laboratory
5900 Folsom Boulevard
Sacramento, California 95819

10. WORK UNIT No.

11. CONTRACT OR GRANT No.

12. SPONSORING AGENCY NAME AND ADDRESS
Department of Transportation
Division of Highways
Sacramento, California 95807

13. TYPE OF REPORT & PERIOD COVERED
Final

14. SPONSORING AGENCY CODE
19-3121

15. SUPPLEMENTARY NOTES
Final report for study titled "K ID Determination from the Instrumented Precracked Charpy Impact Test".

16. ABSTRACT
The fracture behavior under dynamic load rates of seven heats of ASTM A514/517 steel (Grades H and F) is investigated. Material properties including dynamic yield strength and dynamic fracture toughness are determined using the instrumented Charpy impact test. These dynamic properties are contrasted with previously determined static propertiers for the same steel heats. Also discussed is the determination of nil ductility transition temperature (NDTT) and the analysis of the different cracking energy components (initiation and propagation) from Charpy impact tests. Alleged correlations between Charpy impact energy and dynamic fracture toughness are evaluated with respect to this study. The practicality of a fracture control program for bridge steel based on dynamic loading behavior is discussed.

17. KEYWORDS
Dynamic fracture toughness, brittle fracture, steel toughness, instrumented impact test, fracture mechanics, Charpy impact test.

18. No. OF PAGES:
148

19. DRI WEBSITE LINK
http://www.dot.ca.gov/hq/research/researchreports/1974-1975/74-18.pdf

20. FILE NAME
74-18.pdf

This page was created to provide searchable keywords and abstract text for older scanned research reports.
November 2005, Division of Research and Innovation

InterScan
International Scanning Systems

Batch Tracking

[redacted]

Initials Date

ClibPDF - www.fastio.com

TECHNICAL REPORT STANDARD TITLE PAGE

1. REPORT NO.	2. GOVERNMENT ACCESSION NO.	3. RECIPIENT'S CATALOG NO.
4. TITLE AND SUBTITLE Dynamic Fracture Toughness Determination by The Instrumented Charpy Impact Test		5. REPORT DATE June 1974
		6. PERFORMING ORGANIZATION CODE 19603-762504
		8. PERFORMING ORGANIZATION REPORT NO. CA-DOT-TL-6666-1-74-18
7. AUTHOR(S) Smith, Roger D.; Jonas, Paul G.		10. WORK UNIT NO.
9. PERFORMING ORGANIZATION NAME AND ADDRESS Transportation Laboratory 5900 Folsom Boulevard Sacramento, California 95819		11. CONTRACT OR GRANT NO.
		13. TYPE OF REPORT & PERIOD COVERED Final
12. SPONSORING AGENCY NAME AND ADDRESS Department of Transportation Division of Highways Sacramento, California 95807		14. SPONSORING AGENCY CODE 19-3121

15. SUPPLEMENTARY NOTES
Final report for study titled "K_{Id} Determination from the Instrumented Precracked Charpy Impact Test".

16. ABSTRACT

The fracture behavior under dynamic load rates of seven heats of ASTM A514/517 steel (Grades H and F) is investigated. Material properties including dynamic yield strength and dynamic fracture toughness are determined using the instrumented Charpy impact test. These dynamic properties are contrasted with previously determined static properties for the same steel heats. Also discussed is the determination of nil ductility transition temperature (NDTT) and the analysis of the different cracking energy components (initiation and propagation) from Charpy impact tests. Alleged correlations between Charpy impact energy and dynamic fracture toughness are evaluated with respect to this study. The practicality of a fracture control program for bridge steel based on dynamic loading behavior is discussed.

17. KEY WORDS Dynamic fracture toughness, brittle fracture, steel toughness, instrumented impact test, fracture mechanics, Charpy impact test.		18. DISTRIBUTION STATEMENT Limited	
19. SECURITY CLASSIF. (OF THIS REPORT) Unclassified	20. SECURITY CLASSIF. (OF THIS PAGE) Unclassified	21. NO. OF PAGES	22. PRICE

ClibPDF - www.fastio.com

TECHNICAL REPORT STANDARD TITLE PAGE

1. REPORT NO.	2. GOVERNMENT ACCESSION NO.	3. RECIPIENT'S CATALOG NO.

4. TITLE AND SUBTITLE	5. REPORT DATE
Dynamic Fracture Toughness Determination by The Instrumented Charpy Impact Test	June 1974
	6. PERFORMING ORGANIZATION CODE 19603-762504
7. AUTHOR(S) Smith, Roger D.; Jonas, Paul G.	8. PERFORMING ORGANIZATION REPORT NO. CA-DOT-TL-6666-1-74-18
9. PERFORMING ORGANIZATION NAME AND ADDRESS Transportation Laboratory 5900 Folsom Boulevard Sacramento, California 95819	10. WORK UNIT NO.
	11. CONTRACT OR GRANT NO.
12. SPONSORING AGENCY NAME AND ADDRESS Department of Transportation Division of Highways Sacramento, California 95807	13. TYPE OF REPORT & PERIOD COVERED Final
	14. SPONSORING AGENCY CODE 19-3121

15. SUPPLEMENTARY NOTES
Final report for study titled "K_{Id} Determination from the Instrumented Precracked Charpy Impact Test".

16. ABSTRACT

The fracture behavior under dynamic load rates of seven heats of ASTM A514/517 steel (Grades H and F) is investigated. Material properties including dynamic yield strength and dynamic fracture toughness are determined using the instrumented Charpy impact test. These dynamic properties are contrasted with previously determined static properties for the same steel heats. Also discussed is the determination of nil ductility transition temperature (NDTT) and the analysis of the different cracking energy components (initiation and propagation) from Charpy impact tests. Alleged correlations between Charpy impact energy and dynamic fracture toughness are evaluated with respect to this study. The practicality of a fracture control program for bridge steel based on dynamic loading behavior is discussed.

17. KEY WORDS	18. DISTRIBUTION STATEMENT
Dynamic fracture toughness, brittle fracture, steel toughness, instrumented impact test, fracture mechanics, Charpy impact test.	Limited

19. SECURITY CLASSIF. (OF THIS REPORT)	20. SECURITY CLASSIF. (OF THIS PAGE)	21. NO. OF PAGES	22. PRICE
Unclassified	Unclassified		

HMRT 1242 ORIG 9 72

ClibPDF - www.fastio.com

STATE OF CALIFORNIA—BUSINESS AND TRANSPORTATION AGENCY

RONALD REAGAN, Governor

DEPARTMENT OF TRANSPORTATION
DIVISION OF HIGHWAYS
TRANSPORTATION LABORATORY
5900 FOLSOM BLVD., SACRAMENTO 95819

June 1974

Trans. Lab. No. 646666

Mr. R. J. Datel
State Highway Engineer

Dear Sir:

Submitted herewith is a final research report titled:

DYNAMIC FRACTURE TOUGHNESS DETERMINATION

BY THE INSTRUMENTED CHARPY IMPACT TEST

Principal Investigator
Roger D. Smith

Co-Investigator
Paul G. Jonas

Assisted By
Charles B. Kendrick

Under the Supervision of
Eric F. Nordlin

Very truly yours,

JOHN L. BEATON
Chief, Transportation Laboratory

ClibPDF - www.fastio.com

ACKNOWLEDGEMENTS

The authors of this report wish to express their appreciation to Carl Hartbower, Consulting Metallurgical Engineer, for his valuable assistance throughout the project, and to the staff of Effects Technology, Inc., for their counsel and instruction in the performance and application of the instrumented Charpy impact test.

We would also like to cite the Transportation Laboratory Machine Shop staff, particularly Floyd Martin, Joe Wilson, and Ervin Eisenbraun, for their precise and expeditious preparation of the test specimens.

The contents of this report reflect the views of the Transportation Laboratory which is responsible for the facts and the accuracy of the data presented herein. The contents do not necessarily reflect the official views or policies of the State of California, nor do they constitute a specification or regulation.

ClibPDF - www.fastio.com

TABLE OF CONTENTS

		Page
I.	INTRODUCTION	1
II.	CONCLUSIONS	6
III.	IMPLEMENTATION	7
IV.	RECOMMENDATIONS	8
V.	TECHNICAL DISCUSSION	9
	1. Dynamic Fracture Toughness	10
	2. Dynamic vs. Static Fracture Toughness	10
	3. Initiation vs. Propagation Energy	10
	4. Dynamic vs. Static Yield Strength	11
	5. Nil Ductility Transition Temperature	11
	6. K_{Id}-PCI Correlation	12
	7. K_{Id}-CVN Correlation	14
	8. Through-Thickness Yielding Criteria	14
VI.	BIBLIOGRAPHY	18
APPENDIX - A (Tables and Figures)		20-34
APPENDIX - (Report by Effects Technology, Inc., titled "Dynamic Fracture Toughness of Bridge Steels")		

ClibPDF - www.fastio.com

LIST OF TABLES AND FIGURES

		Page
Table I	Bridge Failure Data	21
Table II	Test Data Summary	22
Table III	Data for Evaluation of the Through Thickness Yielding Criteria	24
Figure 1	K_{Ic} and K_{Id} as a Function of Temperature for Plate A	25
Figure 2	K_{Ic} and K_{Id} as a Function of Temperature for Plate AL	26
Figure 3	K_{Ic} and K_{Id} as a Function of Temperature for Plate L	27
Figure 4	K_{Ic} and K_{Id} as a Function of Temperature for Plate M	28
Figure 5	K_{Ic} and K_{Id} as a Function of Temperature for Plate Q	29
Figure 6	K_{Ic} and K_{Id} as a Function of Temperature for Plate R	30
Figure 7	K_{Ic} and K_{Id} as a Function of Temperature for Plate Z	31
Figure 8	Dynamic Fracture Toughness Vs Precracked Charpy Impact Energy	32
Figure 9	Dynamic Fracture Toughness Vs Standard Charpy V-Notch Energy	33
Figure 10	Typical Oscilloscope Trace When Yielding Precedes Fracturing	34
Figure 11	Typical Oscilloscope Trace for a Brittle Test Specimen	34

ClibPDF - www.fastio.com

commonly used the dynamic standard Charpy V-notch impact test to estimate the result of the more complicated and expensive static "compact tension" test for fracture toughness. However, this approach, in effect, characterizes the steel in terms of resistance to fracture under static loading conditions, and is a valid approach only if, in fact, the most severe strain rate acting locally on any flaw in the structural member is in the static range.

Two basic philosophies concerning the selection of a realistic test loading rate are offered by fracture mechanics theorists. The first holds that because the overall bridge structure (and therefore each individual structural member) is subjected to relatively static loading rates (1), a static test for fracture toughness is realistic. The second philosophy, which advocates dynamic fracture toughness testing, alleges that slow crack growth is frequently incremental, and that during these increments of growth the rate of crack tip extension approaches the speed of sound, so that the metal at the crack tip separates very rapidly. Thus the strain rate at the tip of an active sub-critical crack is dynamic during each increment of growth, and final fracture is initiated dynamically by the growth increment that extends the crack to critical size based on dynamic toughness.

Advocates of static testing contend that a statically loaded toughness test fails by this same mechanism and hence a static test should provide a measure of the toughness available in a loaded, cracked structure.

Advocates of dynamic testing contend that overall or integrated slow crack growth rates depend on fatigue loading, stress corrosion, hydrogen embrittlement, strain aging and other diffusion or stress controlled, time dependent phenomena which are active in real structures where time is available but not in static toughness tests where neither time, cyclic stress nor environment are present to activate these mechanisms. Hence an increment of slow crack growth is not likely to occur and provide a dynamic crack tip strain rate during the limited time required to conduct a static toughness test.

This theory also contends that in materials which may be non-homogeneous (in terms of toughness level), cracks may initiate and/or jump abruptly through highly localized zones of low toughness. As these cracks emerge into tougher material, they create dynamic crack tip loading conditions, and thus the dynamic fracture toughness of the material will control. These areas of nonhomogeneity could be any local zone where stress intensity is elevated due to stress concentration, impurity inclusion, etc.,

ClibPDF - www.fastio.com

I. INTRODUCTION

Until recently, structural steel bridge design had been based primarily on conventional yield strength design theory and the use of appropriate safety factors which allow designers to avoid the analysis of obscure effects caused by residual stresses, local overloads, local hardening, strain aging, corrosion and stress concentrations. However, recent structural steel failures at stresses well below yield strength have demonstrated the need to consider these factors and the definitive material properties and failure mechanisms which relate them to design.

The phenomenon to which most of these premature failures can be attributed is known as "brittle fracture". Brittle fracturing results from a material's inability to resist the rapid extension of a crack or other sharp flaw under a particular combination of variables (temperature, loading rate, stress intensity, etc.).

It is a basic fact of materials science that all materials contain flaws - sometimes in the form of microscopic disruptions in the regular arrangement of atoms, or in the form of macroscopic inclusions or cracks often resulting from fabrication. In structural steels all of the commonly occurring flaw-types have the propensity to initiate cracking, the most dangerous flaw-type in terms of brittle fracture.

For brittle fracture to occur, these small cracks must be grown by such mechanisms as fatigue, stress corrosion, or hydrogen embrittlement, to some critical size, after which the crack will extend abruptly across the full section of the member, constituting a brittle fracture. The measure of a material's ability to resist this rapid extension of a crack (brittle fracture) is its "fracture toughness", commonly represented by the symbol "K_{Ic}".

Since the occurrence of extensive brittle fracture in Liberty ships during World War II, the simple, inexpensive standard Charpy V-notch impact test has often been used to measure the relative impact strengths of steels. Although the terms "impact strength" and "toughness" are commonly used synonymously, it should be kept in mind that "toughness" is a measurable value that the designer can relate to stress and flaw size in a structural member; whereas "impact strength", measured in foot-pounds, can only be applied to design on an empirical and qualitative basis. It has been shown (2), however, that empirical correlations exist between these two properties, which accounts for their mistaken synonymity. As a result of these empirical correlations, fracture control programs have

ClibPDF - www.fastio.com

is increased, the probability of exceeding the material's energy absorbing capacity (toughness) is increased, making fracture likely to occur prior to yielding.

It might be said, then, that the loss of toughness with increased strain rate is really an apparent loss of toughness commensurate with the increase in yield strength that results from the higher strain rate.

Other research (2) by this department investigated the effectiveness of the compact tension test (ASTM E399) in determining static fracture toughness and verifying purported correlations (11) between static fracture toughness (K_{Ic}) and Charpy impact energy. Certain of the correlations were proven sound, and on the basis of those findings tentative steel toughness guidelines were established by the California Division of Highways. These guidelines were considered sufficient to guarantee "through-thickness yielding" (3)(12) under static strain rates, and were stated in terms of standard Charpy V-notch impact energies. The Charpy energy values correlate to the calculated static K_{Ic} values considered necessary to guarantee general yielding prior to brittle fracture in a structural steel member. But if the actual failure conditions are, in fact, dictated by dynamic material properties, as suggested above, it would seem more reasonable to establish toughness requirements on the basis of dynamic fracture toughness (K_{Id}) values.

Another desirable feature in any toughness test specimen is sharp notch acuity provided by the use of a precracked (rather than a machined V-notch) specimen. A sharp test specimen precrack best simulates the situation in a cracked service member. Because the effect of notch sharpness is not always predictable it is important that a precracked test specimen be used. There have been instances of brittle fracture in material which exhibited adequate toughness at the failure temperature in post-failure standard (not precracked) Charpy tests, but which behaved brittley in precracked tests at the same temperature. These cases illustrate the dangers associated with the use of non-precracked acceptance tests for steel toughness.

This study, therefore, evaluates the instrumented precracked Charpy impact (IPCI) test as a meaningful measure of dynamic fracture properties of high strength ($\sigma_y \approx 100$ ksi) bridge steel. Included as Appendix A of this report is the report titled "Dynamic Fracture Toughness of Bridge Steels" prepared by Effects Technology, Incorporated, under contract with the California Division of Highways.

ClibPDF - www.fastio.com

which would make that area fracture prior to surrounding material. A common example of this nonhomogeneity would be a welding arc strike, where a zone of local residual stress and embrittled material exists. Another example of this effect would be the case of a growing crack encountering a void. A rapid increase in effective crack length and the accompanying abrupt increase in stress intensity would constitute a dynamic loading situation.

Only a dynamic test therefore will duplicate the high crack extension strain rates that are likely to occur in a real bridge structure under relatively static external loading conditions. Since steels exhibit less toughness under dynamic loading rates, a toughness criteria based on a dynamic test is more demanding (and conservative).

Reported investigations of failed bridge structures tend to support these views since dynamic rather than static toughnesses, as determined either directly or by impact correlation formulae, are usually more consistent with the toughnesses estimated from failure analyses. The value and practicality of a dynamic toughness test was demonstrated in the post-failure fracture mechanics analyses of the Point Pleasant Bridge (4), where the findings (see Table I) suggested that the material's dynamic properties dictated failure conditions.

Since loading rates imposed on a structure by normal service loads are usually in the "static" range, it was logically concluded that local dynamic strain conditions were imposed on the crack tip as the result of the abrupt consolidation of the adjacent flaws, evidence by the appearance of the fracture face.

In the case of the King's bridge near Melbourne, Australia, a failure analysis based on estimates from tests of steel similar to the failed steel, concluded that, here also, failure conditions were dictated by other than the static fracture toughness of the material (see Table I). Other instances of catastrophic brittle fracturing of material that exhibited ductile behavior in static toughness testing, also suggest that brittle failure conditions are often dictated by dynamic material properties.

A simplified explanation is offered for this strain (loading) rate dependency of steel toughness. As the strain rate in a material is increased, that material's yield strength (σ_Y) is similarly increased. The effect of increasing strength level, for all metals, is to cause a decrease in ductility (5).

Also, the elevated yield "ceiling" enables the material to endure a higher applied stress, thereby necessitating higher elastic energy storage if failure is to be averted (3). As stored energy

ClibPDF - www.fastio.com

II. CONCLUSIONS

1. The material property known as fracture toughness is a lesser value under dynamic (impact) loading than under relatively static loading.

2. Dynamic yield strength is significantly greater than static yield strength for the steels tested herein.

3. The Hartbower technique (9) for estimating a steel's nil ductility transition temperature (NDTT) from the transition in the precracked Charpy impact (PCI) vs. temperature curve agrees closely with the instrumented Charpy method (10), which utilizes the $\frac{K_{Id}}{\sigma_{yd}} \simeq 0.4$ criteria.

4. The Corten-Sailors (6) correlation between standard (not precracked) Charpy energy absorption (CVN) and dynamic fracture toughness (K_{Id}) is not verified by Transportation Laboratory data for ASTM A514/517 steel. However, a new correlation expression is developed.

5. Neither the Corten-Sailors (6) nor the Barsom (8) correlation between PCI energy and dynamic fracture toughness (K_{Id}) is verified by Transportation Laboratory data for ASTM A514/517 steel. A new correlation expression is developed.

6. A toughness specification for ASTM A514/517 steel which guarantees through thickness yielding and is based on dynamic fracture toughness converted to PCI energies imposes material requirements not usually attained by current steel-making practice.

ClibPDF - www.fastio.com

In all, seven (7) heats of ASTM A514/A517 high strength, quenched and tempered, alloy steel plate - Grades H and F - were tested. These seven steel heats, representing two manufacturers, were well characterized in terms of chemistry, tensile properties, impact properties, and static fracture toughness in previous testing programs (2). Three of the seven heats were tested using both standard and precracked Charpy specimens. Use of the standard (V-notch) specimen enabled the determination of dynamic yield strength and crack initiation energy in addition to the dynamic fracture toughness values from the precracked specimen.

The IPCI test is unique and valuable in that it's able to depict specimen fracture behavior as a function of time. Where the normal (uninstrumented) Charpy test indicates only the total energy absorbed by the breaking specimen, the IPCI test allows the definition of both load and energy characteristics at any point in the short "fracture life" of the specimen. Therefore, it becomes a simple task to separate the elastic zone of the energy-time curve from the plastic zone, enabling the application of linear elastic fracture mechanics (LEFM) theory in determining dynamic fracture toughness.

ClibPDF - www.fastio.com

IV. RECOMMENDATIONS

As a result of this research, it is recommended:

1. That the precracked Charpy impact (PCI) test be adopted as a routine check test for the fracture toughness of bridge steels.

2. That dynamic fracture toughness (K_{Id}) be related to energy absorption in the precracked Charpy impact test (PCI) by the expression;

$$K_{Id} = \sqrt{7E\ (PCI)},$$

where: K_{Id} = psi $\sqrt{in}$

PCI = ft-lb

E = psi.

3. That a future research effort be directed towards determining the actual strain rate that instigates unstable crack growth in a highway bridge element.

ClibPDF - www.fastio.com

III. IMPLEMENTATION

Although the findings of this study are not conclusive enough to justify the use of dynamic fracture toughness testing as a routine acceptance test for highway bridge steels, a great deal of useful fracture behavior knowledge has been gained.

It is hoped that in the near future, a research study can be initiated which will investigate the same seven heats of ASTM A514/517 steel with respect to their behavior in the static (slow bend) standard Charpy test. This would provide a full complement of information encompassing static and dynamic tests for both impact energy and fracture toughness. However, this information can only be of practical use if the strain rates experienced by an actual highway bridge element are known. When these in-service crack tip strain rates are better known, it should be a relatively simple task to select the most realistic testing requirement for quality control purposes. At that time, the knowledge of dynamic fracture toughness gained from this research will be used in establishing the K_I "extremes" of the loading rate spectrum.

ClibPDF - www.fastio.com

Instrumented impact testing of precracked Charpy (PCI) specimens enables the determination of dynamic fracture toughness, precracked Charpy impact energy, and Nil Ductility Transition Temperature (NDTT). Testing of the standard Charpy V-notch (CVN) specimen enables the determination of dynamic yield strength, CVN energy, and the isolation of crack initiation energy with respect to crack propagation energy. Although the primary concern of this study was dynamic fracture toughness, it was decided to take full advantage of the test's capabilities by running instrumented CVN tests on additional specimens from three of the seven plates.

Our findings with respect to each of the above objectives are presented below;

1. Dynamic Fracture Toughness

Dynamic fracture toughness (K_{Id}) vs. temperature curves for the seven ASTM A517 steel heats tested are found in Appendix B, Figures 19 through 25. The K_{Id} values are calculated using the fracture load (P_f) from the load-time oscilloscope trace when fracture precedes yield. In those cases where fracture did not precede yielding, the "equivalent energy" method (see Appendix B) provided reasonable estimates of K_{Id}. Examples of oscilloscope traces for each of the above two cases are shown in Figures 10 and 11.

2. Dynamic (K_{Id}) vs. Static (K_{Ic}) Fracture Toughness

As expected, the K_{Id} testing yielded lower values than the K_{Ic} values previously determined from compact tension tests (ASTM E399) (2). Both K_{Id} and K_{Ic} values are plotted in Figures 1 through 7. Also plotted are K values which did not satisfy the "validity" criteria set forth in ASTM E399-72. The validity of the K_{Id} test method used in this study is allegedly confirmed by previous findings (see Appendix B) that K_{Id} values from instrumented Charpy tests are consistent with K_{Id} values obtained from thick section (up to 8 inches) compact tension specimens for temperatures up to NDTT + 60°F. It can be seen that any design based on dynamic fracture toughness would be more conservative, i.e., would require higher quality (tougher) steel.

3. Initiation vs. Propagation Energy

Three of the seven steel heats were subjected to standard Charpy (CVN) testing as well as the precracked Charpy (PCI) tests from which K_{Id} determinations were made. Having both the CVN and PCI value enables the separation of "total" energy (CVN) into "propagation" (PCI) and "initiation" (CVN-PCI) energy components.

ClibPDF - www.fastio.com

V. TECHNICAL DISCUSSION

The State of California, Department of Transportation, Division of Highways has heretofore never measured the K_{Id} values for any steels, thus it was necessary to perform this investigatory testing program on an "out-of-house" contractural basis. Effects Technology Incorporated of Santa Barbara, California, was awarded the contract for determining the dynamic fracture toughness (K_{Id}) and related properties of seven (7) steel heats using the instrumented precracked Charpy Impact Test (IPCI).

The IPCI test method (10) was chosen to enable the use of the familiar inexpensive Charpy specimen to determine K_{Id}, thereby reducing the amount of sample steel necessary to complete the testing program.

In all, seven heats of ASTM A517/A514 steel were studied using the instrumented precracked Charpy impact test. Three of these seven heats were also used for instrumented standard (not precracked) Charpy V-notch testing. The objectives of the study were:

(1) to determine the critical dynamic fracture toughness (K_{Id}) of seven (7) heats of steel at various temperatures

(2) to analyse the effects of strain rate on toughness by comparing the K_{Id} values with previously determined "static" K_{Ic} values for the same steel heats

(3) to isolate crack initiation energy from crack propagation energy and study the effect of the different variables on them

(4) to measure dynamic yield stress and compare it to static yield stress for ASTM A517 steel

(5) to verify previously suspected NDTT temperatures

(6) to verify the purported correlations (6) (8) between dynamic fracture toughness (K_{Id}) and precracked Charpy impact (PCI) energy

(7) to verify the purported correlation (6) between dynamic fracture toughness (K_{Id}) and standard Charpy V-notch (CVN) energy

(8) to relate the "through thickness yielding" (7) criteria to dynamic fracture toughness values.

ClibPDF - www.fastio.com

for CVN as well as PCI values, were the only plates for which dynamic yield strength (σ_{yd}) determinations were able to be made (see Appendix B, Figures 35, 36 and 37). Knowledge of the NDTT is necessary from the standpoint that a structure's lowest expected service temperature should be above the NDTT of the material, if brittle fracture is to be averted.

6. K_{Id} - PCI Correlation

An empirical correlation between precracked Charpy impact energy (PCI) and dynamic fracture toughness (K_{Id}) has been reported by Corten and Sailors (6). Their investigation, like this one, involved A517 (Grade F) steels (among others) and generated the following relationship:

$$K_{Id} = 15.87\ (PCI)^{3/8}, \qquad (1)$$

where: $K_{Id} = ksi\sqrt{in}$

$PCI = ft\text{-}lb.$

Figure 8 shows this expression in graphical form juxtaposed with data obtained in this (Transportation Laboratory) study. It is evident that the Corten-Sailor general expression defines a rather conservative lower bound curve for the Transportation Laboratory A517/A514 steel data.

A more realistic expression for the K_{Id}-PCI relationship is given by the expression:

$$K_{Id} = 21(PCI)^{3/8}, \quad \text{where: } K_{Id} = ksi\sqrt{in} \qquad (2)$$

$PCI = ft\text{-}lbs.$

This expression defines a realistically conservative curve that generally agrees with the 95% confidence limit established by a least squares regression analysis of the Transportation Laboratory data (see Figure 8).

An empirical correlation between precracked Charpy impact energy (PCI) and dynamic fracture toughness (K_{Id}), reported (8) by Barsom, involved A517-Grade F steel (among others) and yielded the following relationship:

ClibPDF - www.fastio.com

In other words, the initiation energy is defined as the decrease in total energy resulting from the precracking (see Appendix B, Figures 29, 30 and 31).

Although this information has little quantitative significance, it is interesting to note that fracture propagation energy turns out to be roughly twice fracture initiation energy. Or, from a different viewpoint, the standard (not precracked) Charpy test misleadingly indicates a material's impact strength to be roughly 30% higher than the more realistic precracked specimen. The precracked specimen understandably provides a more realistic indication of the steel's behavior in the presence of a crack by offering greater sensitivity to variables such as temperature and loading rate, and by enabling an approximation of the steel's NDTT.

4. Dynamic vs. Static Yield Strength

This investigation found the following relationships to exist between static and dynamic yield strength:

For Grade H Steels: $\frac{\sigma_{ys}}{\sigma_{\sigma d}} = 0.77$

For Grade F Steels: $\frac{\sigma_{ys}}{\sigma_{yd}} = 0.82$

It is well established that fracture toughness is a function of yield strength. Therefore, any fracture control program which intends to protect against dynamic crack tip loading situations should specify testing requirements commmensurate with dynamic yield strength.

5. Nil Ductility Transition Temperature

The nil ductility transition temperatue is conventionally defined by the "drop weight test" (sometimes referred to as the DW-NDT test) developed by the Naval Research Laboratory. Hartbower and Orner (9) have found that the inflection characteristics of the precracked Charpy vs. temperature plot can also be used to estimate the NDTT. Still another method of NDTT determination is available using the IPCI test, which defines the NDTT as the temperature at which $\frac{K_{Id}}{\sigma_{yd}} \simeq 0.4$. Corresponding values of this ratio for steel plates L and M of this study were 0.353 and 0.379, respectively. Plates L, M, and Q, tested

ClibPDF - www.fastio.com

PCI testing has not been widely used because no standard test method has yet been developed, and because of alleged difficulties encountered in fatigue cracking the small Charpy specimen. This test method should gain greater acceptance with the development of a standardized test method, a project now being undertaken by ASTM Committee E-28.

7. K_{Id} - CVN Correlation

Corten and Sailor(6) also suggest that Equation 1 defines the relationship between standard (not precracked) Charpy V-notch energy (CVN) and dynamic fracture toughness (K_{Id}). This, effectively, is saying that fracture toughness is independent of notch root radius. Equation 1 has already been proven invalid with respect to the findings of this study, but it would seem likely that Equation 2, similarly, would represent the K_{Id}-CVN correlation as well as the K_{Id}-PCI correlation for this study. This was not found true (see Figure 9). The expression which best defines the Transportation Laboratory correlation is:

$$K_{Id} = \sqrt{4E(CVN)}, \quad \text{where: } K_{Id} = \text{psi}\sqrt{\text{in}} \qquad (6)$$

$$E = 30 \times 10^6 \text{ psi}$$

$$CVN = \text{ft-lb.}$$

This expression defines a realistically conservative curve that generally agrees with the 95% confidence limit established by a least squares regression analysis of the Transportation Laboratory data (see Figure 9).

Although it appears from the results of this study that no K_{Id} values less than 40 ksi $\sqrt{in}$ will be realized in A514/517 steel, a curve with "y-intercept" equal to 40 ksi $\sqrt{in}$ was not chosen as the basis for the correlation expression because K_{Id} values less than 40 ksi $\sqrt{in}$ were measured in other studies (11)(6) of A514/517 steel.

Caution should be exercised in using Equation 6 to estimate K_{Id} values from CVN values, as the effects of the difference in notch root radius between the K_{Id} and CVN specimens may not be consistent.

8. Applicability of the "Through Thickness Yielding" (3)(7)(12) Criteria to K_{Id} Testing

Determination of just what level of toughness is adequate for any given steel structure is a difficult and controversial task. One popular approach, known as the "through thickness yielding"

ClibPDF - www.fastio.com

$$\frac{K_{Id}^2}{E} = 5\ \overline{PCI} \quad \text{or,} \tag{3}$$

$$K_{Id} = \sqrt{5E\ \overline{PCI}}, \quad \text{where:} \quad K_{Id} = \text{psi}\ \sqrt{\text{in}} \tag{4}$$

$$E = \text{psi}$$

$$PCI = \text{ft-lbs.}$$

This expression is shown in graphical form juxtaposed with data points from the Transportation Laboratory study in Figure 8. Barsom feels that for PCI values of 5 ft-lb or less, the K_{Id} value is minimized at about 20 ksi $\sqrt{in}$. The failure of the Transportation Laboratory data to reinforce the Barsom curve is evident. Although Barsom calls Equation 4 a "conservative estimate" of K_{Id}, the degree of conservatism with respect to the Transportation Laboratory findings is considerable. A more realistic expression of the Transportation Laboratory findings is given by the expression:

$$K_{Id} = \sqrt{7E(PCI)} \tag{5}$$

This expression defines a realistically conservative curve that generally agrees with the 95% confidence limit established by a least squares regression analysis of the Transportation Laboratory data (see Figure 8).

Of these two correlation expressions (Equations (2) and (5)), Equation (5) is preferred for its better fit with the Transportation Laboratory data and its simpler mathematical form. This correlation will enable estimates of dynamic fracture toughness from the familiar, inexpensive PCI test. The precracked Charpy specimen is generally preferred to the standard (not precracked) specimen because it better simulates an actual crack tip situation in a structural member (and in the K_{Id} test). In addition to enabling K_{Id} estimations, the PCI test can provide a close approximation of the steel's nil ductility transition temperature (NDTT) (9).

It is sometimes considered desirable to express PCI test results in terms of lateral expansion of the broken specimen halves. Previous research (2) by this agency disclosed the existence of a 1:1 relationship between PCI energy and lateral expansion (measured in mils) for A514/A517 steel. That is, a 15 ft-lb PCI energy absorption value corresponds to 15 mils of lateral expansion in the same specimen. So it stands that K_{Id}, in turn, can be estimated from lateral expansion.

ClibPDF - www.fastio.com

require in a Charpy test. The Charpy impact test is sometimes said (13) to represent the "plane strain" (most severe) state of stress, with respect to brittle fracture. If this test does in fact represent the most dangerous situation, it is able to predict the behavior of structural members many times thicker, as the state of stress cannot worsen.

But when the fracture toughness adequacy of these seven steels is evaluated with respect to their originally intended use (i.e., bridge girder flange, 2-1/4 inches thick) the required K_{Id} (PCI) values defined by Equation 8 are too high (due to the increased thickness) to be met by any of the steels (see Table III) in this study. In fact no A514/517 steel ever tested by the Transportation Laboratory could have met the toughness requirement for through thickness yielding based on dynamic testing. (The toughest A514/517 steel ever tested by the State of California exhibited 52 ft-lbs @ 0°F in the PCI test.)

At is evident that the through thickness yielding criteria, when applied to stressed bridge members, is highly demanding by current steel quality standards. However, with seemingly no A514/A517 bridge steels tough enough to meet the above criteria, there has been only one known instance of brittle fracture in California highway bridges. Possible explanations for this anomaly are:

A. Structural redundancy exists to the extent that as one girder cracks, the load is easily transferred to adjacent girders causing the crack to arrest and never reach critical size.

B. Cracks initiating in localized zones of yield-level concentrated stress often arrest as they grow into a field of decreasing stress and, therefore, decreasing crack tip stress intensity.

C. The strain rate in effect at the tips of cracks in service members possibly does not approach the impact strain rate (10^3 in/min) used in the test for dynamic fracture toughness.

In general then, the ability of a steel to perform satisfactorily at toughness levels below those necessary for through thickness yielding probably stems from the fact that the nominal stresses (i.e., those remaining after zones of concentrated stress have been relieved by cracking) which challenge the toughness of a steel bridge member are usually able to remain below a critical level.

ClibPDF - www.fastio.com

criteria, was introduced by Hahn and Rosenfield (12) in 1968. This theory advocates the importance of toughness levels adequate to insure a zone of plastic deformation at the crack tip, that encompasses the plate thickness, thereby insuring that conventional yield-type failure would precede any brittle fracturing. This toughness level is characterized by an increase in surface displacement, or in other terms, a relaxation of crack tip triaxial stress, more popularly termed "constraint". The level of fracture toughness necessary to insure this "through thickness yielding" (T.T.Y.) according to Hahn and Rosenfield is obtained from the expression:

$$K_{Ic} = \sigma_y \sqrt{t}, \qquad (7)$$

where: K_{Ic} = critical plane strain fracture toughness (ksi $\sqrt{in}$)

σ_y = yield strength (ksi)

t = plate thickness (in.).

For dynamic loading conditions, Equation 7 becomes:

$$K_{Id} = \sigma_{yd} \sqrt{t}, \qquad (8)$$

where: K_{Id} = critical plane strain dynamic fracture toughness (ksi $\sqrt{in}$)

σ_{yd} = dynamic yield strength (ksi)

t = plate thickness (in.).

The validity of this theory can be verified by treating the Charpy specimen as a small service member and using the values of K_{Id} and σ_{yd} for the temperature at which general yielding is realized in the IPCI test. The K_{Id} values calculated using Equation 8 (with t = 0.394 in.) are in general agreement with the actual K_{Id} values measured at the temperature of general yielding for each steel (see Table III). Thus the basic theory seems valid.

It would seem logical to assume that the minimum energy level at which "general yielding" in the Charpy specimen precedes any degree of plane strain fracturing would be a suitable level to

ClibPDF - www.fastio.com

VI. BIBLIOGRAPHY

1. Highway Research Board of the NAS-NRC Division of Engineering and Industrial Research, the AASHO Road Test, Report 4, Bridge Research, Special Report CID, Publication No. 953, National Academy of Science - National Research Council, Washington, D.C. 1962.

2. "Fracture Toughness Testing of High Strength Bridge Steel", R. D. Smith and C. B. Kendrick, California Division of Highways, June 1974.

3. "Designing to Prevent Fracture or Fatigue Failure in Bridges" -Paper II- S. T. Rolfe for California Division of Highways, July 1971.

4. "Application of Fracture Mechanics to Analysis of Bridge Failure", Karl H. Frank and C. F. Galambos, Federal Highway Administration.

5. "Criteria for Fracture Control Plans", W. S. Pelini, Naval Research Laboratory, Washington, D. C., 1972.

6. "Relationship Between Material Fracture Toughness Using Fracture Mechanics and Transition Temperature Tests", R. H. Sailors and H. T. Corten, ASTM-STP 514, 1972.

7. "Sources of Fracture Toughness: The Relation Between K_{Ic} and the Ordinary Tensile Properties of Metals", ASTM-STP 432, 1968.

8. "Toughness Criteria for Structural Steels: Investigation of Toughness Criteria for Bridge Steels" (97.018-001(5)) AISI Project 168, February 8, 1973, John M. Barsom.

9. "Transition-Temperature Correlations in Constructional Alloy Steels", The Welding Journal, Vol. 40(9), P 459-S, October 1961, C. E. Hartbower and G. M. Orner.

10. "The Use of Precracked Charpy Specimens to Determine Dynamic Fracture Toughness", Engineering Fracture Mechanics, Vol. 4, 1972, pp. 367-375, W. L. Server and A. S. Tetelman.

11. Barsom, J. M. and Rolfe, S. T., "Correlations Between K_{Ic} and Charpy V-Notch Test Results in the Transition - Temperature Range", Impact Testing of Metals, STP 466, ASTM, Philadelphia, Pa., June, 1969, pp. 281-302.

ClibPDF - www.fastio.com

This would suggest that the lack of brittle fracturing in California highway bridges might be attributed to the lower-than-expected stress levels, as well as to the sufficiently high inherent toughness in most bridge steels to date and the relatively thorough inspection programs instituted by this department. Future bridge design will no doubt "trim" safety factors to the extent that the margin of protection that, fortunately, was (is) present in older structures may not be available in future designs. This fact, coupled with the fact that the popularity of high strength steels (those most susceptible to brittle fracturing) is ever increasing, makes the use of the most <u>realistic</u> routine check test for steel toughness imperative.

ClibPDF - www.fastio.com

APPENDIX A

TABLES AND FIGURES

ClibPDF - www.fastio.com

12. G. T. Hahn and A. R. Rosenfield, "Plastic Flow in the Locale of Notches and Cracks in Fe-3Si Steel Under Conditions Approaching Plane Strain", Ship Structure Committee Report, SSC-191, November, 1968.

13. Gross, J. H., "Effect of Strength and Thickness on Notch Ductility", ASTM STP 466, 1970, pp. 21-52.

ClibPDF - www.fastio.com

	Test Temp. (°F)	K_{Id} (ksi $\sqrt{in}$)	CVN (ft-lbs)	PCI (ft-lbs)
Plate A*	-80	35	-	1
	-40	39	14	1
	- 0	48	16	1
	40	46	17	4
	72	49	20	6
	120	61	24	1
	160	73	29	18
Plate AL*	-80	33	-	3
	-40	46	7	4
	0	51	10	6
	40	60	12	9
	72	61	22	12
	120	65	28	17
	160	71	-	20
	200	75	42	28
Plate L	-160	39	7	2
	-120	51	12	2
	-80	49	12	5
	-40	54	13	7
	-20	50	52	13
	0	61	62	14
	40	88	79	29
	72	80	84	37
Plate M	-320	30	-	1
	-240	42	5	2
	-200	46	7	2
	-160	47	8	4
	-120	47	42	7
	-80	66	34	16
	-40	130	56	26
	0	100	70	46
	40	-	70	-
Plate Q	-40	45	4	3
	0	54	6	4
	40	53	7	6
	60	39	-	7
	72	56	11	6
	120	47	13	8
	160	55	17	8
	200	61	18	12

*CVN energy values are from Transportation Laboratory testing.

Table II. Test Data Summary

ClibPDF - www.fastio.com

	Measured K_{Ic} (Static)	Measured K_{Id} (dynamic)	Calculated K @ failure
Kings Bridge[4]	125	65	98
Point Pleasant[4]	41	26	26

NOTE: Data from numerous other bridge failures attributed to brittle fracture has not yet been made available.

Table I. Bridge Failure Data

ClibPDF - www.fastio.com

Steel Plate Code	General Yield Temp. (T.G.Y.) from K_{Id} vs temp. plot (°F)	K_{Id} @ P max (ksi $\sqrt{in}$)	Position of T.G.Y. on PCI vs Temp. Curve	σ_{yd} @T.G.Y. (ksi)	K_{Id} req'd for T.T.Y. in PCI (ksi $\sqrt{in}$)	K_{Id} req'd for T.T.Y. in service (ksi $\sqrt{in}$)	PCI req'd for T.T.Y. in service (ft-lbs)
A	>160	>75	unknown	-	-	-	-
AL	200	75	upper shelf	122.6	78.5	184	160
L	70	80	upper shelf	137.5	86.3	207	204
M	-40	105	upper shelf	179.1	112.0	268	342
R	>120	>70	unknown	-	-	-	-
Z	120	80	transition slope	137.0	86	205	200
Q	>240	>70	unknown	-	-	-	-

where: T.G.Y. = temperature of general yield in PCI test
P max = maximum load on specimen

Table III. Data for evaluation of the through-thickness yielding criteria.

ClibPDF - www.fastio.com

Table II. (continued) Test Data Summary

	Test Temp. (°F)	K_{Id} (ksi $\sqrt{in}$)	CVN (ft-lbs)	PCI (ft-lbs)
Plate R*	-160	38	-	1
	-120	46	-	2
	-80	46	6	4
	-40	44	10	5
	0	55	18	8
	40	62	-	13
	72	60	34	18
	120	70	43	23
Plate Z	-160	38	-	2
	-120	49	-	2
	-80	52	8	4
	-40	50	11	6
	0	57	22	17
	40	72	-	12
	72	76	36	17
	120	79	46	26
	160	84	-	34

*CVN energy values are from Transportation Laboratory testing.

ClibPDF - www.fastio.com

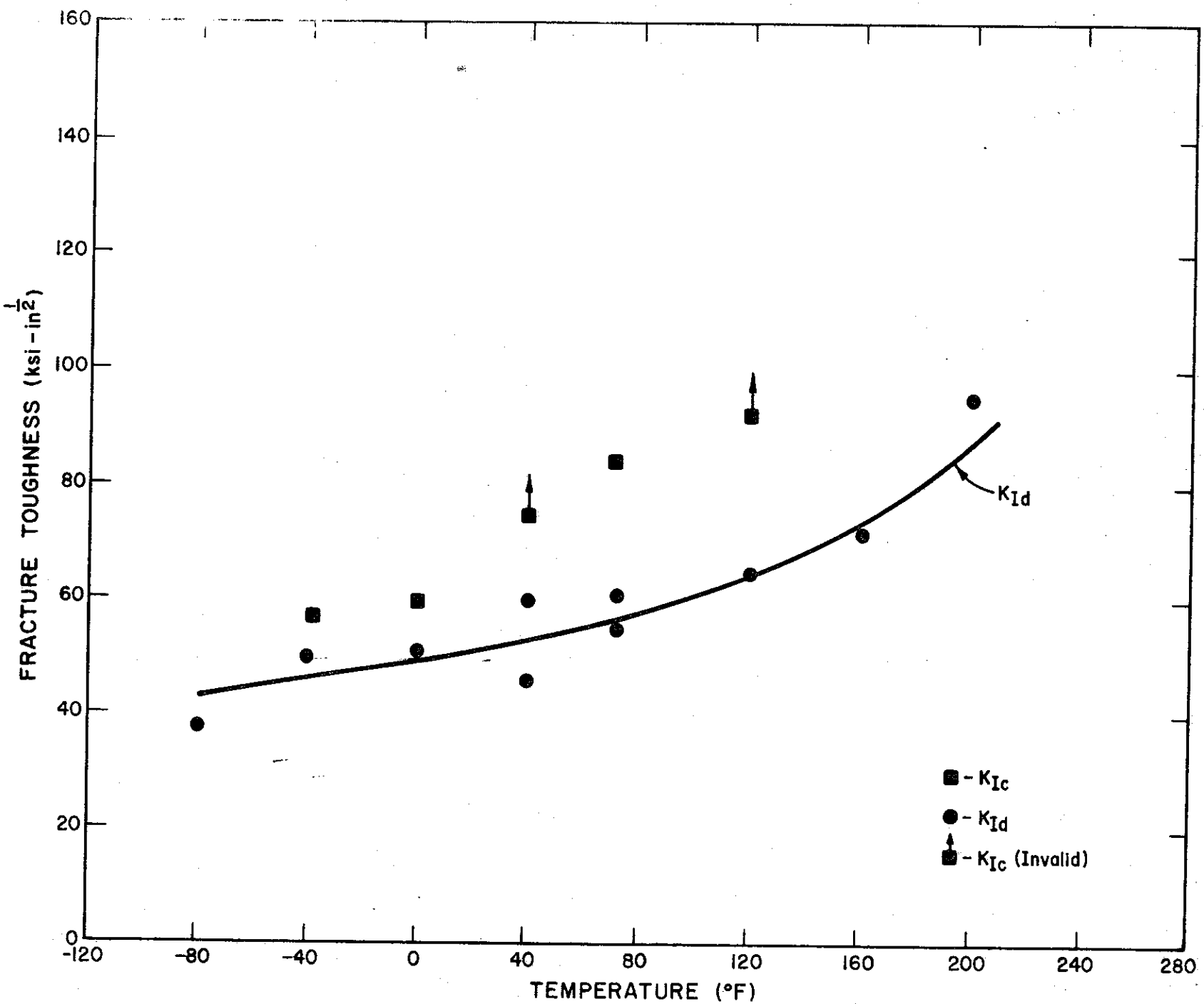

Figure 2. K_{Ic} AND K_{Id} AS A FUNCTION OF TEMPERATURE FOR PLATE AL

ClibPDF - www.fastio.com

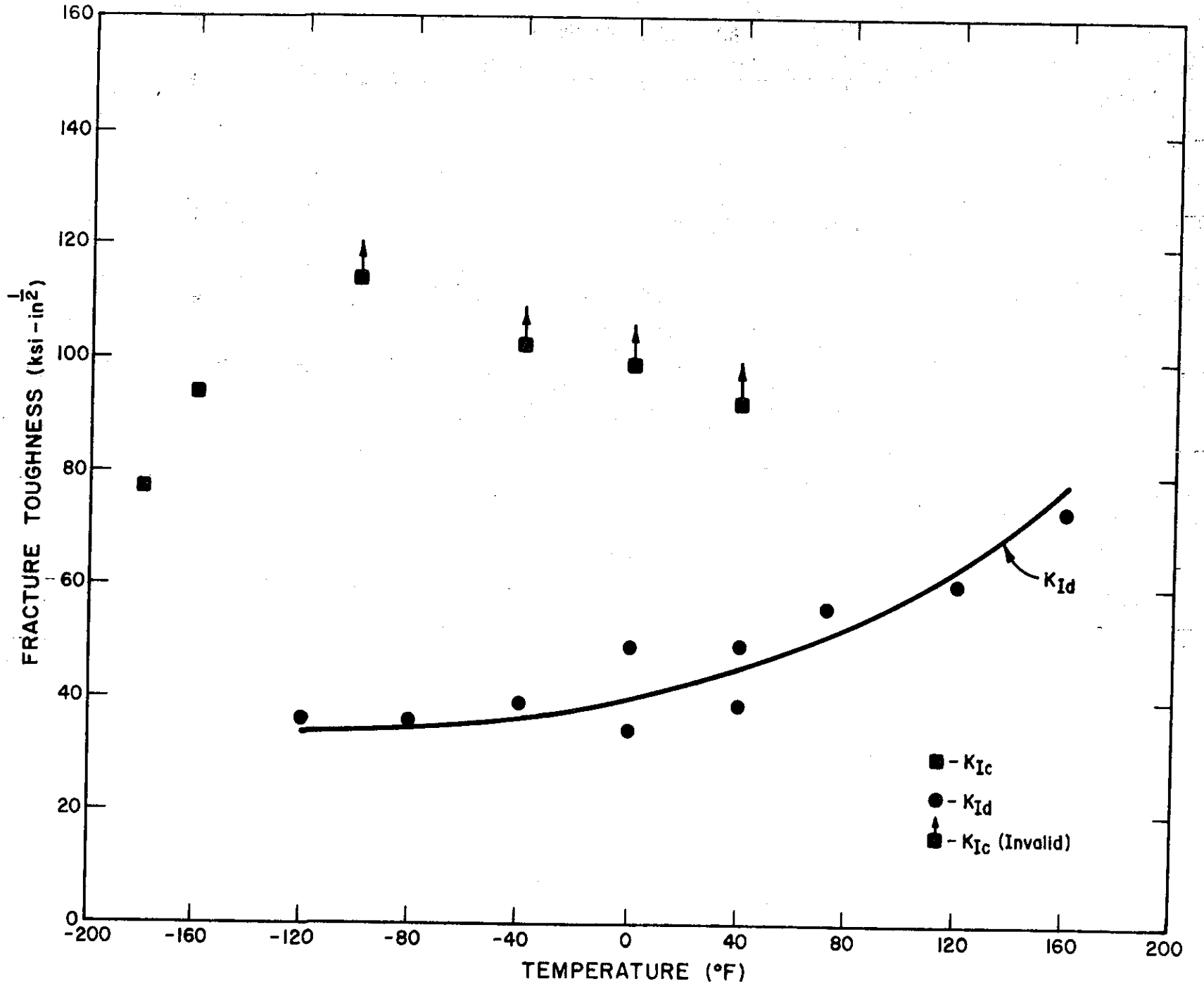

Figure [illegible] K_{Ic} AND K_{Id} AS A FUNCTION OF TEMPERATURE [illegible]

ClibPDF - www.fastio.com

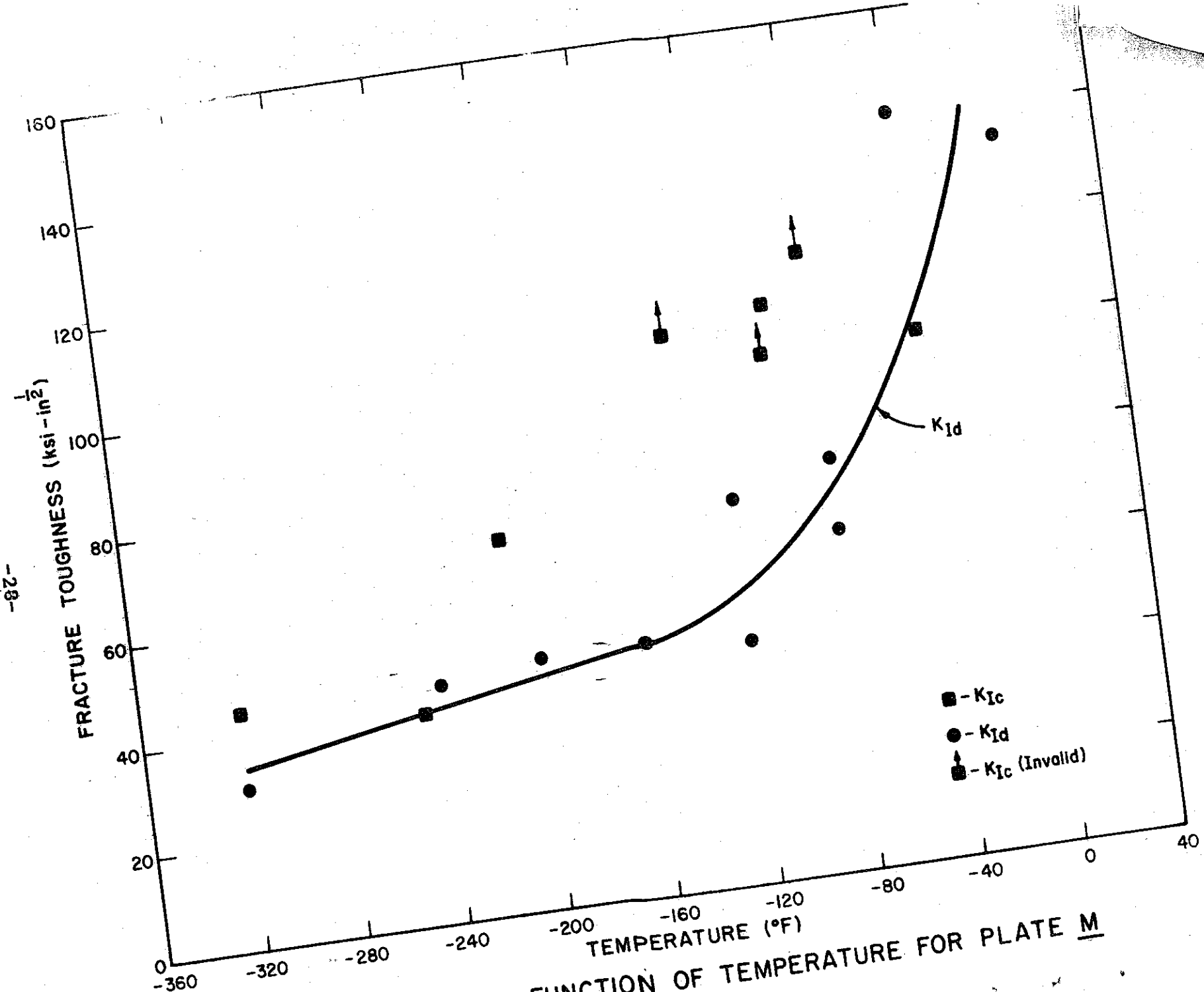

Figure 4. K_{Ic} AND K_{Id} AS A FUNCTION OF TEMPERATURE FOR PLATE M

ClibPDF - www.fastio.com

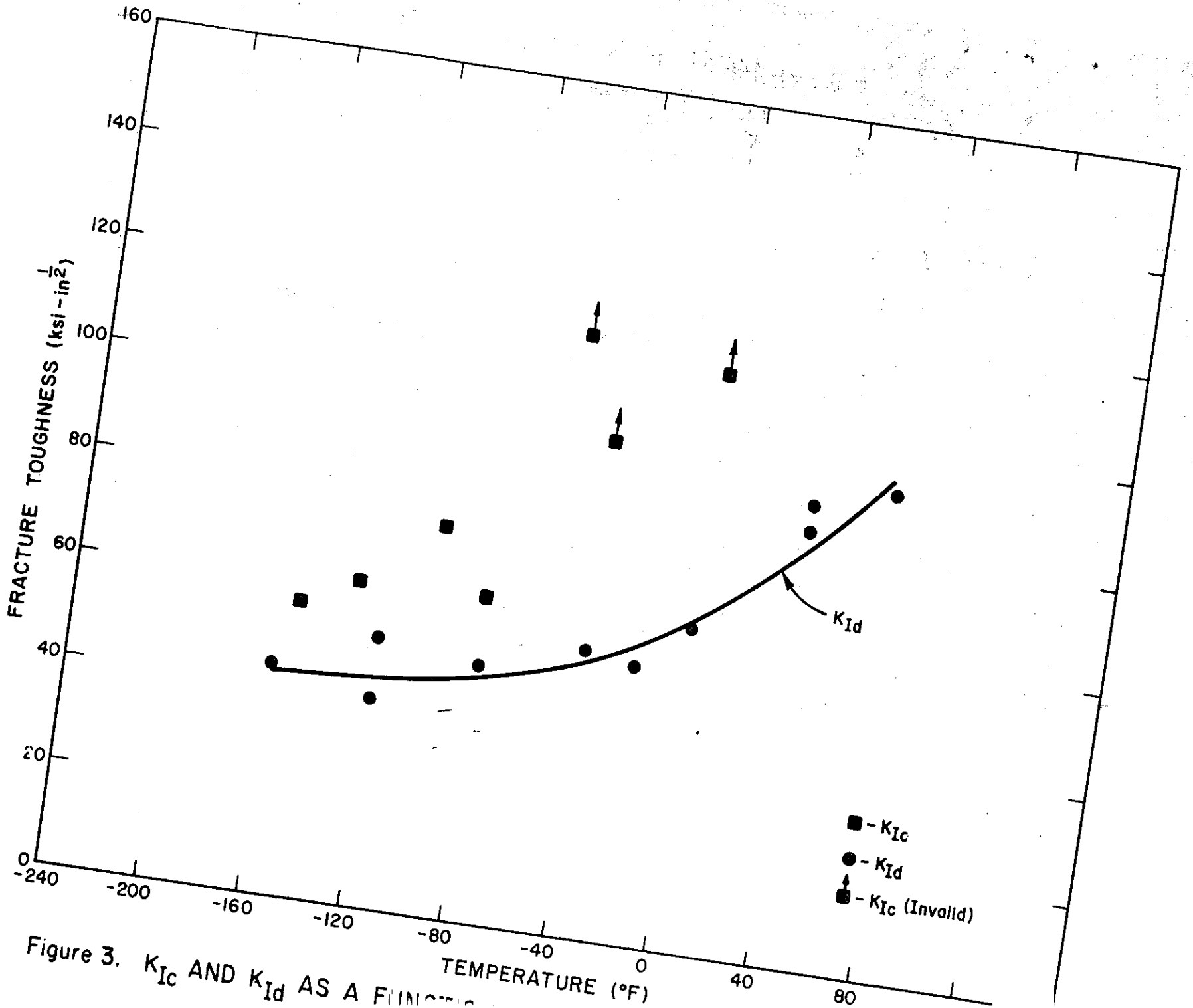

Figure 3. K_{Ic} AND K_{Id} AS A FUNCTION

ClibPDF - www.fastio.com

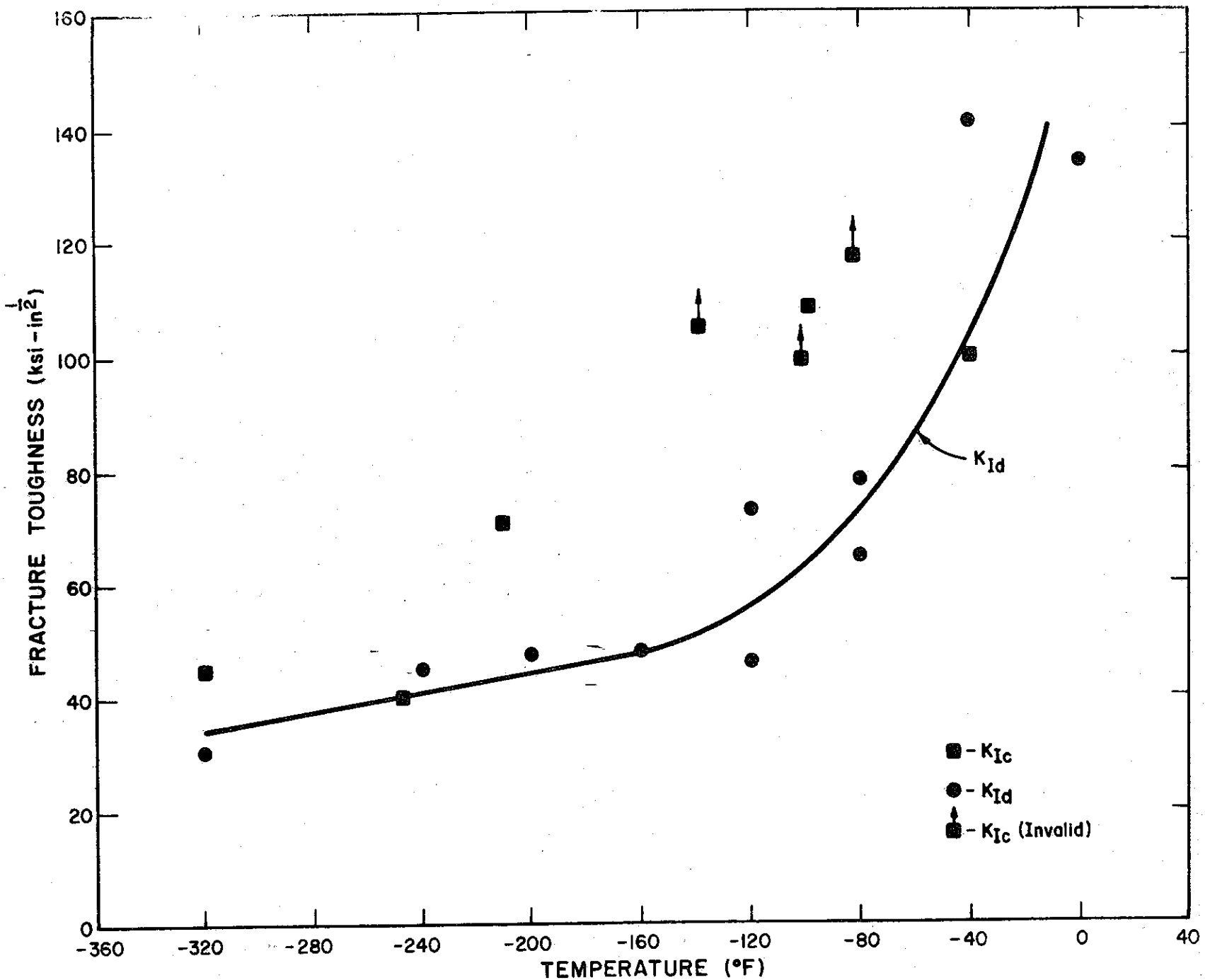

Figure 4. K_{Ic} AND K_{Id} AS A FUNCTION OF TEMPERATURE FOR PLATE M

ClibPDF - www.fastio.com

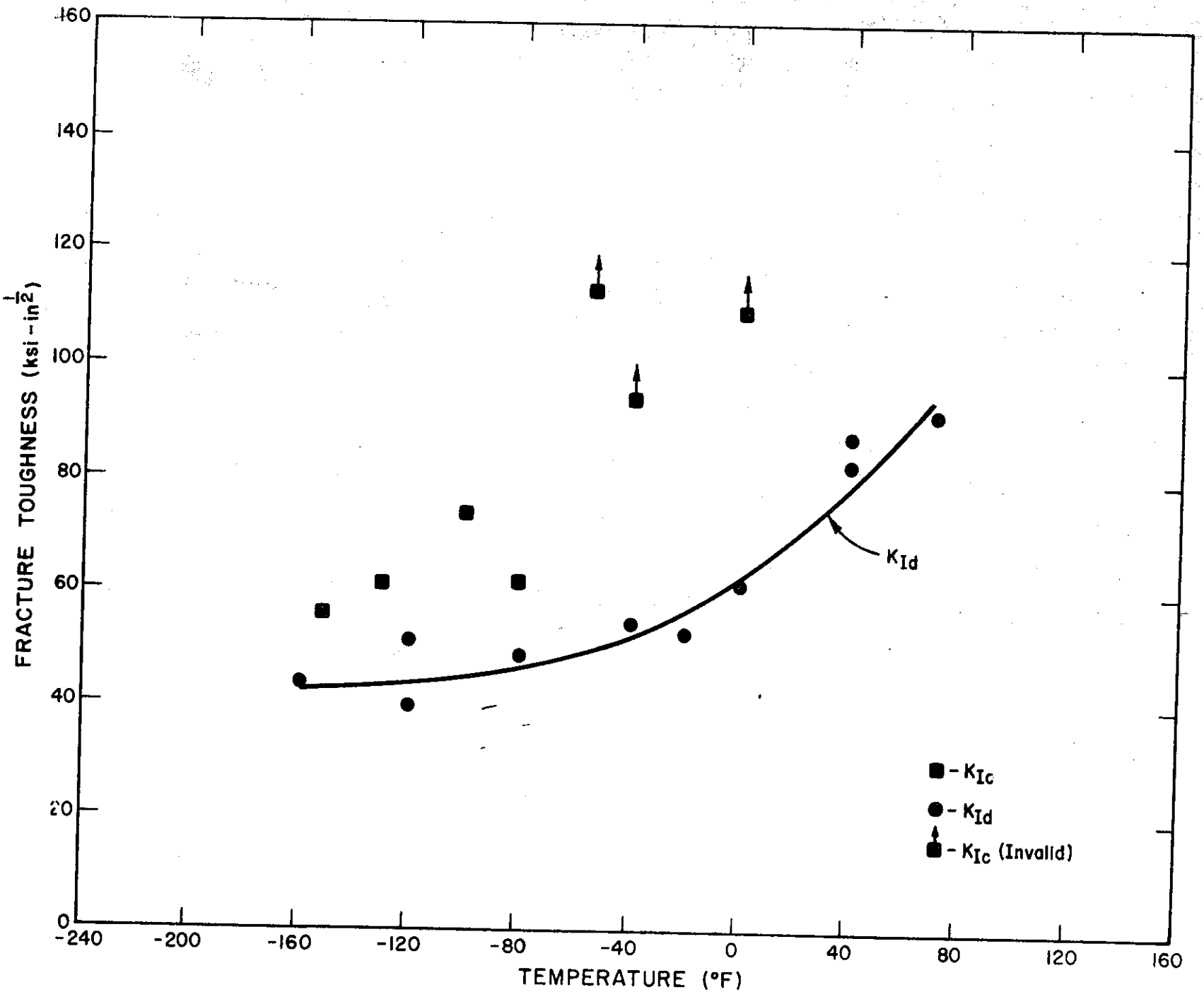

ClibPDF - www.fastio.com

ClibPDF - www.fastio.com

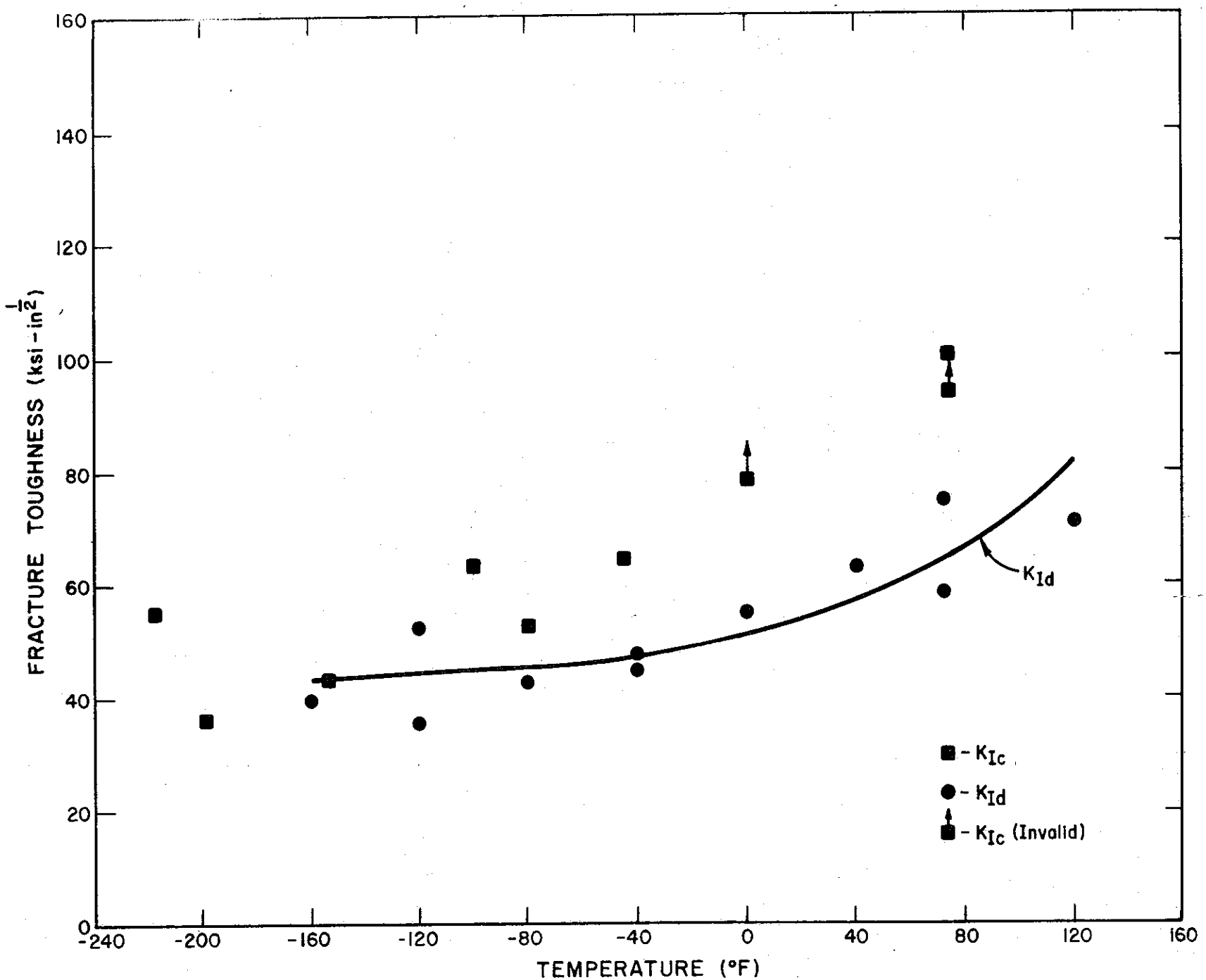

Figure 6. K_{Ic} AND K_{Id} AS A FUNCTION OF TEMPERATURE FOR PLATE R

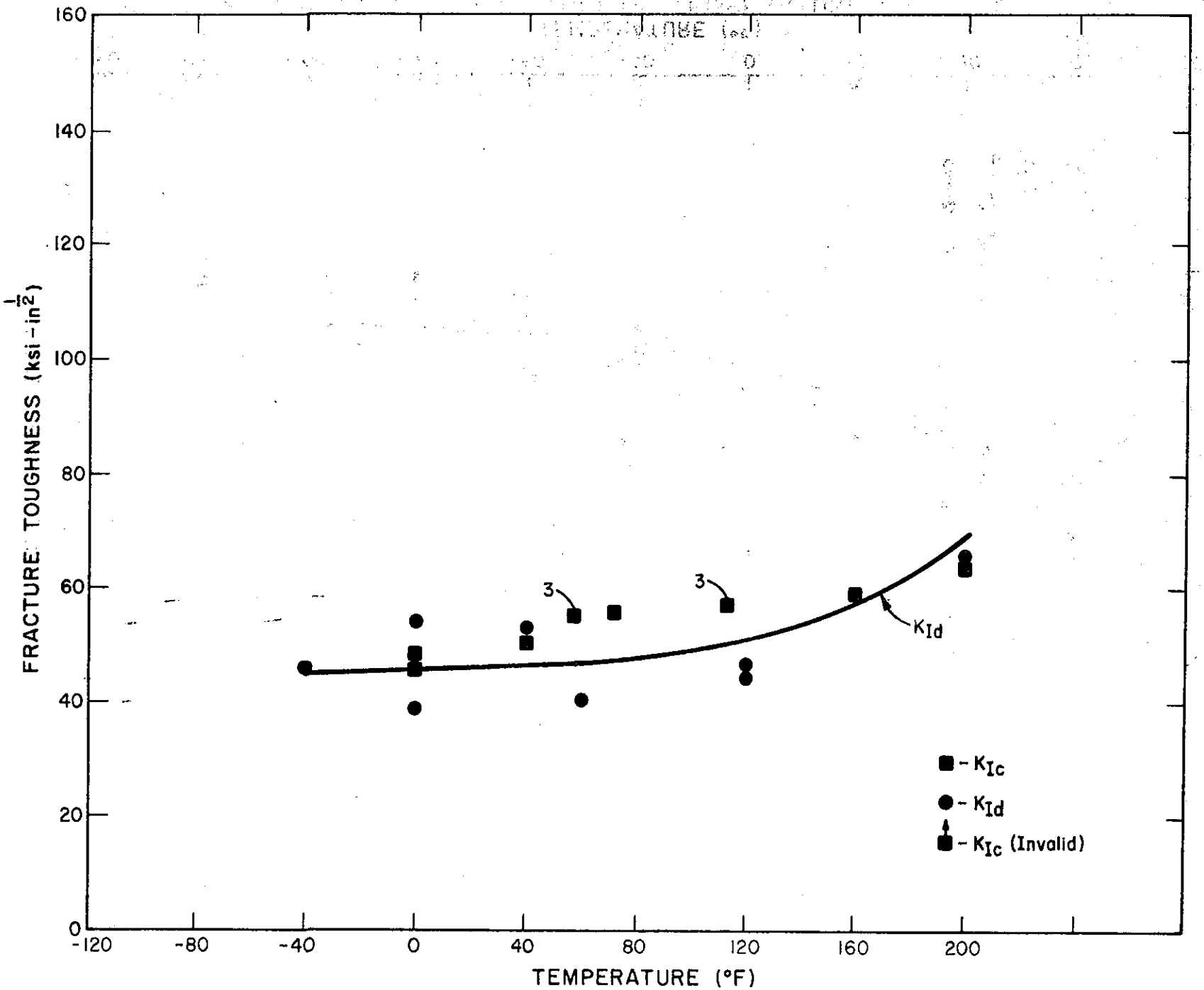

ClibPDF - www.fastio.com

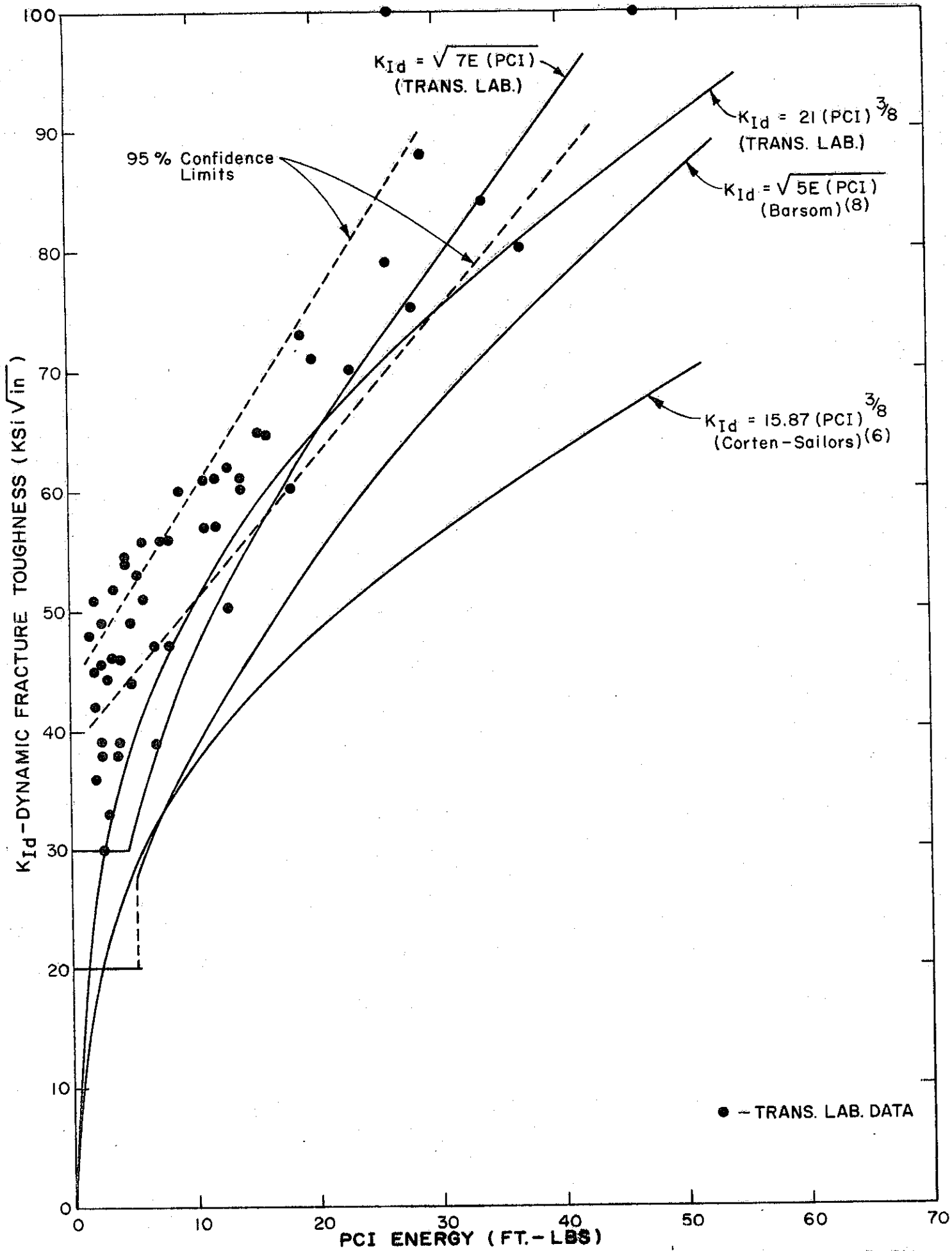

FIG. 8. DYNAMIC FRACTURE TOUGHNESS vs PRECRACKED CHARPY IMPACT ENERGY

ClibPDF - www.fastio.com

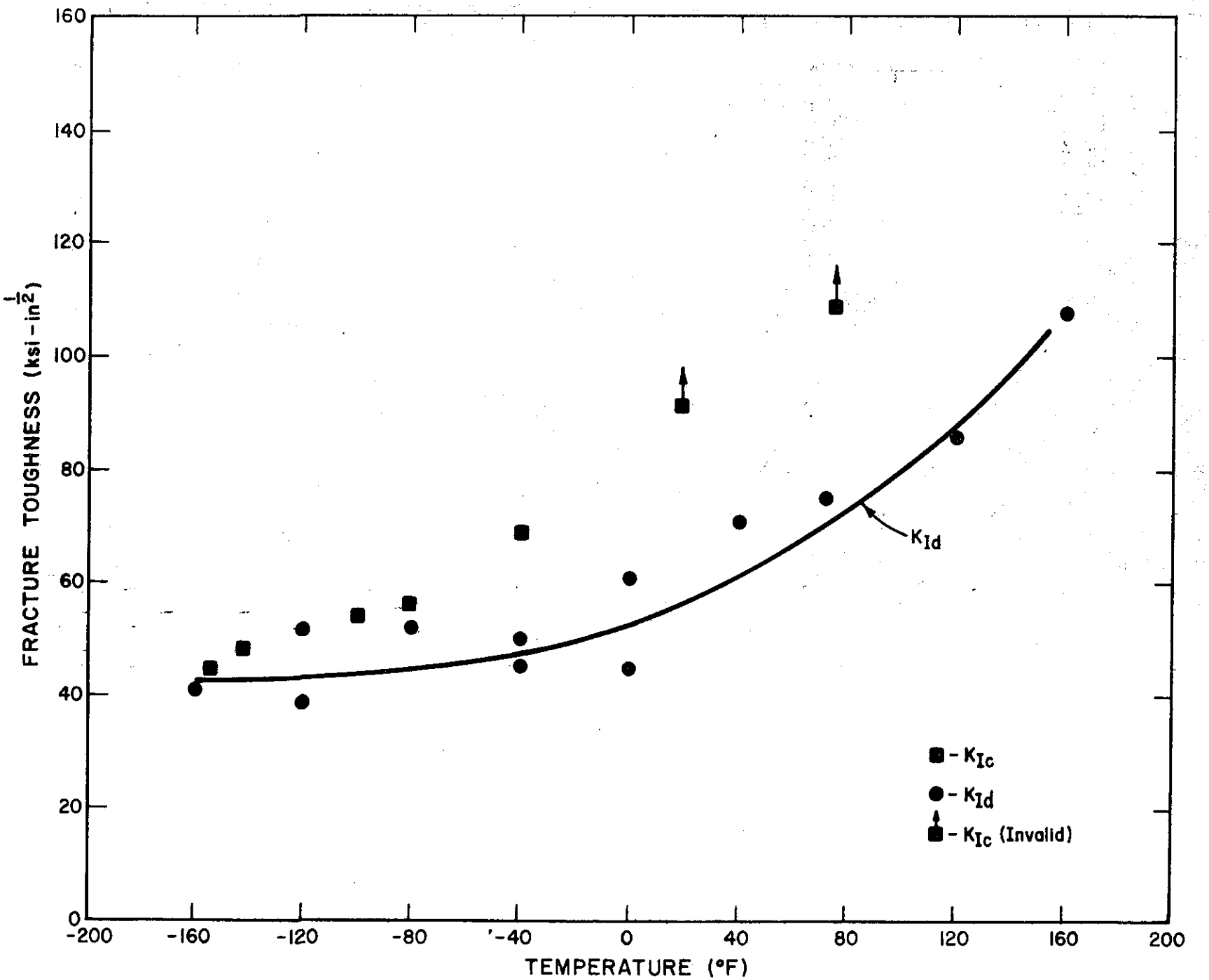

ClibPDF - www.fastio.com

Specimen: L15L (PCI)
Test Temp: +40° F
Total Energy: 35 ft-lb
Load Setting: 1000 lb/div.
Energy Set: 5 ft-lb/div.

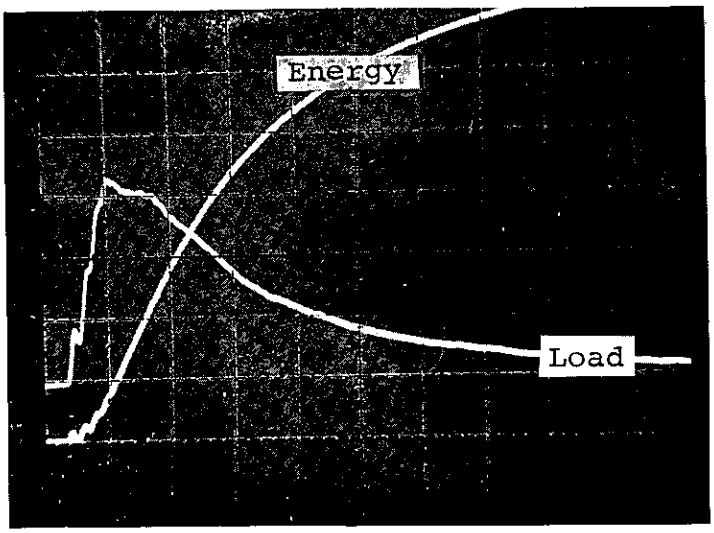

Load (lbs.) or Energy (ft-lbs)

time (milliseconds)

Figure 10. Typical Oscilloscope Trace When Yielding Precedes Fracturing

Specimen: L22L (PCI)
Test Temp: +160° F
Total Energy: 1.8 ft-lb
Load Setting: 500 lb/div.
Energy Setting: 1 ft-lb/div.

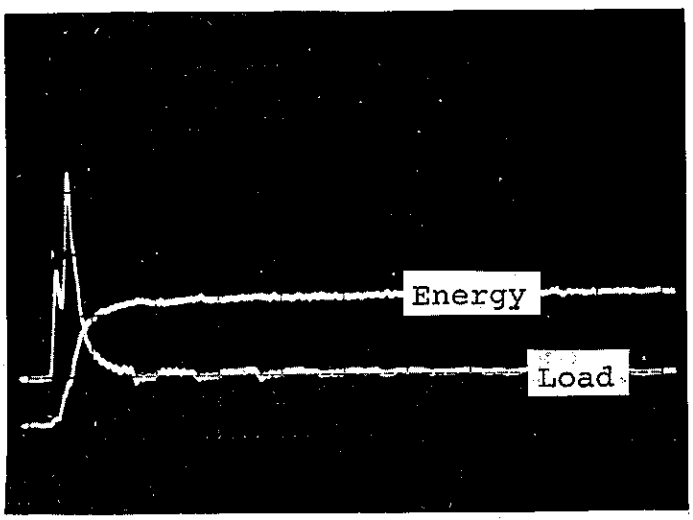

Load (lbs.) or Energy (ft-lbs)

time (milliseconds)

Figure 11. Typical Oscilloscope Trace for a Brittle Test Specimen

ClibPDF - www.fastio.com

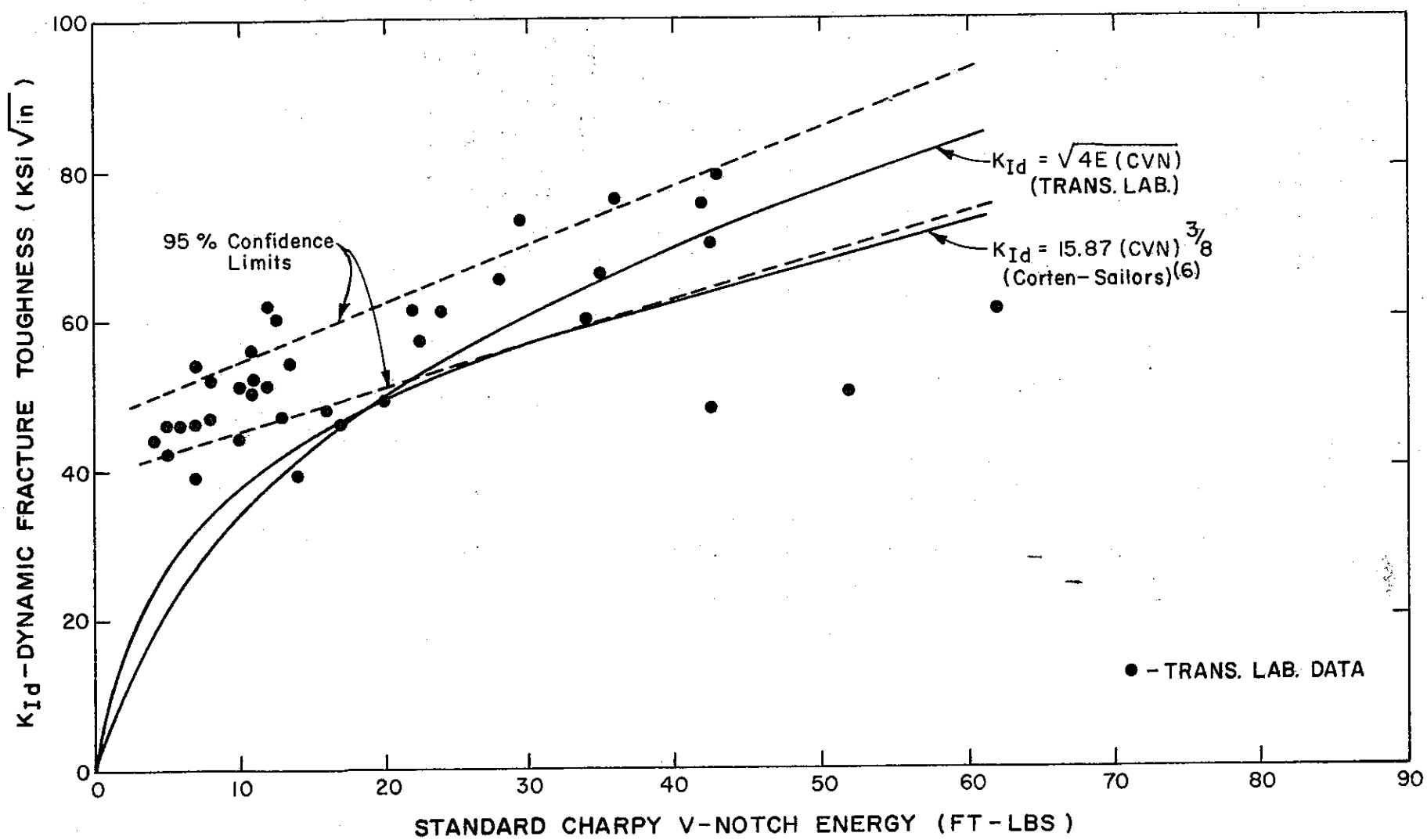

FIG. 9 DYNAMIC FRACTURE TOUGHNESS vs STANDARD CHARPY V-NOTCH ENERGY

ClibPDF - www.fastio.com

APPENDIX

"DYNAMIC FRACTURE TOUGHNESS

OF BRIDGE STEELS"

Report By

EFFECTS TECHNOLOGY, INC.

ClibPDF - www.fastio.com

ABSTRACT

The dynamic strength and toughness properties of seven heats of A514 and A517 bridge steels in Grades F and H were determined by DYNATUP instrumented impact testing of fatigue precracked Charpy and standard Charpy V-notch specimens. The tests employed an initial impact velocity of 16.8 ft per sec which resulted in stress intensity rates $\dot{K}$ of approximately 10^8 to 10^9 psi-$\sqrt{\text{in}}$ per second. The results of these tests were used to determine the NDT temperature, dynamic plane strain fracture toughness, and dynamic yield strength. These values, conventional impact energy transition curves, and load-temperature curves are presented for subsequent comparisons with known metallurgical and static strength properties.

ClibPDF - www.fastio.com

TABLE OF CONTENTS

INTRODUCTION - 1

TEST PROGRAM - 3

EXPERIMENTAL PROCEDURE - 4

A. Materials - 4
B. Fatigue Crack Measurement - 4
C. Instrumented Impact Tests - 5
D. Temperature Measurement - 7
E. Impact Machine Calibration- 8

RAW DATA REDUCTION - 8

STRENGTH AND FRACTURE TOUGHNESS CALCULATIONS - - - - - - - - - - - - - - -12

RESULTS- -17

A. Precracked Charpy Results and Calculations- - - - - - - - - - - -17
B. Charpy V-Notch Results and Calculations - - - - - - - - - - - - -18

DISCUSSION- 20

A. Dynamic Fracture Toughness- -20
B. Other Toughness Considerations- - - - - - - - - - - - - - - - - - -23
C. Significance of Dynamic Fracture Toughness- - - - - - - - - - -25

CONCLUSIONS- -27

REFERENCES -28

ClibPDF - www.fastio.com

INTRODUCTION

The application of fracture-prevention principles to structural design is becoming more important to a rapidly expanding number of concerned parties. This technology has forced development of tests to determine the type and extent of fracture to be expected for various materials at temperatures of structural design. These tests include the drop weight, Charpy V-notch, Izod and drop weight tear tests; these particular tests are identified as transition temperature tests. Fracture research specialists have also developed tests for determining a material property known as plane strain fracture toughness (K_{Ic}), which can be directly related to design stresses and expected flaw sizes. More recently, the instrumented Charpy impact test has been developed to provide a most valuable link between the transition temperature and plane strain fracture toughness concepts. This test retains the advantages of the absorbed energy, fracture appearance, and lateral expansion values while adding the new dimensions of dynamic load-time histories for three-point bend specimens.

The science of fracture mechanics has been developed in the last ten years to provide the designer with more of the information he requires for fracture safe designs. When a material property called fracture toughness (K_{Ic}) is known, the designer can then establish the trade-off between the possible stresses (σ) and flaws (a) present in his structure, since

ClibPDF - www.fastio.com

$$K_{Ic} \propto \sigma\ (a)^{1/2} . \qquad (1)$$

Until recently, the fracture toughness for plane strain (thick section) conditions was primarily measured under quasi-static conditions, and K_{Ic} is referred to as the static fracture toughness. However, K_{Ic} is not necessarily the lowest and therefore most conservative value of fracture toughness for materials such as pressure vessel steels. The yield strength of low and medium strength steels can be very strain rate ($\dot{\varepsilon}$) sensitive. For example, the yield strength of a mild steel can double by increasing the strain rate from 10^{-3} per second to 10^{2} per second. For a given steel, fracture toughness will decrease as the yield strength is increased through strain rate changes. Thus for ferritic pressure vessel steels, the following is true

$$K_{Ic}\ (\dot{\varepsilon}_2) \leq K_{Ic}\ (\dot{\varepsilon}_1) \quad [\dot{\varepsilon}_1 < \dot{\varepsilon}_2] \quad . \qquad (2)$$

The fracture toughness under dynamic loading conditions is generally referred to as K_{Id}. In general, for ferritic materials an environmental or loading condition that increases the yield strength will have an attendant decrease in fracture resistance. A decrease in temperature will raise the yield strength and lower the toughness K_{Ic}. Thus

$$K_{Ic}\ (T_1) \leq K_{Ic}\ (T_2) \quad [T_1 < T_2] \quad . \qquad (3)$$

The change in yield strength with temperature for pressure vessel steels leads to a transition in the fracture mode from brittle cleavage fracture at low temperatures to ductile fibrous tearing at

ClibPDF - www.fastio.com

higher temperatures. This fracture mode transition is responsible for the ductile-brittle transition measured by the standard Charpy test. This fracture mode transition will also cause the fracture toughness (K_{Ic} or K_{Id}) to increase rapidly above a certain temperature (usually around the Nil Ductility Transition Temperature, NDTT).

Effects Technology, Inc. has pioneered in the development of the instrumented Charpy test. This test permits both the energy and the load-deflection behavior of the Charpy specimen to be measured during the normal impact test. Thus instrumented Charpy tests performed on precracked Charpy specimens will yield both the ductile-brittle energy transition behavior of the material and the dynamic fracture toughness-temperature curve. For a steel such as A533B, it has been shown that K_{Id} values obtained from an instrumented Charpy test are consistent with K_{Id} values obtained from thick section (up to 8 inches) compact tension specimens for temperatures up to NDTT + 60°F.

TEST PROGRAM

The primary objective of the program was to measure the dynamic fracture toughness (K_{Id}) for seven heats of A514 and A517 steel in grades F and H, and to evaluate differences in K_{Id} values for the various heats of steel. The test program was also formulated so that the effects of notch acuity on fracture toughness for three of the steels could be studied. Additional data to be obtained from the test program includes the various components of energy, total energy per

ClibPDF - www.fastio.com

unit area (W/A), and dynamic yield strength as a function of temperature. These values were used to determine transition temperature characteristics.

EXPERIMENTAL PROCEDURES

Materials

The materials were A514 and A517 steels in grades F and H from seven heats. The specimens were supplied by the California Department of Highways in the form of standard Charpy V-notch specimens. Fatigue precracking was performed by Aerojet Solid Propulsion Company. A specimen-designation code was stamped on the end of each Charpy specimen; the first letters in each code designated the steel "heat" and the subsequent numbers represented the specimen number. A total of 104 specimens were supplied to Effects Technology, Inc., 30 standard Charpy V-notch specimens and 74 precracked specimens. The test temperature ranges and intervals were determined by the Department of Highways with consultation from Mr. Carl Hartbower based on previous tests performed at the Aerojet Company. The test matrix is listed in Table 1.*

Fatigue Precrack Measurement

The depth of the fatigue precrack was measured by taking 4-5X photographs of the fractured surfaces. The magnification for each photograph was determined, and measurements of the crack depth were

* All tables and figures are at the end of the text.

ClibPDF - www.fastio.com

taken at the middle and at the quarter points of the specimen width. These three values were then averaged to obtain the crack depth. A typical fracture surface with a fatigue precrack is shown in Figure 1.

Instrumented Impact Tests

Instrumented impact testing with a DYNATUP* System provides valuable additional information for analysis of materials tested in three-point bending[1-7]. This general technique is often identified as the instrumented Charpy test, where the name Charpy implies adherence to ASTM E-23 specimen design[8]. However, the test is applicable to specimens with a wide range of dimensions and notch types. The DYNATUP Systems are specifically designed for impact tests of small three-point bend specimens which can be either notched or unnotched.

The discussion in this report is applicable for three-point bend tests of notched specimens having V-notch angles less than approximately 60 degrees and notch root radii less than approximately 0.010 in. (including precracked specimens with zero flank angle and root radius). The basic principles and procedure for reduction of raw data obtained in the form of oscilloscope traces are discussed. The utilization of the data must, of course, be related to the material performance of interest. The discussion in this report includes techniques for determination of yield strength, plane-strain fracture toughness, crack opening displacement and hypothetical critical flaw size [9]. This latter value is useful for comparisons which account for

* Registered trademark.

ClibPDF - www.fastio.com

both the fracture toughness and yield strength variations. These discussions are intended to be an introduction to utilization of instrumented impact data.

The DYNATUP System is essentially a three-component system for use with conventional impact testing machines to monitor the dynamic behavior and supply a precision analog output signal of the load-time history of the impacted test piece. The major components of this system are the instrumented tup, Velocometer and Dynamic Response Module. A schematic of a typical DYNATUP System in operation with a standard Charpy impact machine is shown in Figure 2.

The instrumented tup is the load cell and, as the name implies, is securely fixed in the head of the striking portion of the pendulum. This device employs semiconductor strain gages to sense the compression loading of the tup while in contact with the specimen. These gages receive a constant d.c. power supply from the Dynamic Response Module (DRM).

The DRM is operated in the same manner as a conventional oscilloscope plug-in unit. The signal produced by the instrumented tup is passed through the DRM where it is amplified and integrated to produce a second signal. This integrated signal represents the area under the load-time curve, and therefore, is a measure of the energy absorbed at any time during the impact loading of the test piece. The direct load signal and the energy signal are displayed simultaneously on the cathode ray tube (CRT) of a Tektronix oscilloscope.

ClibPDF - www.fastio.com

The other major component of a DYNATUP System is the Velocometer which supplies a controlled light beam and photosensor to insure accurate and reliable triggering of the oscilloscope. In addition, this component is a non-contacting velocity measuring device specifically designed to detect the head velocity of the pendulum. The Velocometer component is composed of the following subassemblies: mainframe, light source, fiber optic holder, and flag assembly. The latter, not clearly shown in Figure 2, is essentially a thin grid which is firmly attached to the head of the pendulum and passes through a light beam in the fiber optic holder before, during, and after the tup is in contact with the test piece. A more detailed description of the functions of the Velocometer is presented in Reference 10.

An oscilloscope can be used to record all three data signals: load, energy and velocity. This CRT recording is photographed and the desired raw data is obtained by making measurements of signal positions on the film. A typical data record for a structural steel specimen is shown in Figure 3.

Temperature Measurement

Test temperatures were obtained by immersion of the specimen in liquid baths (isopentane, alcohol, oil, liquid nitrogen, etc.). The temperatures were measured with calibrated dial-type thermometers (when possible) and thermocouples. The time intervals between the transfer of the specimen and the impact test was kept to a minimum

ClibPDF - www.fastio.com

(never more than 4 seconds) so as not to allow any warming of the specimen. These procedures employed for the temperature baths and transfer time are in accordance with those of ASTM E23 for standard Charpy tests.[8]

After testing, specimens were coated with KRYLON clear coat to protect the fracture surfaces in case later fractography studies are required.

Impact Machine Calibration

Army Materials and Mechanics Research Center calibration specimens were broken at the end of October 1972 to ensure the reliability of the dial energy values. The results from these tests are listed in Table 2. The deviation from the nominal values for this set of specimens is within the allowable range of $\pm$ 1.0 ft-lbs or $\pm$ 5% of the nominal value (whichever is greater) at all energy levels. Since the impact machine and temperature measuring equipment meet the requirements stated in ASTM E23[8], a calibrated system was used for impact testing.

RAW DATA REDUCTION

The initial step for data reduction is to obtain clear photographic records of the signals displayed on the CRT. This must be accompanied by a reliable recording of all pertinent DRM and oscilloscope scale factors. These factors are shown in Figure 3, and a typical table

ClibPDF - www.fastio.com

employed for recording these values is shown in Figure 4. Definitions of the values recorded in each column of this table are as follows:

SPECIMEN CODE	The specific identification is carefully maintained or identification is begun with reference to testing sequence.
TEMPERATURE (°F)	The temperature of the specimen is noted. The designation RT signifies a room temperature of 72 ± 5°F.
DIAL ENERGY (ft-lbs)	The total energy reduction of the pendulum as a result of impact with the test specimen is measured in foot-pounds by a dial gage connected to the pendulum axis.
LOAD SETTING (lbs/div)	The vertical scale factor for the load signal is selected to be in units of pounds per major division of the oscilloscope graticule.
ENERGY SETTING (ft-lbs/div)	The vertical scale factor for the energy signal is selected to be in units of foot-pounds per major division of the oscilloscope graticule.
SWEEP TIME (msec/div)	The scale factor for the horizontal sweep rate of the oscilloscope beam is selected to be in units of milliseconds per major division of the oscilloscope graticule.
COMMENTS	Special remarks regarding test variables or specimen behavior are recorded.

Other important parameters for data reduction are the specimen geometry, dimensions and orientation, see Figure 5. The indicated support span of 1.57 in. is that specified by ASTM Standard E-23.[8] In this figure, d is the specimen deflection for an applied load P.

The data obtained by measurements made on the photograph are defined on the idealized load-deflection record shown in Figure 6. The values usually measured from the load-time signal are P_{GY}, P_M and

ClibPDF - www.fastio.com

P_1. The deflection is obtained by the product of the average tup velocity $\bar{v}$ and the time as measured on the photograph. Deflection values usually measured are d_{GY}, d_{max} and d_1. The subscripts are references to the load values defined in Figure 6. The values obtained from the energy-time record are referenced to the load-deflection curve of Figure 6 and are defined in this figure. The values usually measured from the energy-time signal are W_T, W_I and W_F. The DRM is calibrated so that the integrated signal (energy) represents that for a constant initial impact velocity. However, substantial decreases in pendulum velocity can occur and, therefore, the energy measurements from the photograph should be appropriately corrected as follows:

$$W \text{ (corrected)} = W \text{ (photograph)} \times \bar{v} \quad . \tag{4}$$

The $\bar{v}$ values are clearly functions of the energy absorbed and the total available kinetic energy of the pendulum.[10] The latter value is usually obtained by the relationship $1/2\ mv_o^2$, where m is the effective mass of the pendulum and v_o is the velocity of the tup just prior to contacting the specimen.

The total energy absorbed by the specimen can also be obtained by the usual[8] dial measurements of pendulum swing retardation. The value obtained from the dial is defined as E_T and should clearly be equal to W_T, which is defined in Figure 6.

The specimen dimensions are defined as shown in Figure 7 and discussed below:

ClibPDF - www.fastio.com

$a \equiv$ the total crack or notch depth

$B \equiv$ the thickness

$w \equiv$ the width

$L \equiv$ the support span length (1.57 in. as shown in Figure 5)

A typical table of raw data is shown in Figure 8. In addition to the parameters discussed above, the table includes test temperature and the average static yield strength at that temperature. The table was printed by computer techniques which did not permit use of subscripts. Therefore, the following equivalence of terms between those discussed above and those listed in the table should be noted:

PF is P_M for the case $P_M < P_{GY}$,

PGY is P_{GY},

PM is P_M,

P1 is P_1,

DGY is d_{GY},

DM is d_{max},

D1 is d_1,

WT is W_T,

WI is W_I,

WF is W_F .

Also included in Figure 8 is the parameter ET/area which corresponds to the total energy to break the specimen divided by the cross-sectional area of the specimen over which the process occurred, i.e. B x(w-a).

ClibPDF - www.fastio.com

STRENGTH AND FRACTURE TOUGHNESS CALCULATION

When general yielding occurs, the P_{GY} value can be used to calculate the dynamic yield strength, which is dependent on deflection rates.* The general equation for conversion is

$$\sigma_{yd} = P_{GY} \frac{L}{B\ (w-a)^2\ C} \quad , \tag{5}$$

where the constant C is dependent on the notch flank angle (2β), notch root radius (ρ), and the type of loading (i.e., pure bending or three-point bending). For our purposes of three-point bending, $2\beta = 45°$, and ρ varying between 0 and 0.010", Equation (5) is valid with $C \approx 1.21$. Therefore,

$$\sigma_{yd} = P_{GY} \frac{L}{B\ (w-a)^2\ (1.21)} \tag{6}$$

The derivation and limitations of Equation (6) are discussed in Reference 11.

Fracture toughness is the major interest of most investigations. In these cases, fracture toughness refers to a critical stress intensity parameter, K_c or K_{Ic}, that can be related to structural service performance by a relationship of the form

$$K_c \propto \sigma\sqrt{\pi c} \quad , \tag{7}$$

where σ is the nominal stress in the vicinity of a flaw having a size indicative of the linear dimension c. There is considerable controversy

---

* The importance of clearly identifying specimen strain rates or deflection rates is without question. In this report, the distinction between dynamic and static is assumed to be that of 10^1 to 10^2 and 10^{-4} sec^{-1}, respectively.

ClibPDF - www.fastio.com

regarding the calculation of a meaningful fracture toughness value based on data derived from a specimen which fractures after general yielding. For this reason, five different approaches to the calculation of fracture toughness are employed.

The first is based on linear elastic fracture mechanics:[12]

$$K_{Ic} = \frac{1.5YL\ (P_F)}{Bw^2}\ a^{1/2} \quad , \tag{8}$$

where (for $w = \frac{L}{4}$)

$$Y = 1.93 - 3.07\left(\frac{a}{w}\right) + 14.53\left(\frac{a}{w}\right)^2 - 25.11\left(\frac{a}{w}\right)^3 + 25.8\left(\frac{a}{w}\right)^4$$

and P_F is the applied load at fracture pop-in, when fracture occurs before general yielding, i.e. with fracture loads less than general yield loads ($P_F < P_{GY}$).

The second method employs the assumption of equivalence of critical strain energy release rates, G_c, to the ratio of impact energy to fracture surface area, W/A, where area (A) = B·(w-a). It has been found experimentally for static tests that using twice the area many times results in a better correlation [13]. The relationships used to calculate fracture toughness are:

$$K_c = \left(\frac{G_c \times E}{1 - \nu^2}\right)^{1/2} \quad , \tag{9}$$

or

$$K_c = \left[\frac{W \times E}{B(w-a)\ (1-\nu^2)}\right] \tag{10}$$

where E is the elastic modulus and W is the impact energy (either W_T, W_I, or W_F). A value of 0.3 is assumed for Poisson's ratio ν.

ClibPDF - www.fastio.com

The value most commonly used to calculate G_c or K_c is the total impact energy (W_T). Intuitively, these toughness values should be based either on the energy required to initiate fracture (W_I) or the energy consumed in creating the new surface (W_F). The K_c values determined by these energy values are presented for comparison of the relative contributions of the initiation and propagation processes to the total apparent toughness.

The third method employed for calculation of fracture toughness uses a lower-bound equivalent-energy approach.[14] This method assumes that if a sufficiently large specimen had been employed, fracture would have occurred before general yielding and at an energy corresponding to that measured for the smaller specimen. From this method, values of P* are estimated by extrapolating the linear slope of the elastic region of the load curve until the area (energy) under the linear curve corresponds to the energy measured (see Figure 9). These P* values are then used to calculate K_{Ic} from Equation (8). Both the initiation energy, W_I, and the energy to fast crack propagation, W_F, are used to calculate fracture toughness values (i.e., P^*_I, and P^*_F, or in computer terminology, P*I and P*F).

The fourth method employed for calculation of fracture toughness uses a crack-opening-displacement (COD) approach. The COD approach essentially uses the deflection measurements to calculate the strain at the root of the notch.[15] COD is intended to represent this strain and can be calculated from the following:

ClibPDF - www.fastio.com

$$COD = 0.51\ (w-a)\ d \quad , \tag{11}$$

where d is the appropriate deflection (d_1 or d_{max}). The generally accepted relation of COD to G_c is

$$G_c = COD \times \sigma_{yd} \quad , \tag{12}$$

and K_c is found from combining Equations (13), (15), and (16):

$$K_c = (COD \times \sigma_{yd} \times E)^{1/2} \quad . \tag{13}$$

For impact tests, σ_{yd} in Equation (13) is that determined by Equations (5) and (6). If the specimen breaks before general yielding occurs, either the static yield strength or a σ_{yd} calculated from the fracture load is used depending upon which is the largest. CODM is the computer code for this measurement.

Equation (11) is also used to evaluate COD at d_{max} and at d_1. These values are shown in Figure 10 in the columns identified as DM and D1 under the COD heading.

The fifth and last method uses the maximum load measurement (P_M) to calculate fracture toughness from Equation (8). For fractures occurring before general yielding, the toughness calculated from P_M is the same as that calculated from P_F. The computer designation for this calculation is PMAX.

The J-integral is another good method for determining the toughness of elastic-plastic materials (e.g., bridge steels). However, the valid relationship for utilization of the J concept are currently more fully developed for the compact tension specimens. In addition, preliminary

ClibPDF - www.fastio.com

work by several investigators have shown the equivalent-energy (third method above) and the J-integral approach yield very nearly the same results for the Charpy type specimen.

A cursory examination of these parameters can be performed in the form of an evaluation of a parameter identified as the "critical crack length".[9] This parameter represents the critical size of a hypothetical flaw subjected to a nominal stress indicative of the yield strength of the alloy at a temperature corresponding to the impact specimen test temperature. In this context "critical" reflects the lowest fracture toughness at which the flaw will propagate or grow in size. This flaw is assumed to be a surface flaw in a plate of unit thickness. The flaw is assumed to have the fixed geometrical shape shown in Figure 11. For this arbitrary evaluation of critical crack depth, σ is assumed to be the dynamic yield stress which is determined by Equations (5) or (6), or the largest of the static yield stress or a σ_{yd} calculated using P_F if the specimen does not yield; the fracture toughness is the lowest non-zero value of the eight calculated values described above. The critical crack depth, c, is calculated from the following equation:

$$c = \frac{K_{Ic}^{2}}{1.21\pi\ \sigma_{yd}^{2}}\ \phi \quad , \tag{14}$$

where ϕ is a flaw and structure geometry parameter, and for the case shown in Figure 11, $\phi = 1.24$.

ClibPDF - www.fastio.com

A typical computer output of the above toughness and strength calculations is shown in Figure 10. Again, the computer does not type subscripts, so the subscript letters are on the same line as the primary letters, as described earlier.

RESULTS

Precracked Charpy Results and Calculations

Each DYNATUP test of the fatigue precracked specimens is represented by a cathode ray tube (CRT) display of the load and energy versus time records, see Figure 3.* The CRT settings, test temperature and pendulum dial values for total absorbed energy for each specimen are listed in the work sheets of Tables 3-9. Each of these tables (work sheets) represent the results obtained for a specific plate identification. The raw data derived from these CRT records are listed in Tables 10 through 16 according to specific plate identifications. The values in these tables are those defined and discussed in the Raw Data Reduction section of this report.

The values listed in the last column of Tables 10 through 16 are the area normalized values of total absorbed energy as indicated by the pendulum dial (i.e., W/A). These W/A values are graphically shown as functions of the test temperature in Figures 12 through 18. The Nil Ductility Transition Temperature (NDTT) for each plate was determined by an empirical procedure suggested by Hartbower[16]. This technique is illustrated in these figures, where NDTT is assumed to

*See Appendix for compilation of load-time traces

ClibPDF - www.fastio.com

correspond to the temperature at which the two linear extrapolations of the W/A versus temperature values intersect. This technique derives NDTT values which are more direct representatives of the actual material response than are those obtained by a foot-pound fix method.

The results of the toughness calculations described in the Strength and Fracture Toughness Calculation section of this report are listed in Tables 17 through 23. For this investigation the major fracture toughness (K_{Id}) parameter is that determined from P_F (the fracture load when fracture occurs before general yielding). If general yielding does occur, the P*I fracture toughness determination from equivalent energy is used along with the P_{max} toughness calculation. The equivalent energy approach gives a lower bound for toughness and is always greater than the P_{max} toughness determination. Figures 19-25 show dynamic fracture toughness as a function of temperature for each plate. The P_F linear elastic data points are shown as black circles. The equivalent energy date points (P*I) are shown as a circle with an X inside. Along with the equivalent energy data for post-yield fracture, the P_{max} fracture toughness data are plotted as circles. Note that the Plate M(K_{Id}) data (Figure 22) is plotted at a different scale than the other plate data.

Charpy V-notch Results and Calculations

Each DYNATUP test of the standard Charpy V-notch specimens is also represented by a CRT display of the load and energy records. The work sheets for these tests are shown in Tables 6 through 8 along with the

ClibPDF - www.fastio.com

values for the fatigue precracked specimen tests. The standard specimens are identified by the C_V in the Comments column of these tables. The raw data derived from these CRT records are listed in Tables 24 through 26.

The normalized energy values W/A for these standard specimen tests are compared to the similar values obtained from the fatigue precracked specimens in Figures 26 through 28. The general difference between the energy results for these two types of specimens is the decrease in the fracture initiation energy as a result of the fatigue precracking. The partitioning of fracture energy between initiation (W_I) and propagation (W_T-W_I) for these standard Charpy V-notch specimen tests are shown in Figures 29 through 31.

One of the useful techniques for examining instrumented impact data for trends relatable to metallurgical properties is the load-temperature diagram. The results of these graphical representations of fracture behavior for the standard Charpy V-notch specimens are shown in Figures 32 through 34. The transition from $P_F < P_{GY}$ to $P_{max} > P_{GY}$ and the general shape of the P_{max} curve are the major parameters of interest in these figures.

The dynamic yield strength (σ_{yd}) derived from the P_{GY} values (Tables 27-29) are compared to the general trends of the static yield strength (σ_{ys}) in Figures 35 through 37. These later values were supplied by the California Highways Department. The temperature dependence of σ_{ys} and σ_{yd} and the elevation in σ_{yd} from σ_{ys} by strain rate are of major interest in determining metallurgical influences on strength and toughness properties of these materials.

ClibPDF - www.fastio.com

DISCUSSION

Seven different heats of A514 and A517 steel in grades F and H were evaluated by the DYNATUP testing of sharp and blunt notch Charpy specimens. The primary objective of this study was to determine the dynamic plane strain fracture toughness (K_{Id}) of these materials. The specimens with sharp notches, produced by fatigue precracking, were used for the K_{Id} and NDTT evaluations. Also included in this study were analysis techniques for evaluation of transition temperature and metallurgical properties. These other toughness considerations utilized both the blunt notch data from the standard Charpy V-notch specimens and the sharp notch data.

Dynamic Fracture Toughness

The loading rate employed for this study resulted in stress intensity rates ($\dot{K}$) of approximately 10^8 to 10^9 psi-$\sqrt{in}$ per second.

The K_{Id} results for the seven heats of steel are presented for direct comparison in Figure 38. This figure illustrates the importance of clearly stating the temperature range of interest when making comparisons of the K_{Id} toughness. At temperatures less than -160F, it is doubtful that any appreciable difference in K_{Id} can be found for these materials. At temperature greater than -160F, Plate M clearly has superior K_{Id} toughness and Plate Q is the least tough of the several heats investigated.

The general temperature range for which one of these seven heats

ClibPDF - www.fastio.com

of steel has improved toughness can be viewed as that where the K_{Id} curve begins to rise. That is, for Plate M the improved toughness begins at approximately -120F. For Plate L the improvement begins near -20F.

The rate at which the toughness improves with increased temperature is also very important. It should be noted that there is not a unique shape for the K_{Id}-temperature curve. That is, a translation of the Plate M curve along the temperature scale will not suffice for indicating the K_{Id} properties of any of the other plates.

The Nil Ductility Transition Temperature (NDTT) is the parameter which is sometimes incorrectly used for these K_{Id} curve translations. The NDTT is defined by the drop weight test described in ASTM Method E208[17]. However, this parameter can be estimated from the area normalized energy (W/A) curves for precracked Charpy specimens. The W/A curves for the seven heats of steel are presented in Figures 12-18. The NDTT is determined by the intersection of the two straight lines which are an apparent fit to the W/A data [16]. The NDTT values obtained by this technique are listed in Table 30. The W/A data obtained for Plate Q did not exhibit a distinct temperature transition and therefore, the NDTT could not be estimated by this technique.

For many failure prevention programs the NDTT is exclusively employed as a design parameter. That is, material properties are specified so that the structure will not encounter appreciable service loads at temperatures less than the NDTT. This type of design is identified as the transition temperature approach. The dynamic plane strain frac-

ClibPDF - www.fastio.com

ture toughness (K_{Id}) is an approach based on considerations for service stress and probable flaw size. With nearly all engineering structures the existence of undetected flaws must be acknowledged. As would be expected, the K_{Id} and NDTT approaches are related. That is, the test for measuring NDTT utilizes a sharp crack and dynamic loading as do the tests for measuring K_{Id}. Recent experience[7] with A533 steel has shown that at the NDTT the ratio of $K_{Id}/\sigma_{yd} \approx 0.4$. The similar values for Plates L and M of this study are 0.353 and 0.379, respectively. This agreement of the ratio of K_{Id}/σ_{yd} at NDTT with previous work on A533 implies that the NDTT values obtained by the W/A technique are reasonable estimates.

The values of K_{Id} at NDTT for the six plates of A517 and A514 steels are also shown in Table 31. These values can be used to normalize the K_{Id}-temperature curves for the variations in transition temperature (NDTT) behavior. This technique is identified as the K_{IR} approach, where R indicates the NDTT reference temperature. This approach was suggested by the Pressure Vessel Research Council and is based on their work with A533 and A508 steels [7,18]. The K_{IR} curves for the six plates* of this study are compared to the general A533 and A508 design curve in Figure 39. As shown in this figure, the K_{IR} approach does reduce the variations in apparent K_{Id} behavior shown in Figure 38. In Figure 39, the K_{IR} curves for some of the plates fall below the A533 design curve in the temperature range above NDTT. For temperatures below NDTT the

* Plate Q is not included because an NDTT could not be estimated.

ClibPDF - www.fastio.com

K_{IR} curves for the six heats of A517 and A514 are higher than that for the A533 design curve. Therefore, it is clear that the K_{IR} approach does not permit use of a single curve (e.g., the A533 K_{IR} curve) to represent the K_{Id} behavior of different heats of the same steel.

Although the K_{IR} approach is useful for evaluation of the relative fracture toughness of a steel, the role of the NDTT in fracture safe design must not be overlooked. The service temperature range of the structure must be included by reference to the NDTT. It is also important not to overlook relative K_{Id} properties when utilizing the NDTT temperature for fracture safe design.

Other Toughness Considerations

A further comparison of Plates L, M, and Q is possible based on the results of the standard Charpy V-notch specimens. The load data from Figures 32, 34, and 36 are represented in Figure 40 for convenience. The Plate M data described very well the "ideal" shape for a Charpy V-notch load-temperature diagram. The fracture load curve rises and intersects the general yield load curve at a point defined as T_D; the maximum load curve then rises quickly above T_D and levels off at a temperature near NDTT. The Plate L data is somewhat similar to the Plate M data except that T_D is at a slightly higher temperature, and the shape after T_D is quite different. In general, this shape difference accounts for the higher NDTT for Plate L. There is also a slight difference in the temperature dependence of P_{GY} (or σ_{yd}) between Plates L and M; the Plate L material is slightly more temperature dependent. The Plate Q

ClibPDF - www.fastio.com

data is shifted drastically to higher temperatures and the P_F and P_{max} curves are very flat. The P_{GY} values fall almost exactly on an extrapolated line from the Plates L and M data; therefore, test temperature has approximately the same effect on the yield strength of all three plates.

The reason for the large temperature shift of T_D for Plate Q steel appears to be due to the difference in the microscopic cleavage fracture strength (σ_f^*) between the Plate Q steel and the Plates L and M steel. An estimate of σ_f^* can be obtained[19] by taking the load at T_D and multiplying by 85.8, i.e., σ_f^* (psi) $\approx$ 85.8 x P_{T_D} (lbs.). σ_f^* for Plates L and M is essentially the same and is equal to $\sim$ 420 ksi. σ_f^* determined for Plate Q is about 15% less - $\sigma_f^* \approx$ 360 ksi. Changes in σ_f are largely due to changes in the ratio (γ_m/k_y)[20], where γ_m is the work done near the tip of a cleavage microcrack that is propagating within a grain, and k_y is the grain-size dependence of the yield strength. When the ratio of γ_m/k_y increases, the amount of homogeneous plastic deformation increases and σ_f^* increases (thus, a lower T_D).

The dynamic yield strength is also shown in Figure 40 since the P_{GY} curves are shown. It is only a matter of scale changes as shown by the σ_{yd} scale on the right. Again, there are no large differences in the dynamic yield strengths between the three steels.

Figures 26, 28, and 30 show the Charpy V-notch total energies as compared to the precracked Charpy total energies. The values were normalized to W/A values for more direct comparison. The data from Plates L and M are very similar except for the temperature shift. The

ClibPDF - www.fastio.com

Plate Q data is unusual, because there appear to be no transitions even in the Charpy V-notch energy. A look at the various energy components for the Charpy V-notch data (Figures 27, 29, and 31) reveals a leveling off of the initiation energy for Plates L and M. This leveling off occurs near the NDTT. The Plate Q data shows no leveling off or transitions of any kind.

The unusual behavior of the Plate Q steel is further exemplified by the two precracked tests performed at +120°F. Both of these tests resulted in a series of "pop-in" drops which makes the determination of the fracture toughness quite difficult (Figure 41). In these cases it would be very interesting to perform fractography studies with the broken specimens. It is interesting to note that T_D for Plate Q is quite close to +120°F; near T_D there is always scatter in the data since the material is "trying to decide" whether to break in a linear elastic manner or whether to yield before breaking.

Significance of Dynamic Fracture Toughness

The choice of whether to base design on static K_{Ic} or dynamic K_{Id} plane strain fracture toughness is difficult for many material applications. K_{Id} is the obvious choice for gun barrels and other structures subject to dynamic loads. For structures which appear to be statically loaded, the K_{Ic} approach may not be the most appropriate. That is, the K_{Id} properties generally determine whether a catastrophic fracture is involved. The K_{Ic} properties may reveal limits for crack initiation, but the ability to arrest or stop the crack extension may be represented by the

ClibPDF - www.fastio.com

K_{Id} properties.

The rates of structural loading are not necessarily related to the materials properties which determine a fracture safe design. The sudden separation of a few metal grains under relatively static loads means that dynamic loading rates apply thereafter in controlling fracture extension. K_{Id} always controls fracture extension, irrespective of initiation conditions [21].

ClibPDF - www.fastio.com

CONCLUSIONS

1. Plate Q steel is inferior to the other heats of steel in terms of dynamic fracture toughness.

2. Plate M steel is quite superior to any of the other heats of steel in terms of dynamic fracture toughness.

3. The dynamic yield strength of Plates L, M, and Q are very similar and significantly higher than the static.

4. There are no apparent fracture transitions in the Plate Q steel and its difference from the other steels appears to be due to a lower microscopic cleavage fracture strength.

5. The significance of the K_{Id} values determined in this program should be viewed with respect to the fact that K_{Id} always controls fracture extension, irrespective of initiation conditions.

6. The K_{IR} concept is useful for evaluation of variations in K_{Id} properties, however, the specific NDTT values must also be considered.

ClibPDF - www.fastio.com

REFERENCES

1. Wullaert, R. A., "Applications of the Instrumented Charpy Impact Test," Impact Testing of Metals, ASTM STP 466, 1970, pp. 148-164.

2. Wullaert, R. A., D. R. Ireland, and A. S. Tetelman, "Prediction of Variation in Fracture Toughness K_{Ic} from Small Specimen Tests," presented at Practical Applications of Fracture Mechanics to Pressure Vessel Technology Conference, London, England, May 1971.

3. Tetelman, A. S., D. R. Ireland, R. A. Wullaert, "Prediction of Radiation-Induced Changes in Fracture Toughness K_{Ic} from Small Specimens Tests," presented at the First International Conference on Structural Mechanics in Reactor Technology, Berlin, West Germany, September 1971.

4. Toland, R. A., "Failure Modes in Impact-Loaded Composite Materials," presented at Failure Modes in Composites Symposium, AIME Spring Meeting, Boston, Massachusetts, May 1972.

5. Hoover, W. R., and R. E. Allred, "The Dynamic Fracture Behavior of Borsic-Al Composites," Sandia Laboratories, Albuquerque, New Mexico, SC-DC-721080, June 1972.

6. Wullaert, R. A., D. R. Ireland, and A. S. Tetelman, "The Use of Pre-cracked Charpy Specimen in Fracture Toughness Testing," presented at the Fracture Prevention and Control Symposium, Westec 1972 Meeting, Los Angeles, California, March 1972.

7. Server, W. L. and A. S. Tetelman, "The Use of Pre-cracked Charpy Specimens to Determine Dynamic Fracture Toughness," Engineering Fracture Mechanics, Vol. 4, 1972, pp. 367-375.

8. "Notched Bar Impact Testing of Metallic Materials," ASTM Standards E23-72, 1972 Annual Book of ASTM Standards, ASTM, Philadelphia, Pennsylvania, 1972, pp. 276-292.

9. Ireland, D. R., "Dynamic Properties of Superalloys at Elevated Temperatures," Research Directorate, Weapons Laboratory at Rock Island, Technical Report RE-TR-71-75, February 1972.

10. Ireland, D. R., and W. L. Server, "Utilization of the Dynatup Velocomter", Dynatup Technical Report TR 72-16, Effects Technology, Inc., Santa Barbara, California, 1972.

11. Server, W. L. and D. R. Ireland, "General Yielding of Notched Three-Point Bend Specimens," Dynatup Technical Report TR 72-19, Effects Technology, Inc., Santa Barbara, California, 1972.

ClibPDF - www.fastio.com

12. Brown, W. F., Jr., and J. E. Srawley, Plane Strain Crack Toughness Testing of High Strength Metallic Materials, ASTM STP 410, 1966.

13. Ronald, T. M. F., J. A. Hall, and C. M. Pierce, "Usefulness of Precracked Charpy Specimens for Fracture Toughness Screening Tests of Titanium Alloys", Met Trans, 3, (4) 813 (April, 1972).

14. Witt, F. J., "Equivalent Energy Procedures for Predicting Gross Plastic Fracture", USAEC Report ORNL-TM-3172, Oak Ridge National Laboratory.

15. Wells, A. A., Symposium on Crack Propagation, Paper No. B4, Cranfield, England, 1961.

16. Orner, G. M., and C. E. Hartbower, "Transition-Temperature Correlations in Constructional Alloy Steels", The Welding Journal, Vol. 40 (9), P. 459-S, October 1961.

17. "Standard Method for Conducting Drop Weight Test to Determine Nil-Ductility Transition Temperature of Ferritic Steels", ASTM Standards E208-69, 1972 Annual Book of ASTM Standards, ASTM, Philadelphia, Pennsylvania, 1972, pp 594-613.

18. "PVRC Recommendations on Toughness Requirements for Ferritic Materials", Welding Research Council Bulletin No. 175, August 1972.

19. Server, W. L., "Dynamic Fracture Toughness Determined from Instrumented Pre-Cracked Charpy Tests", Materials Department, University of California, Los Angeles, Technical Report No. 8 (UCLA-ENG-7267), August, 1972.

20. Wullaert, R. A., "The Effect of Nickel on the Microstructure and Mechanical Properties of Ferritic Steels", Department of Materials Science, Stanford University, Ph.D. Thesis, June 1969.

21. Pellini, W. S., "Criteria for Fracture Control Plans", Naval Research Laboratory, Report 7406, May 11, 1972.

ClibPDF - www.fastio.com

TABLE 1. TEST MATRIX FOR PRECRACKED CHARPY AND STANDARD CHARPY V-NOTCH SPECIMENS

Plate	Material	Code Designation	Specimen Type	Quantity	Temperature Range
A	A517-F	A	Precracked Charpy	10	-120°F to +160°F
AL	A517-H	AL	Precracked Charpy	10	-80°F to +200°F
L	A517-F	L	Precracked Charpy	10	-160°F to +80°F
L	A517-F	L	Charpy V-Notch	11	Selected from Precracked Results
M	A514-F	M	Precracked Charpy	10	-320°F to 0°F
M	A514-F	M	Charpy V-Notch	9	Selected from Precracked Results
Q	A517-H	3B	Precracked Charpy	10	-40°F to +200°F
Q	A517-H	1B,2B,3B	Charpy V-Notch	10	Selected from Precracked Charpy
R	A514-H	R	Precracked Charpy	12	-160°F to +120°F
Z	A517-H	Z	Precracked Charpy	12	-160°F to +160°F

ClibPDF - www.fastio.com

TABLE 2. AMMRC IMPACT MACHINE CALIBRATION TESTS (AT -40°F)
OCTOBER 1972

AMMRC Specimen Series	AMMRC Nominal Energy Value (ft-lbs)	Average Energy Value from 5 Tests (ft-lbs)
J10	12.8	13.3
K10	43.2	43.8
M10	71.1	74.1

ClibPDF - www.fastio.com

DYNATUP

CUSTOMER CALIFORNIA DEPT. OF HIGHWAYS (PLATE A) DATE FEBRUARY 1973

SPECIMEN CODE	TEMP (°F)	DIAL ENERGY (ft-lbs)	LOAD SETTING (lbs/div)	ENERGY SETTING (ft-lbs/div)	SWEEP TIME (msec/div)	COMMENTS
A15L	-120	1.0	500	1	.5	
A14L	-80	1.2	500	1	.2	
A11L	-40	1.5	500	1	.2	
A10L	0	2.5	500	2	.5	
A13L	40	4.1	500	2	.2	
A12L	72	6.5	500	2	.5	
A16L	120	14.0	500	5	.5	not seated properly
A17L	0	3.0	500	1	.2	
A18L	40	5.5	500	1	.2	
A19L	160	18.5	500	5	.2	

TABLE 3. WORK SHEET FOR PLATE A

ClibPDF - www.fastio.com

DYNATUP

CUSTOMER California Dept. of Highways (Plate AL) DATE February 1973

SPECIMEN CODE	TEMP (°F)	DIAL ENERGY (ft-lbs)	LOAD SETTING (lbs/div)	ENERGY SETTING (ft-lbs/div)	SWEEP TIME (msec/div)	COMMENTS
AL5L	-40	4.3	500	1	.2	
AL7L	0	6.2	500	2	.2	
AL9L	40	9.0	500	2	.2	
AL8L	72	11.5	500	2	.5	
AL11L	120	17.0	500	5	.5	
AL10L	160	20.3	500	5	.5	
AL1L	-80	2.9	500	1	.1	
AL2L	40	9.2	500	2	.2	
AL3L	72	13.0	500	2	.2	
AL4L	200	28.5	1000	10	.5	

TABLE 4. WORK SHEET FOR PLATE AL

ClibPDF - www.fastio.com

CR-73-142

DYNAMIC FRACTURE TOUGHNESS OF BRIDGE STEELS

FINAL REPORT

to

MATERIALS AND RESEARCH ENGINEERING DEPARTMENT
CALIFORNIA DIVISION OF HIGHWAYS
5900 Folsom Boulevard
Sacramento, California 95819

by

W. L. Server
D. R. Ireland
R. A. Wullaert

March 10, 1973

EFFECTS TECHNOLOGY, INC.
A SUBSIDIARY OF GENERAL RESEARCH CORPORATION
5383 HOLLISTER AVE. • P.O. BOX 30400
SANTA BARBARA, CALIFORNIA 93105
PHONE (805) 967-0116

Contract No. 19-3121

ClibPDF - www.fastio.com

DYNATUP

CUSTOMER CALIFORNIA DEPT. OF HIGHWAYS (PLATE L) DATE FEBRUARY 1973

SPECIMEN CODE	TEMP (°F)	DIAL ENERGY (ft-lbs)	LOAD SETTING (lbs/div)	ENERGY SETTING (ft-lbs/div)	SWEEP TIME (msec/div)	COMMENTS
L22L	-160	1.8	500	1	.2	
L24L	-120	2.0	500	1	.2	
L23L	-80	4.5	500	2	.2	
L19L	-40	7.0	1000	5	.2	
L18L	0	14.0	1000	5	.5	
L20L	40	22.2	1000	10	.2	
L21L	72	37.2	1000	10	.5	
L3L	-200	4.0	1000	1	.2	Cv
L8	-160	7.0	1000	2	.2	"
L2L	-140	6.0	1000	2	.2	"
L9	-120	12.0	1000	2	.2	"
L10L	-80	12.0	1000	2	.2	" - missed energy
L11L	-40	13.5	1000	10	.5	"
L7	-20	51.5	1000	10	.5	"
L6L	0	61.5	1000	20	.5	"
L1L	20	68.5	1000	20	.5	"
L4L	40	78.6	1000	20	.5	"
L5L	72	83.5	1000	20	.5	"
L12L	-120	3.2	500	1	.1	
L13L	-20	13.2	1000	2	.2	
L15L	40	35.0	1000	5	.2	energy off scale

TABLE 5. WORK SHEET FOR PLATE L

ClibPDF - www.fastio.com

DYNATUP

CUSTOMER CALIFORNIA DEPT. OF HIGHWAYS (PLATE M) DATE FEBRUARY 1973

SPECIMEN CODE	TEMP (°F)	DIAL ENERGY (ft-lbs)	LOAD SETTING (lbs/div)	ENERGY SETTING (ft-lbs/div)	SWEEP TIME (msec/div)	COMMENTS
M6L	-240	2.0	500	1	.1	
M5L	-200	2.2	500	1	.1	
M4L	-160	4.0	500	2	.2	
M3L	-120	6.0	1000	5	.2	
M7L	-80	14.0	1000	2	.5	energy off scale
M1L	-40	26.5	1000	10	.5	
M2L	0	46.5	1000	10	.5	
M15L	-240	5.1	1000	2	.1	Cv
M16L	-200	7.0	1000	2	.2	"
M18L	-160	8.2	1000	10	.2	"
M19L	-140	17.5	1000	10	.5	"
M21L	-120	42.5	1000	5	.5	" - energy off scale
M14L	-80	34.5	1000	10	.5	"
M13L	-40	55.8	1000	10	.5	"
M17L	0	40.0	1000	20	.5	"
M20L	40	69.9	1000	20	.5	"
M8L	-320	1.2	500	1	.1	
M9L	-120	8.0	1000	2	.2	missed energy
M10L	-80	18.8	1000	5	.2	

TABLE 6. WORK SHEET FOR PLATE M

ClibPDF - www.fastio.com

DYNATUP

CUSTOMER CALIFORNIA DEPT. OF HIGHWAYS (PLATE Q) DATE FEBRUARY 1973

SPECIMEN CODE	TEMP (°F)	DIAL ENERGY (ft-lbs)	LOAD SETTING (lbs/div)	ENERGY SETTING (ft-lbs/div)	SWEEP TIME (msec/div)	COMMENTS
3B12	-40	3.2	500	1	.2	
3B14	0	4.0	500	1	.2	
3B11	40	5.5	500	2	.2	
3B15	72	6.0	1000	2	.2	
3B13	120	8.2	1000	2	.2	
3B10	160	10.5	1000	2	.2	
3B9	200	12.1	1000	5	.2	
3B19	-40	4.0	1000	1	.2	Cv
2B17	0	6.0	500	2	.2	" load off scale, but extrapolatable
2B16	40	7.0	1000	2	.2	"
1B13	72	11.0	1000	2	.2	"
1B12	100	12.0	1000	2	.2	"
1B16	120	13.0	1000	2	.2	" - energy off scale
1B14	140	14.5	1000	2	.2	" - "
2B13	160	16.9	1000	5	.2	"
2B15	200	18.5	1000	5	.2	"
1B15	240	22.0	1000	5	.2	"
3B16	0	4.7	500	1	.2	
3B17	60	7.0	500	1	.2	energy off scale
3B18	120	8.0	1000	2	.2	

TABLE 7. WORK SHEET FOR PLATE Q

ClibPDF - www.fastio.com

DYNATUP

CUSTOMER California Dept. of Highways (Plate R) DATE February 1973

SPECIMEN CODE	TEMP (°F)	DIAL ENERGY (ft-lbs)	LOAD SETTING (lbs/div)	ENERGY SETTING (ft-lbs/div)	SWEEP TIME (msec/div)	COMMENTS
R6L	-160	1.3	500	1	.1	
R7L	-120	1.5	500	1	.2	
R5L	-80	3.0	500	1	.2	
R1L	-40	5.0	500	2	.2	
R2L	0	7.5	500	2	.2	
R4L	40	13.1	500	5	.5	
R3L	72	16.0	500	5	.5	
R8L	-120	2.4	500	1	.1	
R9L	-80	4.0	500	1	.1	
R10L	-40	4.9	500	2	.2	
R11L	72	20.0	500	5	.2	
R12L	120	23.4	500	5	.2	

FIGURE 8. WORK SHEET FOR PLATE R

ClibPDF - www.fastio.com

DYNATUP

CUSTOMER CALIFORNIA DEPT. OF HIGHWAYS (PLATE Z) DATE FEBRUARY 1973

SPECIMEN CODE	TEMP (°F)	DIAL ENERGY (ft-lbs)	LOAD SETTING (lbs/div)	ENERGY SETTING (ft-lbs/div)	SWEEP TIME (msec/div)	COMMENTS
Z9L	-120	1.9	500	1	.2	
Z10L	-80	3.5	500	1	.2	
Z7L	-40	6.0	500	2	.2	
Z6L	0	8.7	500	2	.2	
Z12L	40	12.2	500	5	.5	
Z11L	72	16.8	500	5	.5	
Z8L	120	26.0	500	10	.5	
Z1L	-160	1.8	500	1	.1	
Z2L	-120	2.8	500	1	.1	
Z3L	-40	7.0	500	2	.2	
Z4L	0	11.7	500	2	.2	
Z5L	160	34.1	1000	10	.5	

TABLE 9. WORK SHEET FOR PLATE Z

ClibPDF - www.fastio.com

TABLE 10. RAW DATA FOR INSTRUMENTED IMPACT EVALUATION OF PRECRACKED CHARPY V-NOTCH SPECIMENS OF PLATE A (A517-F) PROVIDED BY CALIFORNIA DIVISION OF HIGHWAYS - JANUARY 1973

SPECIMEN CODE	TEST TEMPERATURE F	STATIC YIELD STRESS KSI	DIAL IMPACT ENERGY FT-LB	LOAD, LB				DEFLECTION, IN			INTEGRATOR ENERGY FT-LB			CRACK DEPTH IN	ET/AREA LB/IN
				PF	PGY	PM	P1	DGY	DM	D1	WT	WI	WF		
A15L	-120	116.0	1.0	1455	0	1455	1455	0.000	.012	.012	1.5	.6	.6	.121	112
A14L	-80	112.6	1.2	1440	0	1440	1440	0.000	.011	.011	1.6	.6	.6	.122	134
A11L	-40	110.9	1.5	1530	0	1530	1530	0.000	.011	.011	1.7	.7	.7	.125	170
A10L	0	109.1	2.5	1785	0	1785	1785	0.000	.012	.012	1.8	.8	.8	.136	295
A17L	0	109.1	3.0	1410	0	1410	1410	0.000	.013	.013	2.1	.9	.9	.117	330
A13L	40	107.3	4.1	1815	0	1815	1815	0.000	.012	.012	4.1	.8	.8	.135	482
A18L	40	107.3	5.5	1665	0	1665	1665	0.000	.012	.012	5.8	.8	.8	.111	592
A12L	72	105.9	6.5	2025	0	2025	2025	0.000	.012	.012	7.0	.8	.8	.137	770
A16L	120	103.7	14.0	2430	0	2430	2430	0.000	.036	.036	14.8	3.0	3.0	.121	1562
A19L	160	101.8	18.5	3015	0	3015	3015	0.000	.026	.026	19.7	4.1	4.1	.117	2034

ClibPDF - www.fastio.com

TABLE 11. RAW DATA FOR INSTRUMENTED IMPACT EVALUATION OF PRECRACKED CHARPY V-NOTCH SPECIMENS OF PLATE AL (A517-H) PROVIDED BY CALIFORNIA DIVISION OF HIGHWAYS - JANUARY 1973

SPECIMEN CODE	TEST TEMPERATURE F	STATIC YIELD STRESS KSI	DIAL IMPACT ENERGY FT-LB	LOAD, LB				DEFLECTION, IN			INTEGRATOR ENERGY FT-LB			CRACK DEPTH IN	ET/AREA LB/IN
				PF	PGY	PM	P1	DGY	DM	D1	WT	WI	WF		
AL1L	-80	108.0	2.9	1695	0	1695	1695	0.000	.012	.012	2.4	.7	.7	.101	301
AL5L	-40	106.8	4.3	2025	0	2025	2025	0.000	.011	.011	4.2	.8	.8	.118	475
AL7L	0	105.6	6.2	1935	0	1935	1935	0.000	.013	.013	6.3	1.2	1.2	.128	710
AL9L	40	104.3	9.0	2325	0	2325	2325	0.000	.013	.013	9.2	1.4	1.4	.124	1015
AL2L	40	104.3	9.2	1980	0	1980	1980	0.000	.016	.016	9.5	1.7	1.7	.109	983
AL8L	72	103.4	11.5	2250	0	2250	2250	0.000	.018	.018	12.4	1.7	1.7	.133	1342
AL3L	72	103.4	13.0	2355	0	2355	2355	0.000	.018	.018	14.1	1.7	1.7	.110	1394
AL11L	120	101.8	17.0	2580	0	2580	2580	0.000	.024	.024	17.5	2.8	2.8	.121	1897
AL10L	160	100.4	20.3	2655	0	2655	2655	0.000	.024	.024	21.4	2.9	2.9	.132	2360
AL4L	200	99.0	28.5	0	2790	3000	3000	.029	.041	.041	27.6	6.4	6.4	.120	3168

ClibPDF - www.fastio.com

TABLE 12. RAW DATA FOR INSTRUMENTED IMPACT EVALUATION OF PRECRACKED CHARPY V-NOTCH SPECIMENS OF PLATE L (A517-F) PROVIDED BY CALIFORNIA DIVISION OF HIGHWAYS - JANUARY 1973

SPECIMEN CODE	TEST TEMPERATURE F	STATIC YIELD STRESS KSI	DIAL IMPACT ENERGY FT-LB	LOAD, LB				DEFLECTION, IN			INTEGRATOR ENERGY FT-LB			CRACK DEPTH IN	ET/AREA LB/IN
				PF	PGY	PM	PI	DGY	DM	DI	WT	WI	WF		
L22L	-160	123.6	1.8	1650	0	1650	1650	0.000	.012	.012	2.0	.7	.7	.129	207
L24L	-120	119.7	2.0	1830	0	1830	1830	0.000	.011	.011	1.9	.8	.8	.138	238
L12L	-120	119.7	3.2	1830	0	1830	1830	0.000	.011	.011	2.6	.8	.8	.098	329
L23L	-80	115.8	4.5	2100	0	2100	2100	0.000	.012	.012	4.5	1.2	1.2	.109	481
L19L	-40	113.2	7.0	2280	0	2280	2280	0.000	.011	.011	7.1	1.0	1.0	.113	759
L13L	-20	112.2	13.2	2400	0	2400	2400	0.000	.019	.019	12.1	1.8	1.8	.100	1367
L18L	0	111.3	14.0	2490	0	2490	2490	0.000	.018	.018	12.9	2.5	2.5	.118	1545
L20L	40	110.0	22.2	3420	0	3420	3420	0.000	.026	.026	22.0	4.4	4.4	.125	2514
L15L	40	110.0	35.0	3300	0	3300	3300	0.000	.023	.023	0.0	3.6	3.6	.121	3905
L21L	72	109.8	37.2	0	3480	3540	3540	.029	.032	.032	37.4	5.8	5.8	.105	3920

ClibPDF - www.fastio.com

TABLE 13. RAW DATA FOR INSTRUMENTED IMPACT EVALUATION OF PRECRACKED CHARPY V-NOTCH SPECIMENS OF PLATE M (A514-F) PROVIDED BY CALIFORNIA DIVISION OF HIGHWAYS - JANUARY 1973

SPECIMEN CODE	TEST TEMPERATURE F	STATIC YIELD STRESS KSI	DIAL IMPACT ENERGY FT-LB	LOAD, LB				DEFLECTION, IN			INTEGRATOR ENERGY FT-LB			CRACK DEPTH IN	ET/AREA LB/IN
				PF	PGY	PM	PI	DGY	DM	DI	WT	WI	WF		
M8L	-320	176.2	1.2	1305	0	1305	1305	0.000	.012	.012	1.6	.6	.6	.115	131
M6L	-240	142.8	2.0	1770	0	1770	1770	0.000	.011	.011	2.1	.7	.7	.123	225
M5L	-200	134.3	2.2	1770	0	1770	1770	0.000	.012	.012	2.3	.8	.8	.131	255
M4L	-160	129.0	4.0	1770	0	1770	1770	0.000	.013	.013	3.3	1.0	1.0	.132	465
M9L	-120	125.2	8.0	1800	0	1800	1800	0.000	.012	.012	0.0	0.0	0.0	.129	919
M3L	-120	125.2	6.0	2790	0	2790	2790	0.000	.016	.016	6.4	1.8	1.8	.125	679
M7L	-80	122.5	14.0	2730	0	2730	2730	0.000	.018	.018	0.0	2.4	2.4	.115	1528
M10L	-80	122.5	18.8	3120	0	3120	3120	0.000	.019	.019	19.1	2.4	2.4	.117	2067
M1L	-40	120.5	26.5	0	3870	3960	3960	.024	.038	.038	27.1	7.3	7.3	.127	3023
M2L	0	119.0	46.5	0	4080	4320	0	.026	.040	0.000	46.1	8.5	0.0	.110	4987

ClibPDF - www.fastio.com

TABLE 14. RAW DATA FOR INSTRUMENTED IMPACT EVALUATION
OF PRECRACKED CHARPY V-NOTCH SPECIMENS
OF PLATE Q (A517-H)
PROVIDED BY
CALIFORNIA DIVISION OF HIGHWAYS - JANUARY 1973

SPECIMEN CODE	TEST TEMPERATURE F	STATIC YIELD STRESS KSI	DIAL IMPACT ENERGY FT-LB	LOAD, LB				DEFLECTION, IN			INTEGRATOR ENERGY FT-LB			CRACK DEPTH IN	ET/AREA LB/IN
				PF	PGY	PM	P1	DGY	DM	D1	WT	WI	WF		
3812	-40	118.2	3.2	1980	0	1980	1980	0.000	.011	.011	3.7	.8	.8	.110	343
3814	0	115.1	4.0	1950	0	1950	1950	0.000	.012	.012	4.2	1.0	1.0	.137	474
3816	0	115.1	4.7	1860	0	1860	1860	0.000	.012	.012	5.0	.8	.8	.094	477
3811	40	113.0	5.5	2190	0	2190	2190	0.000	.013	.013	5.8	1.3	1.3	.116	603
3817	60	112.2	7.0	1935	0	1935	1935	0.000	.014	.014	0.0	1.1	1.1	.093	708
3815	72	111.8	6.0	2220	0	2220	2220	0.000	.013	.013	6.4	1.4	1.4	.122	672
3813	120	110.5	8.2	1920	0	1920	1920	0.000	.019	.019	8.4	1.6	1.6	.117	902
3818	120	110.5	8.0	1800	0	1800	1800	0.000	.022	.022	8.0	1.9	1.9	.120	889
3810	160	109.6	10.5	2730	0	2730	2730	0.000	.019	.019	11.7	1.9	1.9	.098	1080
389	200	108.8	12.1	3060	0	3060	3060	0.000	.021	.021	12.7	2.4	2.4	.098	1245

ClibPDF - www.fastio.com

TABLE 15. RAW DATA FOR INSTRUMENTED IMPACT EVALUATION OF PRECRACKED CHARPY V-NOTCH SPECIMENS OF PLATE R (A514-H) PROVIDED BY CALIFORNIA DIVISION OF HIGHWAYS - JANUARY 1973

SPECIMEN CODE	TEST TEMPERATURE F	STATIC YIELD STRESS KSI	DIAL IMPACT ENERGY FT-LB	LOAD, LB				DEFLECTION, IN			INTEGRATOR ENERGY FT-LB			CRACK DEPTH IN	ET/AREA LB/IN
				PF	PGY	PM	P1	DGY	DM	D1	WT	WI	WF		
R6L	-160	127.8	1.3	1545	0	1545	1545	0.000	.011	.011	1.9	.7	.7	.123	146
R7L	-120	124.0	1.5	1905	0	1905	1905	0.000	.011	.011	1.9	.7	.7	.135	176
R8L	-120	124.0	2.4	1515	0	1515	1515	0.000	.013	.013	2.2	.8	.8	.111	258
R5L	-80	120.4	3.0	2040	0	2040	2040	0.000	.012	.012	3.0	.8	.8	.126	341
R9L	-80	120.4	4.0	1740	0	1740	1740	0.000	.011	.011	3.5	.8	.8	.118	441
R1L	-40	117.9	5.0	1860	0	1860	1860	0.000	.012	.012	4.7	.8	.8	.123	562
R10L	-40	117.9	4.9	1665	0	1665	1665	0.000	.012	.012	4.2	.8	.8	.131	567
R2L	0	116.0	7.5	2025	0	2025	2025	0.000	.013	.013	7.3	1.2	1.2	.133	875
R4L	40	114.6	13.1	2430	0	2430	2430	0.000	.015	.015	13.6	1.5	1.5	.126	1489
R3L	72	113.6	16.0	2190	0	2190	2190	0.000	.018	.018	16.8	1.8	1.8	.130	1846
R11L	72	113.6	20.0	3390	0	3390	3390	0.000	.024	.024	20.6	3.2	3.2	.101	2079
R12L	120	112.0	23.4	2820	0	2820	2820	0.000	.024	.024	24.9	3.2	3.2	.121	2611

ClibPDF - www.fastio.com

TABLE 16. RAW DATA FOR INSTRUMENTED IMPACT EVALUATION OF PRECRACKED CHARPY V-NOTCH SPECIMENS OF PLATE Z (A517-H) PROVIDED BY CALIFORNIA DIVISION OF HIGHWAYS - JANUARY 1973

SPECIMEN CODE	TEST TEMPERATURE F	STATIC YIELD STRESS KSI	DIAL IMPACT ENERGY FT-LB	LOAD, LB				DEFLECTION, IN			INTEGRATOR ENERGY FT-LB			CRACK DEPTH IN	ET/AREA LB/IN
				PF	PGY	PM	P1	DGY	DM	D1	WT	WI	WF		
Z1L	-160	130.4	1.8	1545	0	1545	1545	0.000	.012	.012	1.9	.7	.7	.131	208
Z9L	-120	126.4	1.9	2040	0	2040	2040	0.000	.012	.012	2.1	.9	.9	.124	214
Z2L	-120	126.4	2.8	1590	0	1590	1590	0.000	.012	.012	2.4	.7	.7	.118	309
Z10L	-80	123.5	3.5	2160	0	2160	2160	0.000	.012	.012	3.3	1.1	1.1	.116	383
Z7L	-40	121.6	6.0	2190	0	2190	2190	0.000	.012	.012	6.2	1.2	1.2	.108	639
Z3L	-40	121.6	7.0	1890	0	1890	1890	0.000	.012	.012	7.1	.9	.9	.115	764
Z6L	0	120.0	8.7	2505	0	2505	2505	0.000	.016	.016	8.6	1.4	1.4	.117	957
Z4L	0	120.0	11.7	1830	0	1830	1830	0.000	.012	.012	11.7	.8	.8	.119	1296
Z12L	40	119.0	12.2	2880	0	2880	2880	0.000	.018	.018	12.3	2.4	2.4	.120	1356
Z11L	72	118.2	16.8	2940	0	2940	2940	0.000	.018	.018	18.0	2.4	2.4	.125	1902
Z8L	120	117.0	26.0	0	3210	3270	3270	.029	.032	.032	26.5	5.2	5.2	.116	2848
Z5L	160	116.2	34.1	0	3060	3330	0	.029	.044	0.000	35.3	7.2	0.0	.123	3832

ClibPDF - www.fastio.com

TABLE 17. RESULTS OF INSTRUMENTED IMPACT EVALUATION OF PRECRACKED CHARPY V-NOTCH SPECIMENS OF PLATE A (A517-F) PROVIDED BY CALIFORNIA DIVISION OF HIGHWAYS - JANUARY 1973

SPECIMEN CODE	TEST TEMPERATURE F	YIELD STRESS KSI		FRACTURE TOUGHNESS CALCULATED FROM THE INDICATED PARAMETER, KSI-SQRT(IN)								CRITICAL CRACK LENGTH IN	COD (0.001 IN)	
		STATIC	DYNAMIC	PF	WT	WI	WF	P*I	P*F	CODM	PMAX		DM	DI
A15L	-120	116.0	0.0	36.4	77.3	48.4	48.4	32.9	32.9	78.8	36.4	.026	1.68	1.68
A14L	-80	112.6	0.0	36.2	77.8	48.2	48.2	34.7	34.7	73.2	36.2	.030	1.51	1.51
A11L	-40	110.9	0.0	39.3	80.7	53.9	53.9	40.8	40.8	71.8	39.3	.040	1.49	1.49
A10L	0	109.1	0.0	49.2	84.8	57.9	57.9	47.6	47.6	73.1	49.2	.061	1.59	1.59
A17L	0	109.1	0.0	34.4	89.0	57.8	57.8	36.9	36.9	79.4	34.4	.032	1.87	1.87
A13L	40	107.3	0.0	49.7	127.5	55.4	55.4	45.9	45.9	72.2	49.7	.058	1.59	1.59
A18L	40	107.3	0.0	39.0	144.2	53.9	53.9	38.3	38.3	75.4	39.0	.041	1.74	1.74
A12L	72	105.9	0.0	56.2	166.5	55.3	55.3	49.2	49.2	71.0	56.2	.069	1.57	1.57
A16L	120	103.7	0.0	60.8	232.6	104.0	104.0	54.9	54.9	126.4	60.8	.083	4.98	4.98
A19L	160	101.8	0.0	73.5	265.1	121.2	121.2	82.3	82.3	118.7	73.5	.102	3.69	3.69

ClibPDF - www.fastio.com

TABLE 18. RESULTS OF INSTRUMENTED IMPACT EVALUATION OF PRECRACKED CHARPY V-NOTCH SPECIMENS OF PLATE AL (A517-H) PROVIDED BY CALIFORNIA DIVISION OF HIGHWAYS - JANUARY 1973

SPECIMEN CODE	TEST TEMPERATURE F	YIELD STRESS KSI		FRACTURE TOUGHNESS CALCULATED FROM THE INDICATED PARAMETER, KSI-SQRT(IN)								CRITICAL CRACK LENGTH IN	COD (0.001 IN)	
		STATIC	DYNAMIC	PF	WT	WI	WF	P*I	P*F	CODM	PMAX		DM	D1
AL1L	-80	108.0	0.0	37.2	92.3	48.7	48.7	32.7	32.7	78.3	37.2	.029	1.80	1.80
AL5L	-40	106.8	0.0	49.7	125.3	54.2	54.2	45.8	45.8	71.3	49.7	.058	1.53	1.53
AL7L	0	105.6	0.0	50.6	155.9	68.1	68.1	53.6	53.6	76.4	50.6	.073	1.79	1.79
AL9L	40	104.3	0.0	59.3	186.7	73.5	73.5	62.7	62.7	76.3	59.3	.101	1.81	1.81
AL2L	40	104.3	0.0	45.8	184.6	77.2	77.2	52.1	52.1	84.9	45.8	.061	2.26	2.26
AL8L	72	103.4	0.0	60.8	219.8	81.7	81.7	61.5	61.5	88.7	60.8	.099	2.39	2.39
AL3L	72	103.4	0.0	54.8	224.1	78.2	78.2	54.2	54.2	90.0	54.8	.087	2.59	2.59
AL11L	120	101.8	0.0	64.5	253.3	101.2	101.2	67.5	67.5	106.2	64.5	.102	3.31	3.31
AL10L	160	100.4	0.0	71.3	284.3	105.2	105.2	75.5	75.5	109.1	71.3	.099	3.16	3.16
AL4L	200	99.0	122.6	0.0	313.9	151.0	151.0	95.0	95.0	143.2	74.5	.118	5.73	5.73

ClibPDF - www.fastio.com

TABLE 19. RESULTS OF INSTRUMENTED IMPACT EVALUATION OF PRECRACKED CHARPY V-NOTCH SPECIMENS OF PLATE L (A517-F) PROVIDED BY CALIFORNIA DIVISION OF HIGHWAYS - JANUARY 1973

SPECIMEN CODE	TEST TEMPERATURE F	YIELD STRESS KSI		FRACTURE TOUGHNESS CALCULATED FROM THE INDICATED PARAMETER, KSI-SQRT(IN)								CRITICAL CRACK LENGTH IN	COD (0.001 IN)	
		STATIC	DYNAMIC	PF	WT	WI	WF	P*I	P*F	CODM	PMAX		DM	DI
L22L	-160	123.6	0.0	43.5	89.7	51.8	51.8	38.7	38.7	80.6	43.5	.031	1.63	1.63
L24L	-120	119.7	0.0	51.1	88.7	59.1	59.1	51.5	51.5	73.5	51.1	.058	1.42	1.42
L12L	-120	119.7	0.0	39.4	96.3	53.9	53.9	37.8	37.8	81.2	39.4	.032	1.73	1.73
L23L	-80	115.8	0.0	48.6	129.7	66.5	66.5	51.7	51.7	79.9	48.6	.056	1.75	1.75
L19L	-40	113.2	0.0	54.1	163.0	62.2	62.2	54.5	54.5	73.9	54.1	.073	1.55	1.55
L13L	-20	112.2	0.0	52.3	207.0	79.2	79.2	50.4	50.4	99.8	52.3	.064	2.86	2.86
L18L	0	111.3	0.0	61.1	219.4	97.0	97.0	71.1	71.1	92.9	61.1	.096	2.52	2.52
L20L	40	110.0	0.0	87.8	288.9	129.2	129.2	95.6	95.6	130.2	87.8	.101	3.56	3.56
L15L	40	110.0	0.0	82.5	362.0	116.2	116.2	87.6	87.6	120.2	82.5	.102	3.24	3.24
L21L	72	109.8	137.5	0.0	362.2	142.1	142.1	91.7	91.7	139.8	79.7	.107	4.70	4.70

ClibPDF - www.fastio.com

TABLE 20. RESULTS OF INSTRUMENTED IMPACT EVALUATION OF PRECRACKED CHARPY V-NOTCH SPECIMENS OF PLATE M (A514-F) PROVIDED BY CALIFORNIA DIVISION OF HIGHWAYS - JANUARY 1973

SPECIMEN CODE	TEST TEMPERATURE F	YIELD STRESS KSI		FRACTURE TOUGHNESS CALCULATED FROM THE INDICATED PARAMETER, KSI-SQRT(IN)								CRITICAL CRACK LENGTH IN	COD (0.001 IN)	
		STATIC	DYNAMIC	PF	WT	WI	WF	P*I	P*F	CODM	PMAX		DM	DI
M8L	-320	176.2	0.0	31.4	80.0	49.1	49.1	30.0	30.0	100.8	31.4	.009	1.72	1.72
M6L	-240	142.8	0.0	44.8	92.9	55.1	55.1	42.2	42.2	86.2	44.8	.028	1.58	1.58
M5L	-200	134.3	0.0	47.2	97.1	58.9	58.9	45.8	45.8	84.1	47.2	.037	1.62	1.62
M4L	-160	129.0	0.0	47.6	116.3	62.7	62.7	47.0	47.0	85.7	47.6	.042	1.77	1.77
M9L	-120	125.2	0.0	47.4	179.5	0.0	0.0	0.0	0.0	80.4	47.4	.046	1.62	1.62
M3L	-120	125.2	0.0	71.6	159.4	84.2	84.2	71.1	71.1	93.2	71.6	.099	2.14	2.14
M7L	-80	122.5	0.0	65.6	230.2	94.6	94.6	70.8	70.8	99.1	65.6	.091	2.54	2.54
M10L	-80	122.5	0.0	76.0	269.9	94.7	94.7	74.2	74.2	106.4	76.0	.097	2.68	2.68
M1L	-40	120.5	179.1	0.0	325.6	168.8	168.8	139.5	139.5	170.4	103.0	.105	5.20	5.20
M2L	0	119.0	166.9	0.0	409.6	176.3	0.0	132.5	0.0	173.1	100.6	.116	5.82	0.00

ClibPDF - www.fastio.com

TABLE 21. RESULTS OF INSTRUMENTED IMPACT EVALUATION OF PRECRACKED CHARPY V-NOTCH SPECIMENS OF PLATE Q (A517-H) PROVIDED BY CALIFORNIA DIVISION OF HIGHWAYS - JANUARY 1973

SPECIMEN CODE	TEST TEMPERATURE F	YIELD STRESS KSI		FRACTURE TOUGHNESS CALCULATED FROM THE INDICATED PARAMETER, KSI-SQRT(IN)								CRITICAL CRACK LENGTH IN	COD (0.001 IN)	
		STATIC	DYNAMIC	PF	WT	WI	WF	P*I	P*F	CODM	PMAX		DM	DI
3812	-40	118.2	0.0	46.1	116.8	55.5	55.5	44.6	44.6	76.1	46.1	.045	1.57	1.57
3814	0	115.1	0.0	54.1	130.6	62.0	62.0	53.5	53.5	74.9	54.1	.069	1.58	1.58
3816	0	115.1	0.0	39.0	130.6	53.7	53.7	36.9	36.9	80.9	39.0	.033	1.84	1.84
3811	40	113.0	0.0	53.0	146.6	69.5	69.5	55.3	55.3	80.4	53.0	.070	1.88	1.88
3817	60	112.2	0.0	40.3	153.7	60.2	60.2	38.7	38.7	86.8	40.3	.038	2.21	2.21
3815	72	111.8	0.0	55.9	154.9	73.0	73.0	60.4	60.4	78.7	55.9	.079	1.83	1.83
3813	120	110.5	0.0	46.8	174.0	76.1	76.1	47.8	47.8	94.5	46.8	.057	2.71	2.71
3818	120	110.5	0.0	44.7	170.5	83.3	83.3	48.5	48.5	99.7	44.7	.052	3.02	3.02
3810	160	109.6	0.0	58.7	197.5	79.6	79.6	54.8	54.8	96.6	58.7	.080	2.89	2.89
389	200	108.8	0.0	65.8	205.0	88.4	88.4	61.2	61.2	104.4	65.8	.090	3.24	3.24

ClibPDF - www.fastio.com

TABLE 22. RESULTS OF INSTRUMENTED IMPACT EVALUATION OF PRECRACKED CHARPY V-NOTCH SPECIMENS OF PLATE R (A514-H) PROVIDED BY CALIFORNIA DIVISION OF HIGHWAYS - JANUARY 1973

SPECIMEN CODE	TEST TEMPERATURE F	YIELD STRESS KSI		FRACTURE TOUGHNESS CALCULATED FROM THE INDICATED PARAMETER, KSI-SQRT(IN)								CRITICAL CRACK LENGTH IN	COD (0.001 IN)	
		STATIC	DYNAMIC	PF	WT	WI	WF	P*I	P*F	CODM	PMAX		DM	DI
R6L	-160	127.8	0.0	39.1	86.0	51.2	51.2	38.0	38.0	78.6	39.1	.028	1.50	1.50
R7L	-120	124.0	0.0	52.2	89.6	52.1	52.1	45.6	45.6	75.3	52.2	.043	1.44	1.44
R8L	-120	124.0	0.0	35.5	90.8	55.2	55.2	34.9	34.9	87.0	35.5	.025	1.92	1.92
R5L	-80	120.4	0.0	52.7	108.5	55.3	55.3	45.9	45.9	79.1	52.7	.046	1.65	1.65
R9L	-80	120.4	0.0	42.7	115.1	54.5	54.5	41.3	41.3	78.2	42.7	.037	1.61	1.61
R1L	-40	117.9	0.0	47.1	134.8	56.7	56.7	44.6	44.6	78.2	47.1	.046	1.66	1.66
R10L	-40	117.9	0.0	44.4	129.7	57.6	57.6	44.5	44.5	77.0	44.4	.045	1.61	1.61
R2L	0	116.0	0.0	54.8	170.3	68.7	68.7	56.6	56.6	79.3	54.8	.071	1.76	1.76
R4L	40	114.6	0.0	62.8	227.8	75.1	75.1	62.1	62.1	84.4	62.8	.094	2.04	2.04
R3L	72	113.6	0.0	58.1	254.0	82.4	82.4	60.5	60.5	90.8	58.1	.083	2.40	2.40
R11L	72	113.6	0.0	74.4	266.6	105.7	105.7	73.1	73.1	118.1	74.4	.100	3.54	3.54
R12L	120	112.0	0.0	70.5	301.7	108.5	108.5	76.0	76.0	110.6	70.5	.102	3.28	3.28

ClibPDF - www.fastio.com

TABLE 23. RESULTS OF INSTRUMENTED IMPACT EVALUATION OF PRECRACKED CHARPY V-NOTCH SPECIMENS OF PLATE Z (A517-H) PROVIDED BY CALIFORNIA DIVISION OF HIGHWAYS - JANUARY 1973

SPECIMEN CODE	TEST TEMPERATURE F	YIELD STRESS KSI		FRACTURE TOUGHNESS CALCULATED FROM THE INDICATED PARAMETER, KSI-SQRT(IN)								CRITICAL CRACK LENGTH IN	COD (0.001 IN)	
		STATIC	DYNAMIC	PF	WT	WI	WF	P*I	P*F	CODM	PMAX		DM	DI
Z1L	-160	130.4	0.0	41.2	87.2	52.0	52.0	38.0	38.0	82.4	41.2	.027	1.62	1.62
Z9L	-120	126.4	0.0	52.0	91.0	59.6	59.6	48.7	48.7	81.8	52.0	.047	1.66	1.66
Z2L	-120	126.4	0.0	39.0	96.2	52.7	52.7	37.0	37.0	82.7	39.0	.027	1.70	1.70
Z10L	-80	123.5	0.0	52.3	111.7	65.7	65.7	53.5	53.5	81.5	52.3	.057	1.71	1.71
Z7L	-40	121.6	0.0	50.3	150.5	66.0	66.0	52.5	52.5	81.5	50.3	.054	1.75	1.75
Z3L	-40	121.6	0.0	45.4	163.6	57.8	57.8	44.2	44.2	80.5	45.4	.042	1.71	1.71
Z6L	0	120.0	0.0	61.0	178.7	73.0	73.0	57.2	57.2	90.3	61.0	.072	2.20	2.20
Z4L	0	120.0	0.0	45.2	210.0	55.8	55.8	43.1	43.1	78.7	45.2	.041	1.68	1.68
Z12L	40	119.0	0.0	71.5	214.1	94.0	94.0	75.1	75.1	98.3	71.5	.102	2.50	2.50
Z11L	72	118.2	0.0	75.5	260.2	94.2	94.2	78.4	78.4	99.5	75.5	.101	2.44	2.44
Z8L	120	117.0	137.0	0.0	308.9	137.4	137.4	89.8	89.8	136.9	79.1	.106	4.58	4.58
Z5L	160	116.2	137.5	0.0	358.5	162.3	0.0	108.1	0.0	156.5	84.4	.120	6.04	0.00

ClibPDF - www.fastio.com

TABLE 24. RAW DATA FOR INSTRUMENTED IMPACT EVALUATION OF STANDARD CHARPY V-NOTCH SPECIMENS OF PLATE L (A517-F) PROVIDED BY CALIFORNIA DIVISION OF HIGHWAYS - JANUARY 1973

SPECIMEN CODE	TEST TEMPERATURE F	STATIC YIELD STRESS KSI	DIAL IMPACT ENERGY FT-LB	LOAD, LB				DEFLECTION, IN			INTEGRATOR ENERGY FT-LB			CRACK DEPTH IN	ET/AREA LB/IN
				PF	PGY	PM	P1	DGY	DM	D1	WT	WI	WF		
L3L	-200	129.7	4.0	3210	0	3210	3210	0.000	.019	.019	4.8	3.0	3.0	.079	387
L8	-160	123.6	7.0	4440	0	4440	4440	0.000	.025	.025	7.9	4.6	4.6	.079	677
L2L	-140	117.9	6.0	4140	0	4140	4140	0.000	.023	.023	6.9	5.4	5.4	.079	580
L9	-120	119.7	12.0	0	4890	5280	5280	.026	.036	.036	12.7	6.5	6.5	.079	1160
L10L	-80	115.8	12.0	0	4680	5160	5160	.026	.041	.041	0.0	0.0	0.0	.079	1160
L11L	-40	113.2	13.5	0	4560	4800	4800	.021	.027	.027	13.6	6.5	6.5	.079	1305
L7	-20	110.0	51.5	0	4350	5190	5190	.029	.074	.083	53.8	25.5	27.2	.079	4979
L6L	0	111.3	61.5	0	4320	5340	5100	.025	.076	.101	60.3	24.0	33.5	.079	5946
L1L	20	108.2	68.5	0	4200	5340	5100	.028	.084	.112	73.1	29.9	39.9	.079	6623
L4L	40	110.0	78.6	0	4410	5310	0	.022	.083	0.000	80.3	27.8	0.0	.079	7600
L5L	72	109.8	83.5	0	4260	5250	0	.027	.098	0.000	84.0	33.1	0.0	.079	8073

ClibPDF - www.fastio.com

TABLE 25. RAW DATA FOR INSTRUMENTED IMPACT EVALUATION OF STANDARD CHARPY V-NOTCH SPECIMENS OF PLATE M (A514-F) PROVIDED BY CALIFORNIA DIVISION OF HIGHWAYS - JANUARY 1973

SPECIMEN CODE	TEST TEMPERATURE F	STATIC YIELD STRESS KSI	DIAL IMPACT ENERGY FT-LB	LOAD, LB				DEFLECTION, IN			INTEGRATOR ENERGY FT-LB			CRACK DEPTH IN	ET/AREA LB/IN
				PF	PGY	PM	P1	DGY	DM	D1	WT	WI	WF		
M15L	-240	142.8	5.1	3810	0	3810	3810	0.000	.021	.021	6.0	3.0	3.0	.079	493
M16L	-200	134.3	7.0	4620	0	4620	4620	0.000	.025	.025	8.1	4.6	4.6	.079	677
M18L	-160	129.0	8.2	4680	0	4680	4680	0.000	.028	.028	8.6	5.4	5.4	.079	793
M19L	-140	126.9	17.5	0	4680	5550	5550	.030	.047	.047	17.7	13.0	13.0	.079	1692
M21L	-120	125.2	42.5	0	4890	5400	5160	.029	.055	.066	0.0	16.3	21.7	.079	4109
M14L	-80	122.5	34.5	0	4800	5730	5730	.026	.064	.064	35.2	21.9	21.9	.079	3336
M13L	-40	120.5	55.8	0	4800	5730	5610	.020	.068	.082	56.8	23.4	31.5	.079	5395
M17L	0	119.0	70.0	0	4530	5220	0	.022	.053	0.000	68.5	16.6	0.0	.079	6768
M20L	40	117.8	69.9	0	4380	5220	0	.025	.064	0.000	70.7	24.9	0.0	.079	6759

ClibPDF - www.fastio.com

TABLE 26. RAW DATA FOR INSTRUMENTED IMPACT EVALUATION OF STANDARD CHARPY V-NOTCH SPECIMENS OF PLATE Q (A517-H) PROVIDED BY CALIFORNIA DIVISION OF HIGHWAYS - JANUARY 1973

SPECIMEN CODE	TEST TEMPERATURE F	STATIC YIELD STRESS KSI	DIAL IMPACT ENERGY FT-LB	LOAD, LB				DEFLECTION, IN			INTEGRATOR ENERGY FT-LB			CRACK DEPTH IN	ET/AREA LB/IN
				PF	PGY	PM	P1	DGY	DM	D1	WT	WI	WF		
3819	-40	118.2	4.0	3420	0	3420	3420	0.000	.017	.017	4.3	1.7	1.7	.079	387
2817	0	115.1	6.0	3750	0	3750	3750	0.000	.019	.019	5.9	2.9	2.9	.079	580
2816	40	113.0	7.0	3960	0	3960	3960	0.000	.019	.019	7.1	2.9	2.9	.079	677
1813	72	111.8	11.0	4620	0	4620	4620	0.000	.024	.024	11.4	4.7	4.7	.079	1064
1812	100	111.0	12.0	3900	0	3900	3900	0.000	.024	.024	12.3	3.9	3.9	.079	1160
1816	120	110.5	13.0	4290	0	4290	4290	0.000	.031	.031	0.0	5.2	5.2	.079	1257
1814	140	110.0	14.5	0	4050	4350	4350	.026	.033	.033	0.0	6.6	6.6	.079	1402
2813	160	109.6	16.9	0	4080	4590	4590	.019	.036	.036	18.1	7.4	7.4	.079	1634
2815	200	108.8	18.5	0	3810	4440	4440	.019	.040	.040	19.3	8.4	8.4	.079	1789
1815	240	108.0	22.0	0	3900	4500	4500	.025	.038	.038	22.9	8.9	8.9	.079	2127

ClibPDF - www.fastio.com

TABLE 27. RESULTS OF INSTRUMENTED IMPACT EVALUATION OF STANDARD CHARPY V-NOTCH SPECIMENS OF PLATE L (A517-F) PROVIDED BY CALIFORNIA DIVISION OF HIGHWAYS - JANUARY 1973

SPECIMEN CODE	TEST TEMPERATURE F	YIELD STRESS KSI		FRACTURE TOUGHNESS CALCULATED FROM THE INDICATED PARAMETER, KSI-SQRT(IN)								CRITICAL CRACK LENGTH IN	COD (0.001 IN)	
		STATIC	DYNAMIC	PF	WT	WI	WF	P*I	P*F	CODM	PMAX		DM	D1
L3L	-200	129.7	0.0	60.6	129.4	102.7	102.7	65.9	65.9	114.3	60.6	.069	3.10	3.10
L8	-160	123.6	0.0	83.8	164.0	126.1	126.1	83.7	83.7	138.7	83.8	.102	4.05	4.05
L2L	-140	117.9	0.0	78.2	153.5	135.2	135.2	91.2	91.2	127.2	78.2	.103	3.67	3.67
L9	-120	119.7	162.6	0.0	207.2	148.6	148.6	101.9	101.9	172.6	99.7	.120	5.76	5.76
L10L	-80	115.8	155.6	0.0	200.5	0.0	0.0	0.0	0.0	178.9	97.4	.125	6.52	6.52
L11L	-40	113.2	151.6	0.0	212.4	146.9	146.9	110.3	110.3	142.7	90.6	.114	4.31	4.31
L7	-20	110.0	144.6	0.0	421.1	289.8	299.3	182.3	188.3	231.2	98.0	.146	11.91	13.29
L6L	0	111.3	143.7	0.0	444.9	280.7	331.6	187.2	221.1	232.6	100.8	.157	12.21	16.29
L1L	20	108.2	139.7	0.0	488.2	312.3	360.6	196.2	226.6	240.0	100.8	.166	13.45	17.93
L4L	40	110.0	146.6	0.0	510.3	300.6	0.0	218.4	0.0	243.6	100.3	.149	13.26	0.00
L5L	72	109.8	141.7	0.0	519.9	326.1	0.0	210.0	0.0	260.2	99.1	.156	15.81	0.00

ClibPDF - www.fastio.com

TABLE 28. RESULTS OF INSTRUMENTED IMPACT EVALUATION OF STANDARD CHARPY V-NOTCH SPECIMENS OF PLATE M (A514-F) PROVIDED BY CALIFORNIA DIVISION OF HIGHWAYS - JANUARY 1973

SPECIMEN CODE	TEST TEMPERATURE F	YIELD STRESS KSI		FRACTURE TOUGHNESS CALCULATED FROM THE INDICATED PARAMETER, KSI-SQRT(IN)								CRITICAL CRACK LENGTH IN	COD (0.001 IN)	
		STATIC	DYNAMIC	PF	WT	WI	WF	P*I	P*F	CODM	PMAX		DM	DI
M15L	-240	142.8	0.0	71.9	144.4	103.1	103.1	68.6	68.6	126.0	71.9	.074	3.38	3.38
M16L	-200	134.3	0.0	87.2	167.4	126.8	126.8	85.3	85.3	142.3	87.2	.098	4.05	4.05
M18L	-160	129.0	0.0	88.4	171.8	135.4	135.4	88.2	88.2	149.0	88.4	.102	4.43	4.43
M19L	-140	126.9	155.6	0.0	245.3	210.0	210.0	132.2	132.2	195.0	104.8	.144	7.63	7.63
M21L	-120	125.2	162.6	0.0	379.4	235.0	271.4	153.8	177.6	213.5	101.9	.125	8.80	10.65
M14L	-80	122.5	159.6	0.0	343.6	271.2	271.2	185.5	185.5	227.5	108.2	.146	10.29	10.29
M13L	-40	120.5	159.6	0.0	434.1	278.3	323.3	219.8	255.3	233.3	108.2	.146	10.94	13.22
M17L	0	119.0	150.6	0.0	474.0	233.2	0.0	169.8	0.0	198.7	98.6	.136	8.50	0.00
M20L	40	117.8	145.6	0.0	479.0	284.0	0.0	192.8	0.0	213.8	98.6	.146	10.29	0.00

ClibPDF - www.fastio.com

TABLE 29. RESULTS OF INSTRUMENTED IMPACT EVALUATION OF STANDARD CHARPY V-NOTCH SPECIMENS OF PLATE Q (A517-H) PROVIDED BY CALIFORNIA DIVISION OF HIGHWAYS - JANUARY 1973

SPECIMEN CODE	TEST TEMPERATURE F	YIELD STRESS KSI		FRACTURE TOUGHNESS CALCULATED FROM THE INDICATED PARAMETER, KSI-SQRT(IN)								CRITICAL CRACK LENGTH IN	COD (0.001 IN)	
		STATIC	DYNAMIC	PF	WT	WI	WF	P*I	P*F	CODM	PMAX		DM	D1
3819	-40	118.2	0.0	64.6	119.0	74.5	74.5	53.9	53.9	99.9	64.6	.066	2.71	2.71
2817	0	115.1	0.0	70.8	139.1	96.9	96.9	69.1	69.1	109.0	70.8	.098	3.09	3.09
2816	40	113.0	0.0	74.8	151.6	97.3	97.3	71.7	71.7	111.3	74.8	.094	3.09	3.09
1813	72	111.8	0.0	87.2	191.4	123.5	123.5	88.6	88.6	133.6	87.2	.103	3.84	3.84
1812	100	111.0	0.0	73.6	198.3	111.7	111.7	73.9	73.9	122.2	73.6	.103	3.84	3.84
1816	120	110.5	0.0	81.0	203.1	128.5	128.5	78.5	78.5	145.6	81.0	.096	4.98	4.98
1814	140	110.0	134.7	0.0	213.9	144.5	144.5	93.5	93.5	146.3	82.1	.118	5.36	5.36
2813	160	109.6	135.7	0.0	238.4	152.0	152.0	116.3	116.3	151.4	86.7	.130	5.73	5.73
2815	200	108.8	126.7	0.0	244.4	161.2	161.2	120.0	120.0	154.7	83.8	.139	6.48	6.48
1815	240	108.0	129.7	0.0	264.7	165.5	165.5	109.6	109.6	150.7	85.0	.137	6.07	6.07

ClibPDF - www.fastio.com

TABLE 30. ESTIMATED NDTT VALUES DETERMINED FROM PRECRACKED W/A CURVES

Plate	Material	Estimated NDTT(°F)	K_{Id} @ NDTT (ksi-in$^{1/2}$)
A	A517-F	+23	43
AL	A517-H	+54	54
L	A517-F	-30	53.5
M	A514-F	-105	60
Q	A517-H	-	-
R	A514-H	-32	47.5
Z	A517-H	-6	52

ClibPDF - www.fastio.com

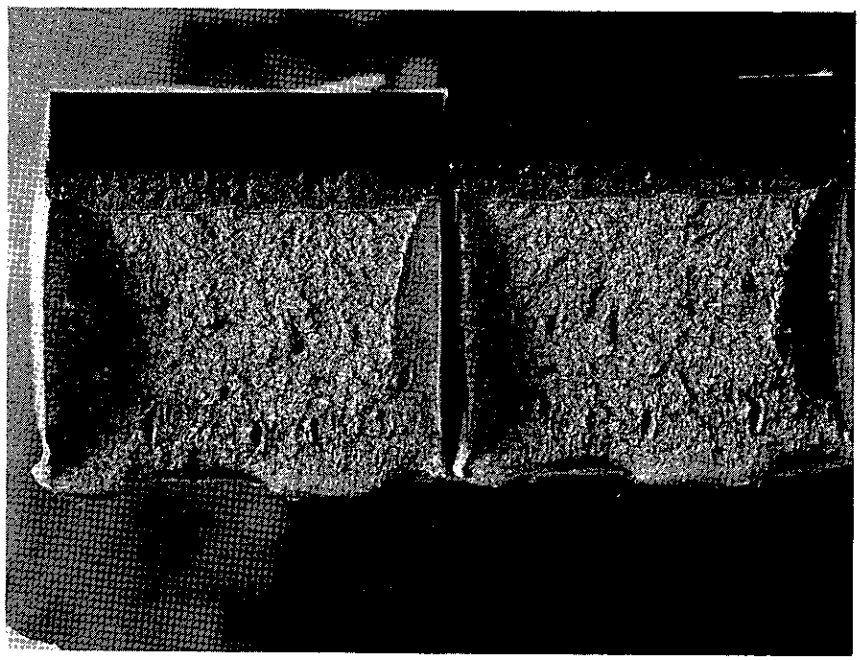

Figure 1. Typical Fatigue Precrack
(Specimen M10L)

ClibPDF - www.fastio.com

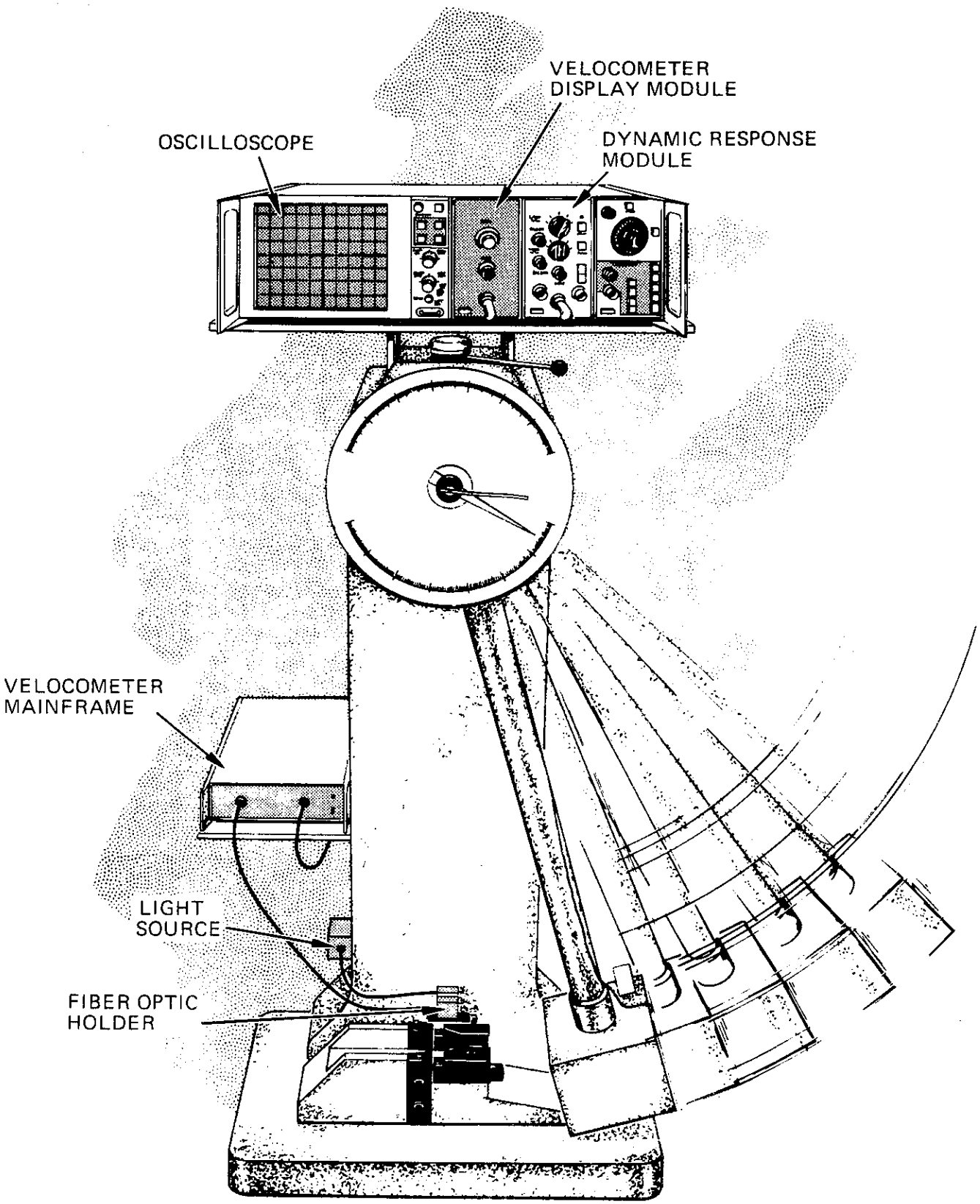

FIGURE 2.

Typical DYNATUP System in Operation
with A Standard Charpy Impact Machine

ClibPDF - www.fastio.com

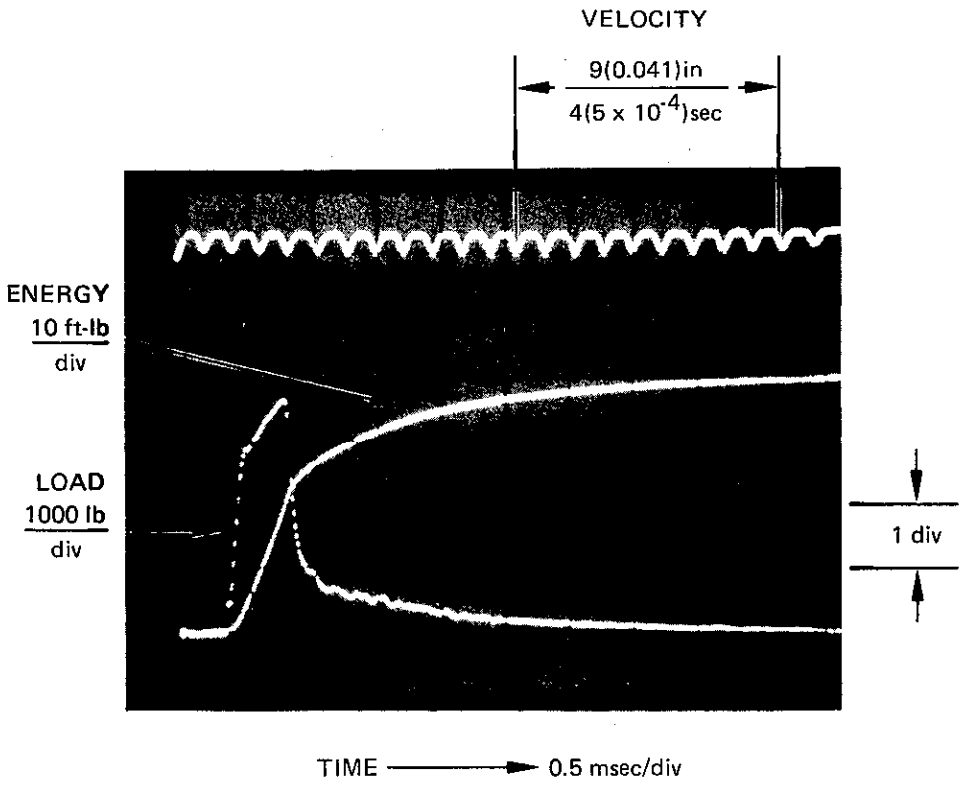

FIGURE 3.

Typical Raw Data Record of

CRT Display for DYNATUP Test of Structural Steel

ClibPDF - www.fastio.com

DYNATUP

CUSTOMER _____ DATE _____

SPECIMEN CODE	TEMP (°F)	DIAL ENERGY (ft-lbs)	LOAD SETTING (lbs/div)	ENERGY SETTING (ft-lbs/div)	SWEEP TIME (msec/div)	COMMENTS

FIGURE 4.

Typical Basic Data Table

ClibPDF - www.fastio.com

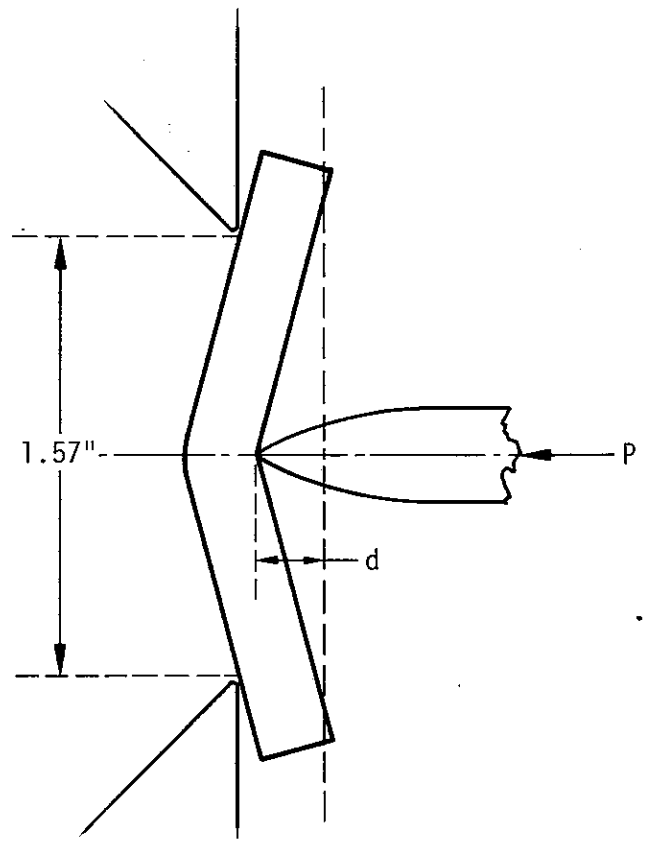

Figure 5. Specimen Orientation for Dynamic Three-Point Bending

ClibPDF - www.fastio.com

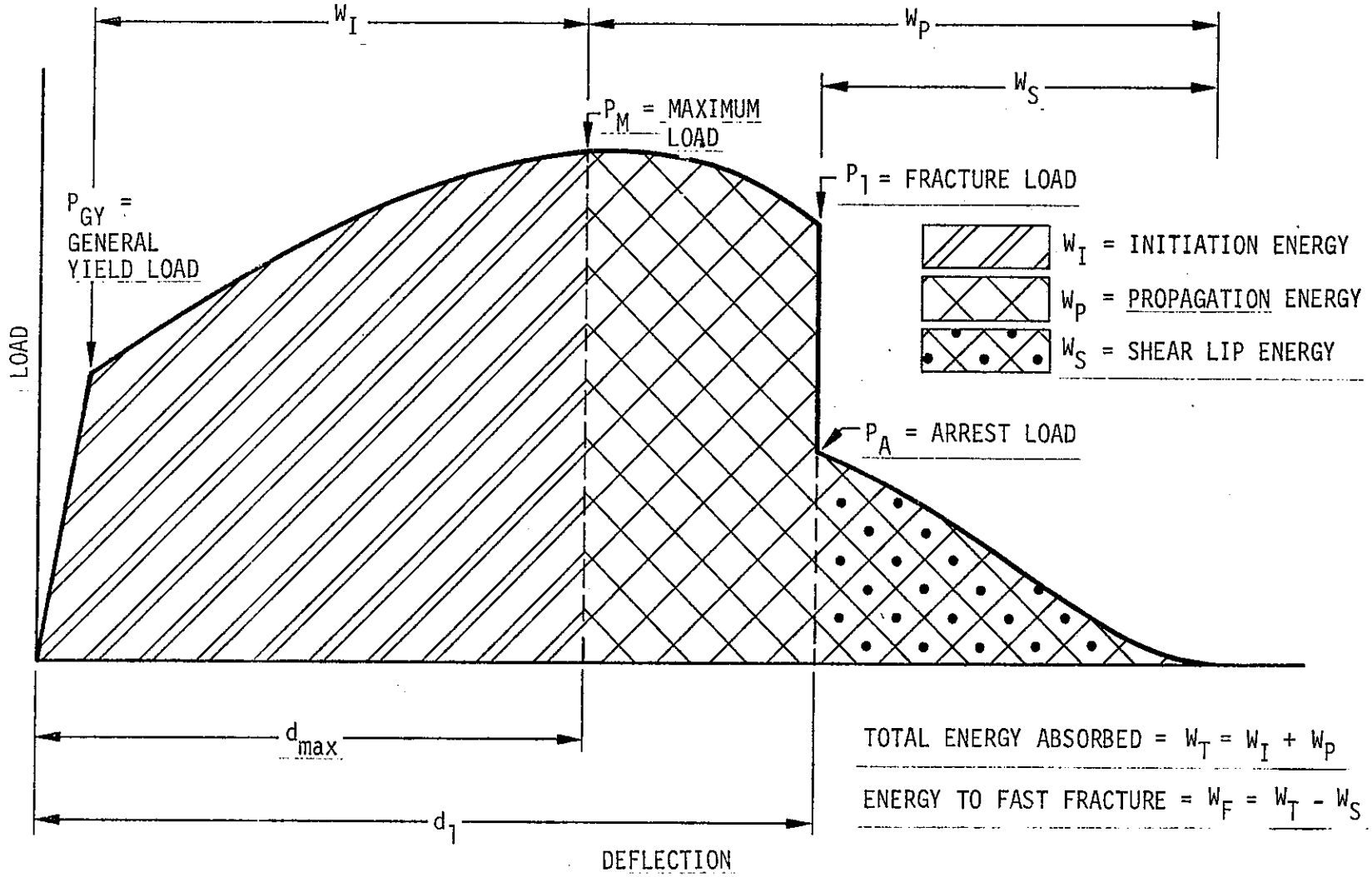

FIGURE 6.

Idealized Load-Deflection Record

ClibPDF - www.fastio.com

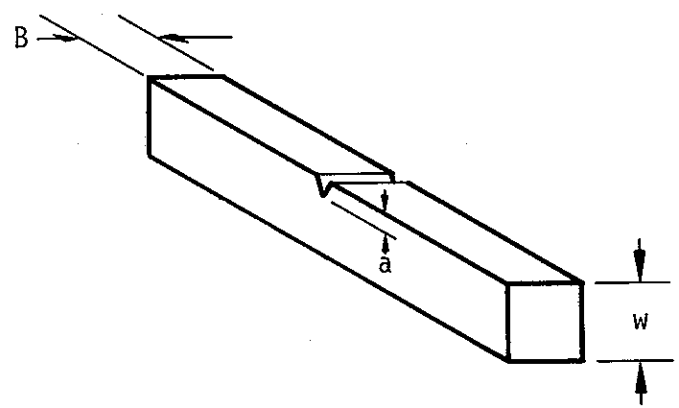

Figure 7. Specimen Dimensions

ClibPDF - www.fastio.com

SPECIMEN CODE	TEST TEMPERATURE F	STATIC YIELD STRESS KSI	DIAL IMPACT ENERGY FT-LB	LOAD , LB				DEFLECTION , IN			INTEGRATOR ENERGY FT-LB			CRACK DEPTH IN	FT/AREA LB/IN
				PF	PGY	PM	P1	DGY	DM	D1	WT	WI	WF		

FIGURE 8.

Typical Raw Data Table

ClibPDF - www.fastio.com

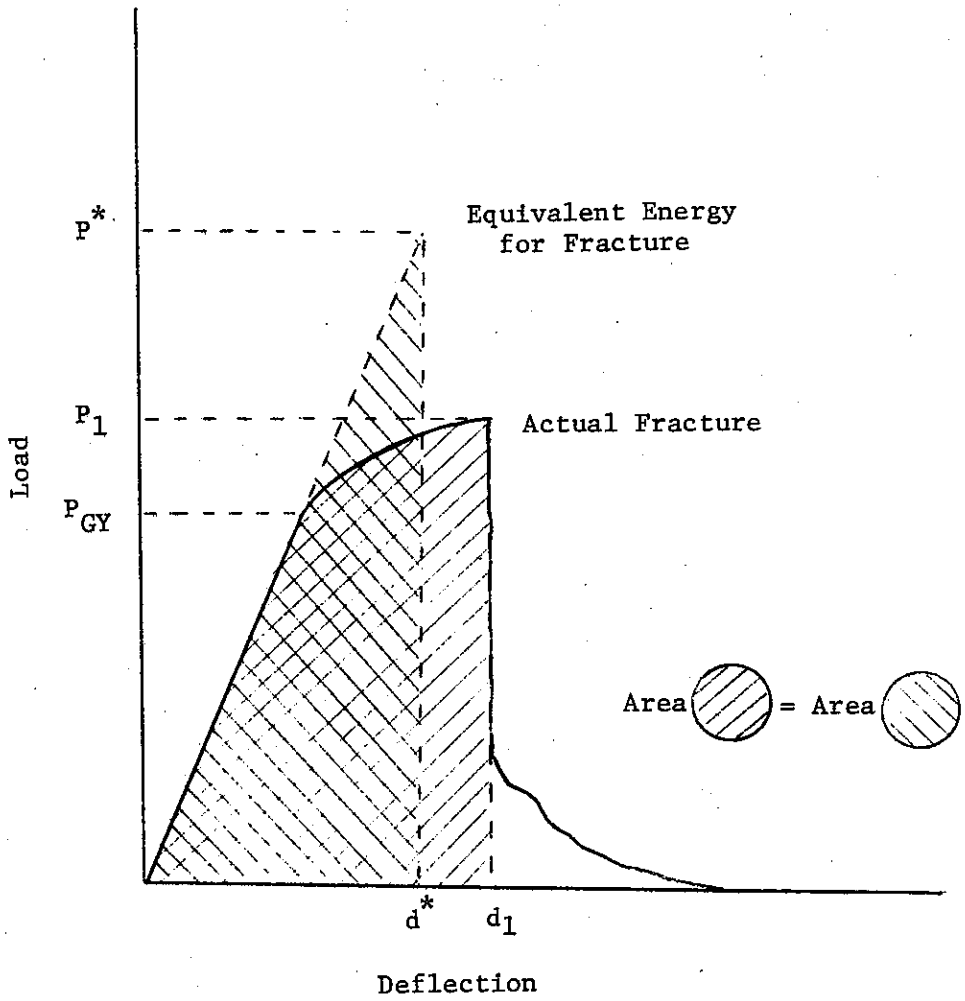

FIGURE 9.

Relationship of Equivalent Energy Fracture Load P^* to the Actual Fracture Load

ClibPDF - www.fastio.com

SPECIMEN CODE	TEST TEMPERATURE F	YIELD STRESS KSI		FRACTURE TOUGHNESS CALCULATED FROM THE INDICATED PARAMETER , KSI-SQRT(IN)								CRITICAL CRACK LENGTH IN	COD (0.001 IN)	
		STATIC	DYNAMIC	PF	WT	WI	WF	P*I	P*F	CODM	PMAX		DM	DI

FIGURE 10.

Typical Fracture Toughness Results Table

ClibPDF - www.fastio.com

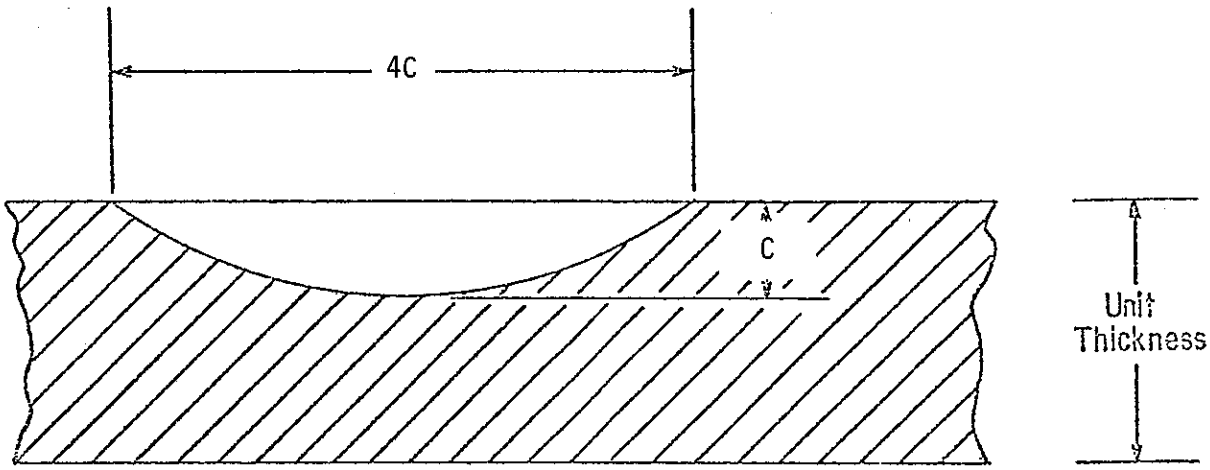

FIGURE 11.
Hypothetical Surface Flaw of Crack Depth, C, in a Plate of Unit Thickness

ClibPDF - www.fastio.com

ClibPDF - www.fastio.com

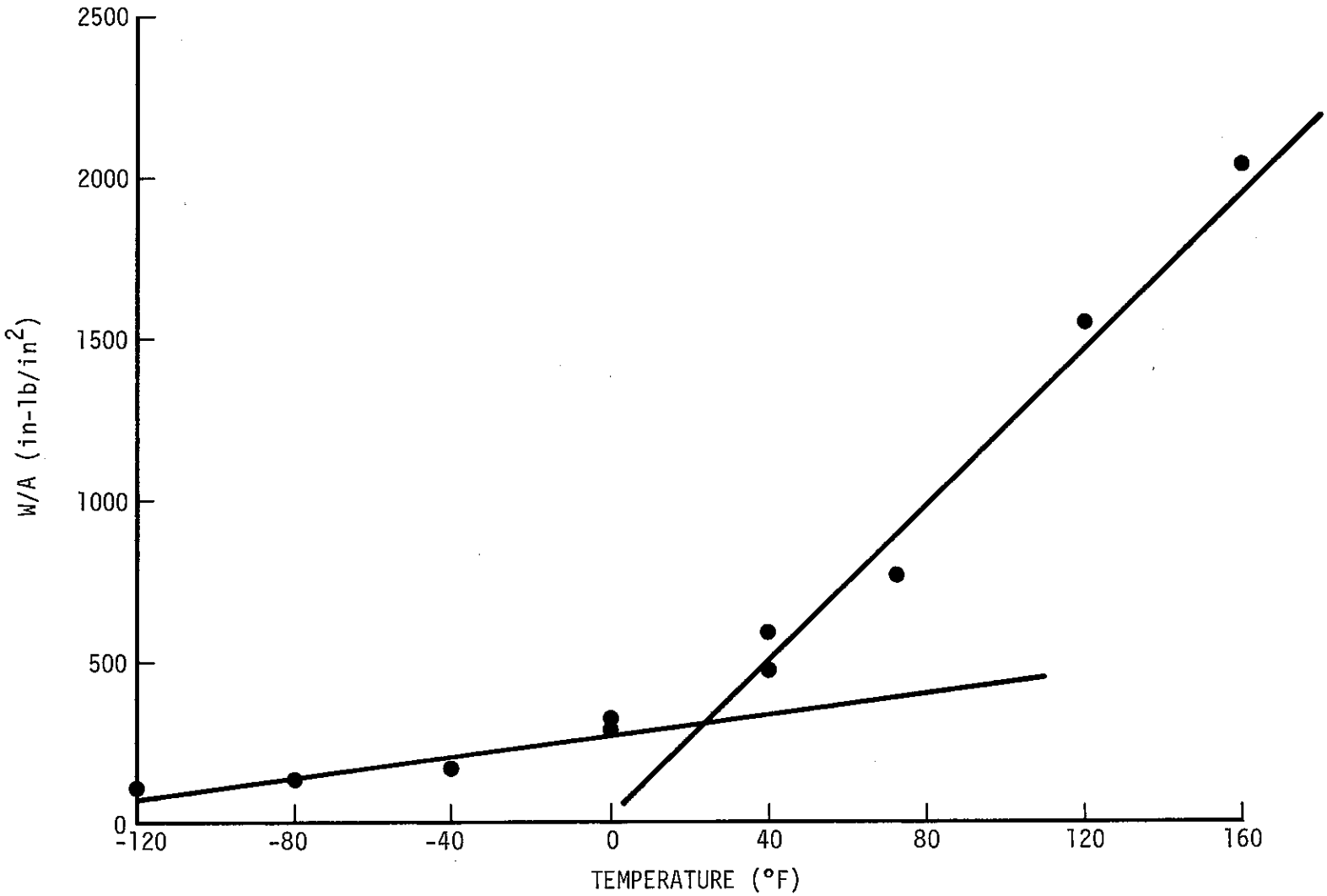

Figure 12. W/A as a Function of Temperature for Plate A

ClibPDF - www.fastio.com

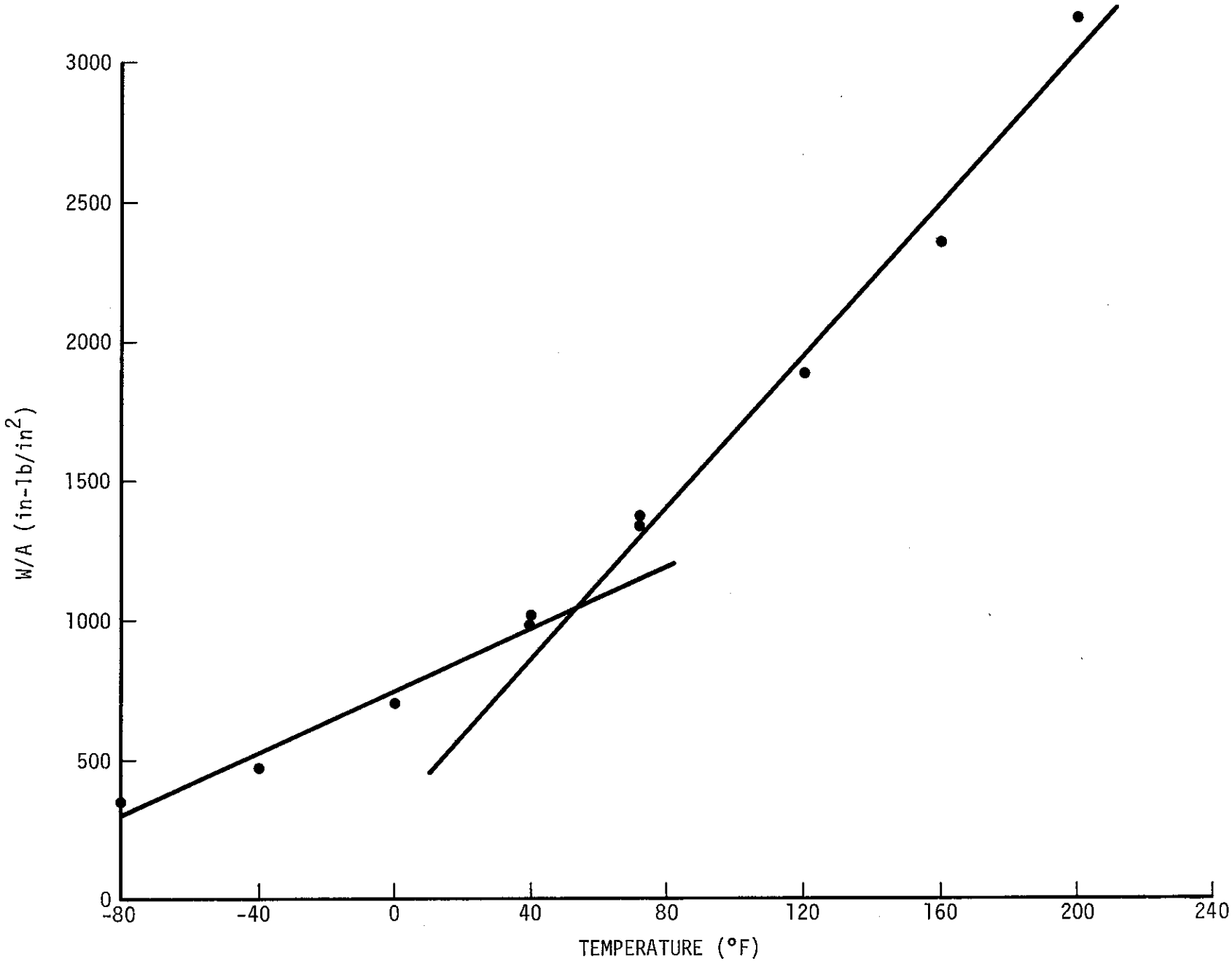

Figure 13. W/A as a Function of Temperature for Plate AL

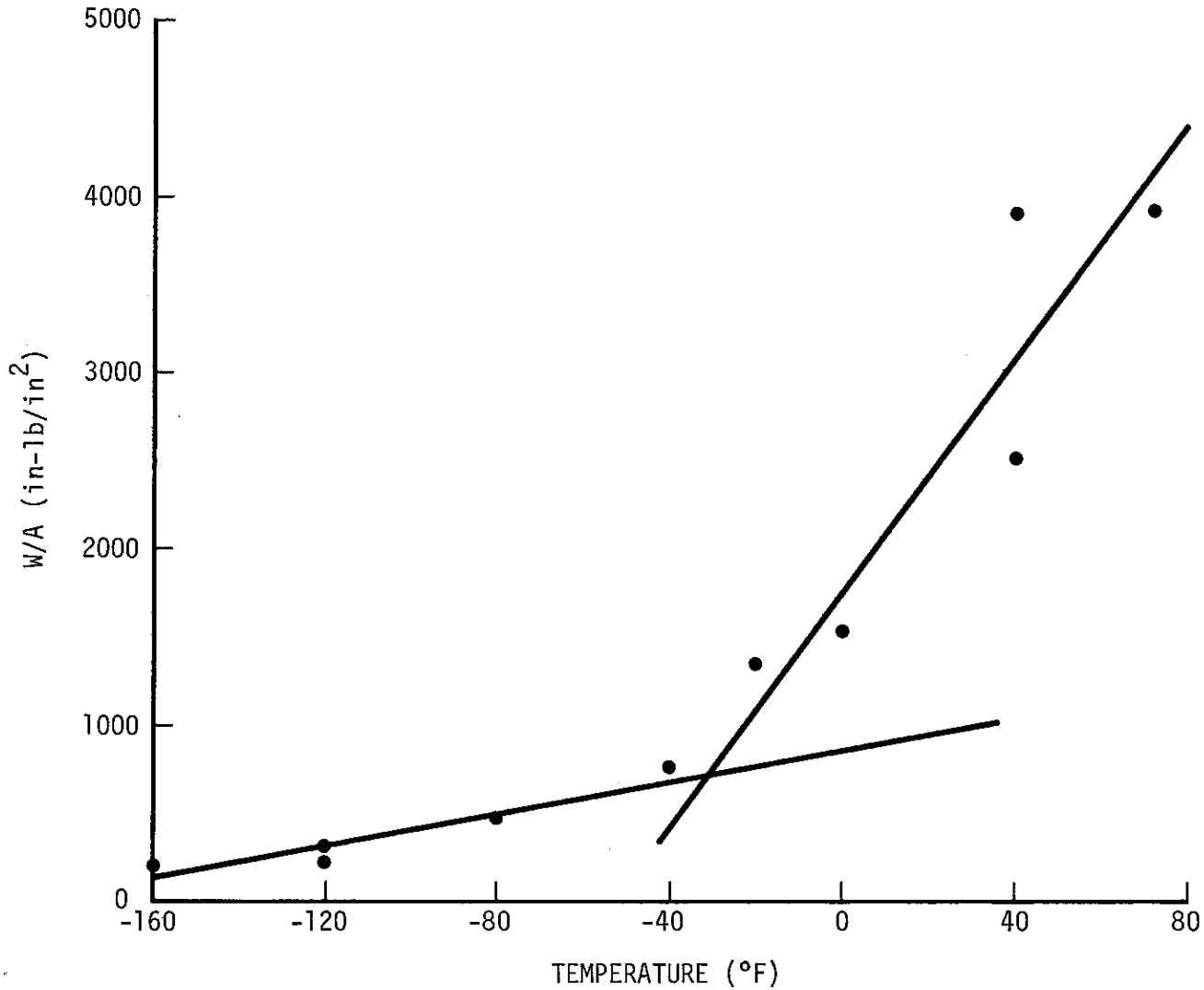

Figure 14. W/A as a Function of Temperature for Plate L

ClibPDF - www.fastio.com

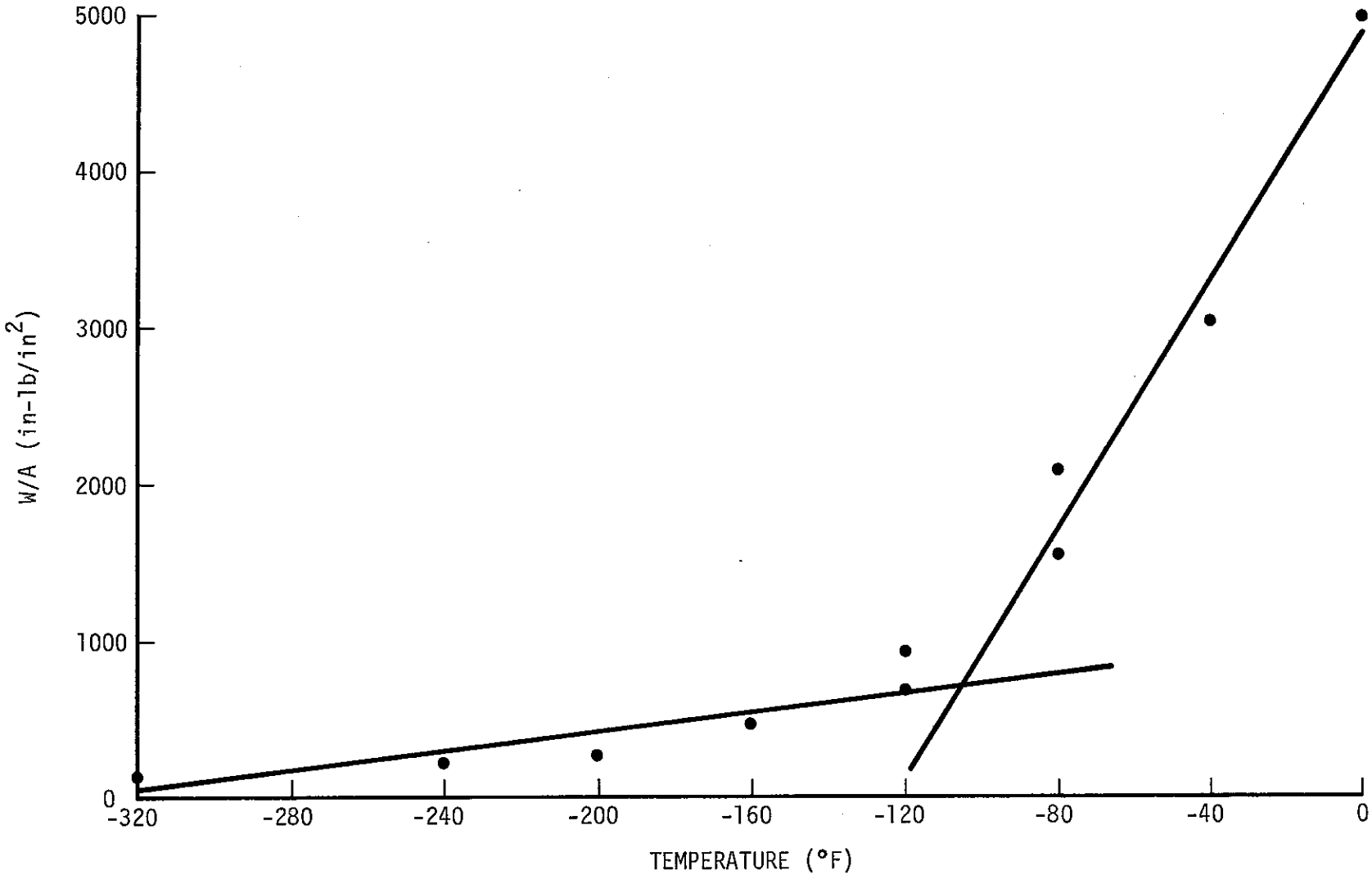

Figure 15. W/A as a Function of Temperature for Plate M

ClibPDF - www.fastio.com

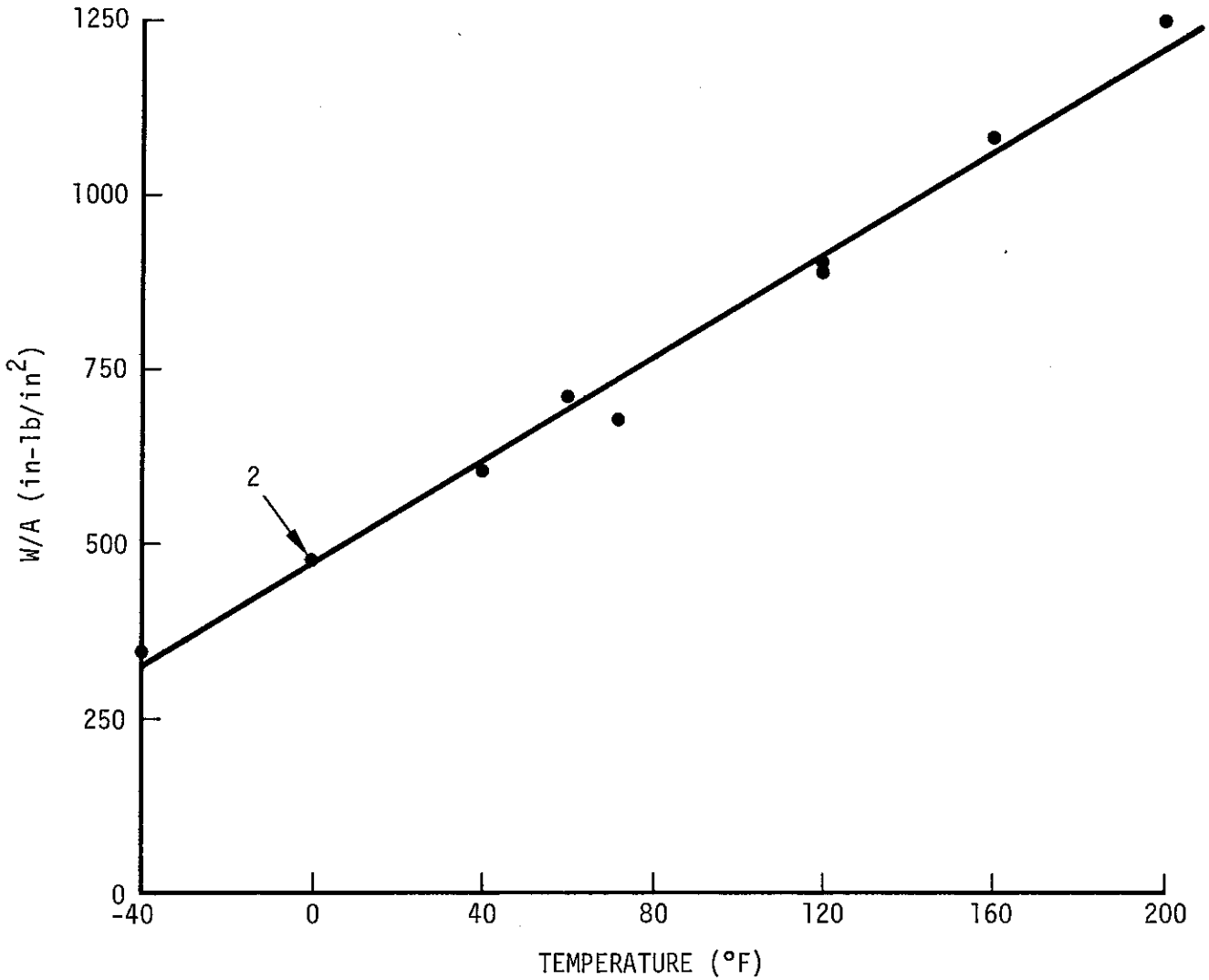

Figure 16. W/A as a Function of Temperature for Plate Q

ClibPDF - www.fastio.com

ClibPDF - www.fastio.com

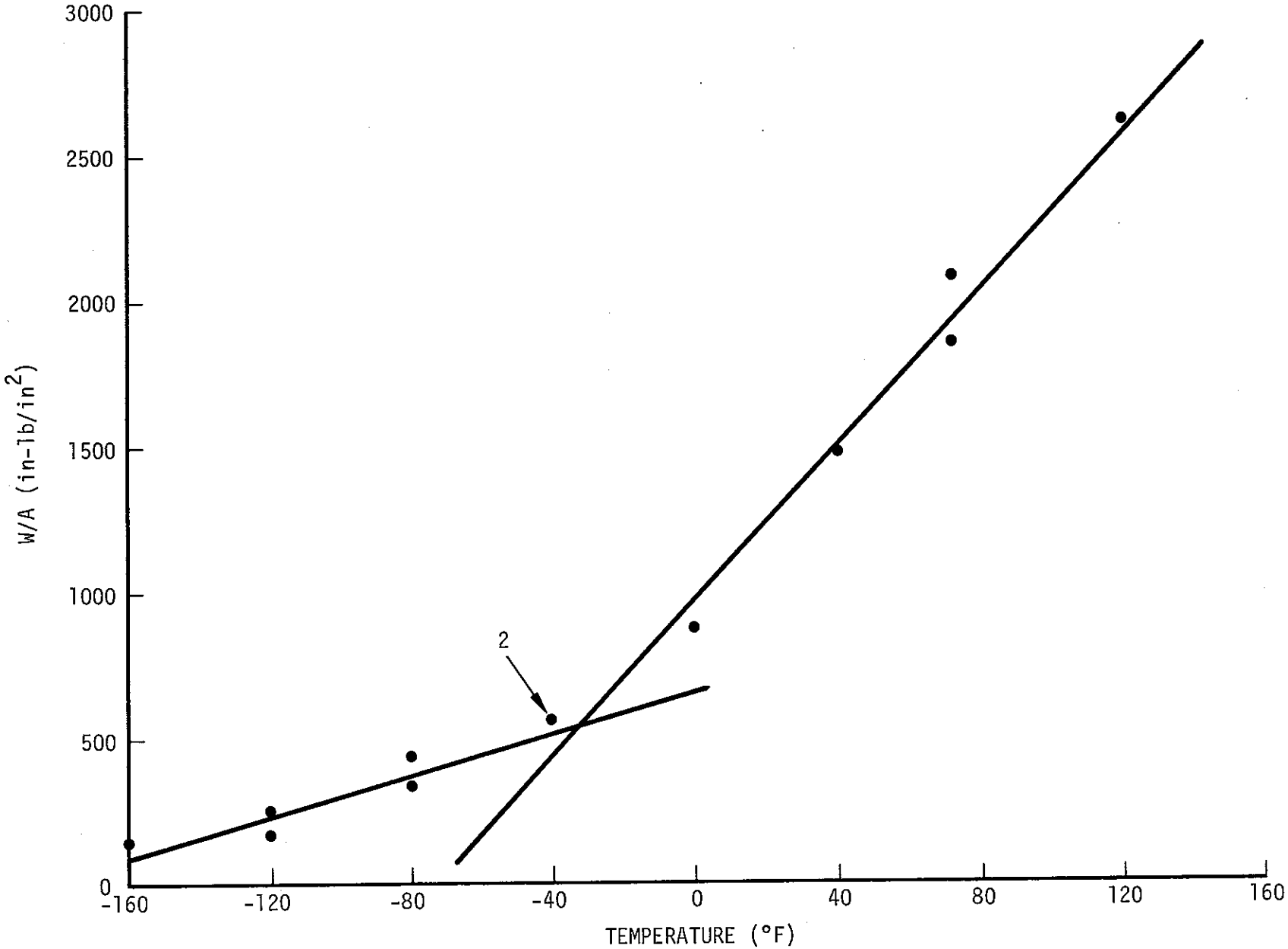

Figure 17. W/A as a Function of Temperature for Plate R

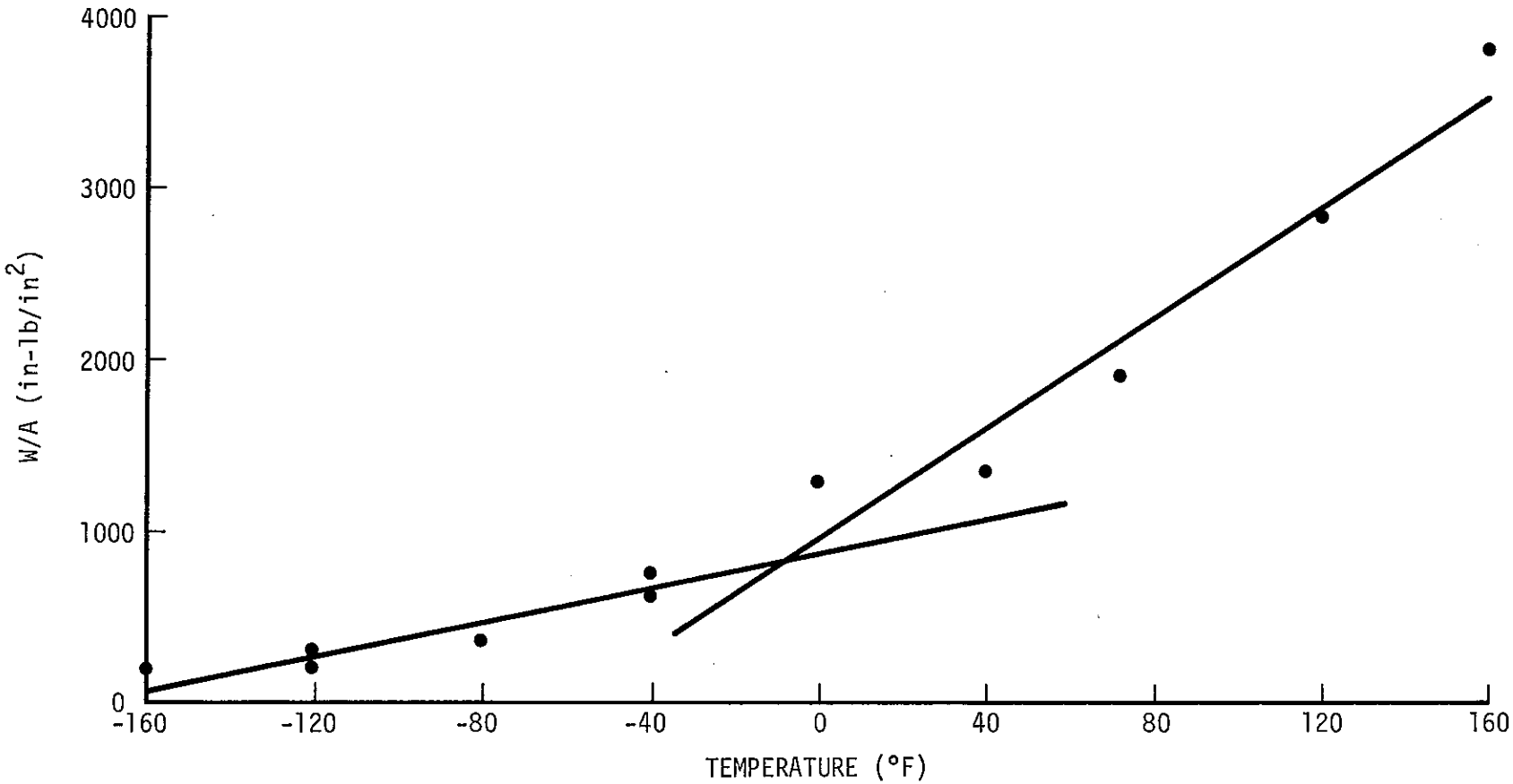

Figure 18. W/A as a Function of Temperature for Plate Z

ClibPDF - www.fastio.com

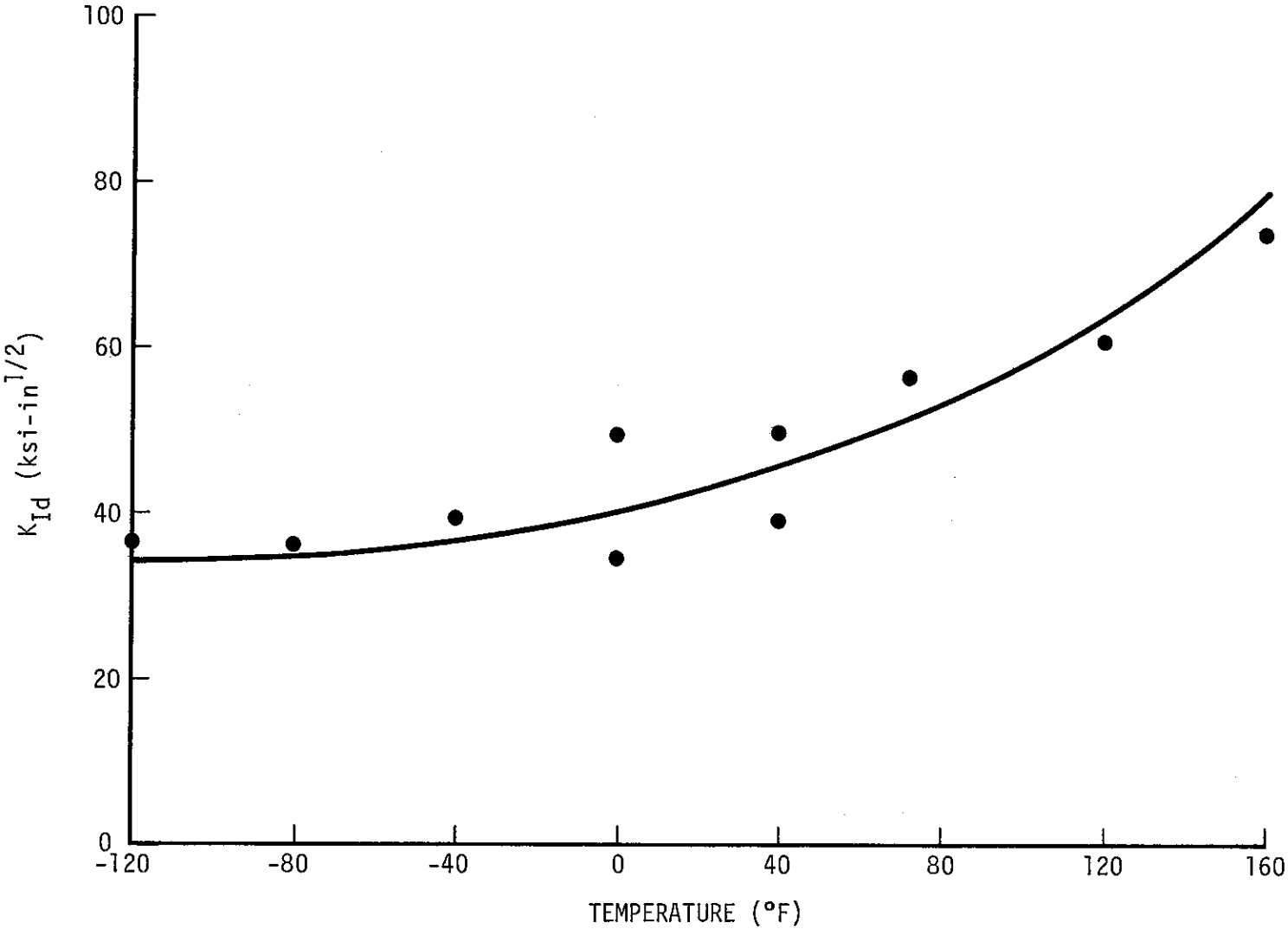

Figure 19. K_{Id} as a Function of Temperature for Plate A

ClibPDF - www.fastio.com

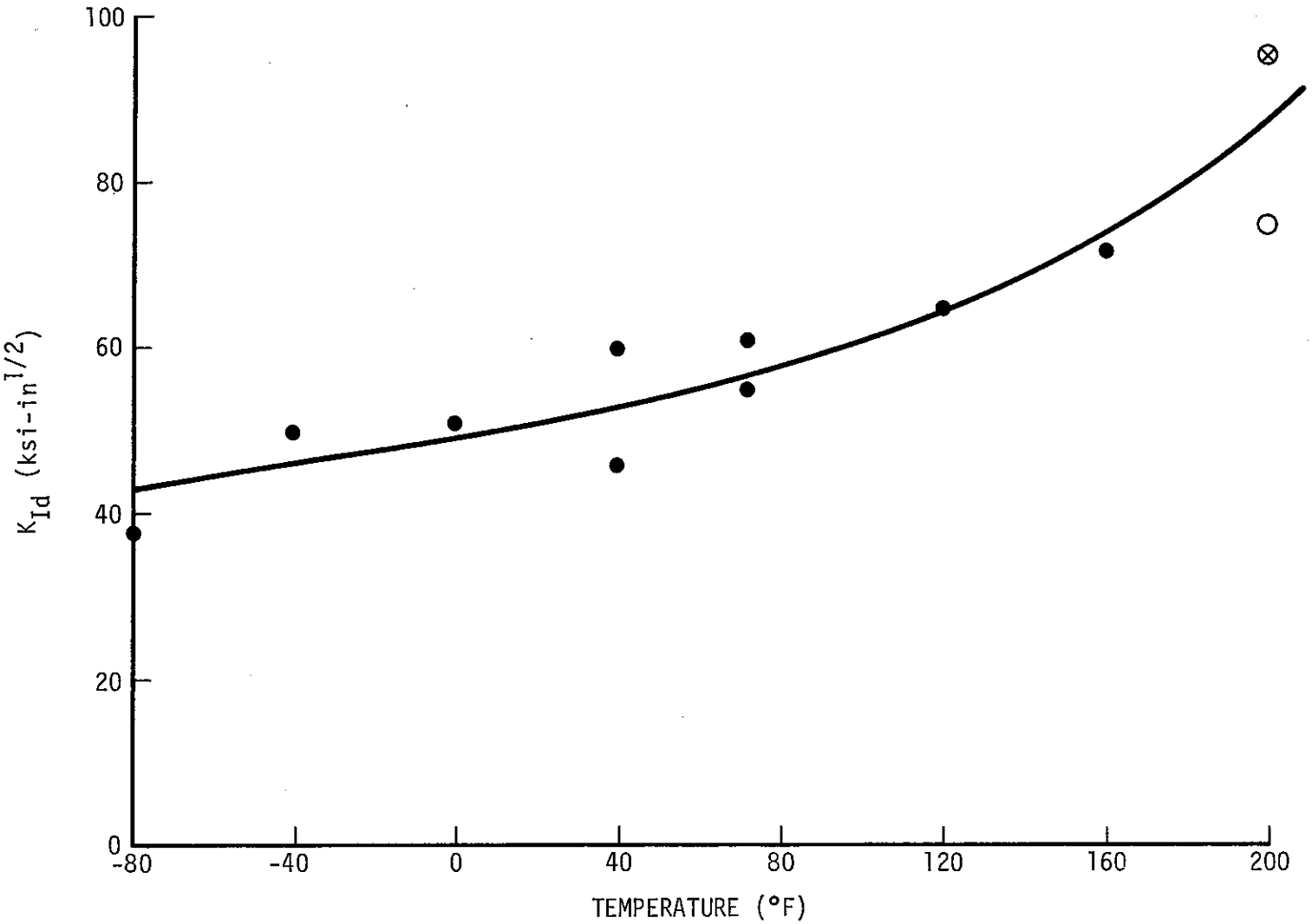

Figure 20. K_{Id} as a Function of Temperature for Plate AL

ClibPDF - www.fastio.com

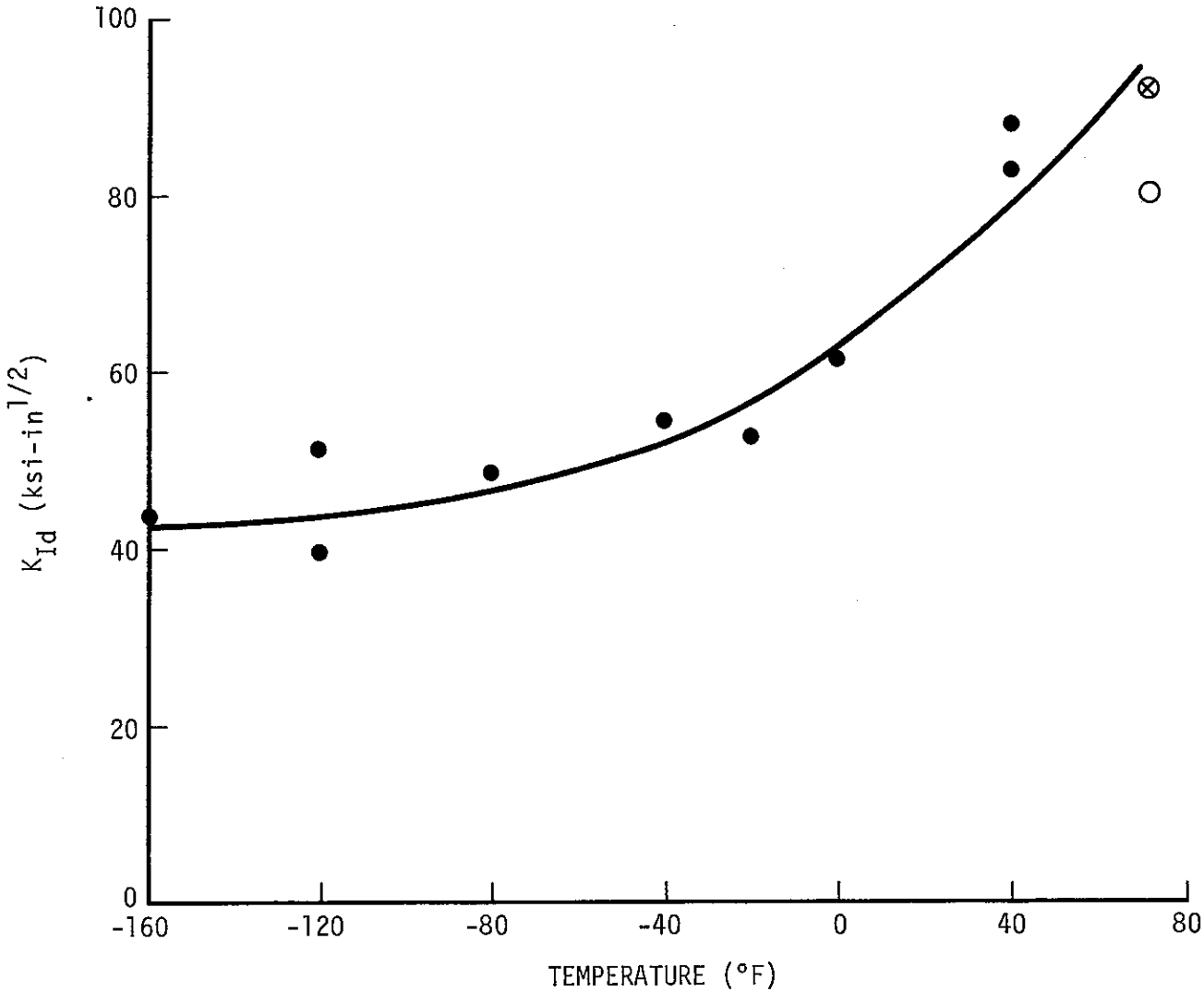

Figure 21. K_{Id} as a Function of Temperature for Plate L

ClibPDF - www.fastio.com

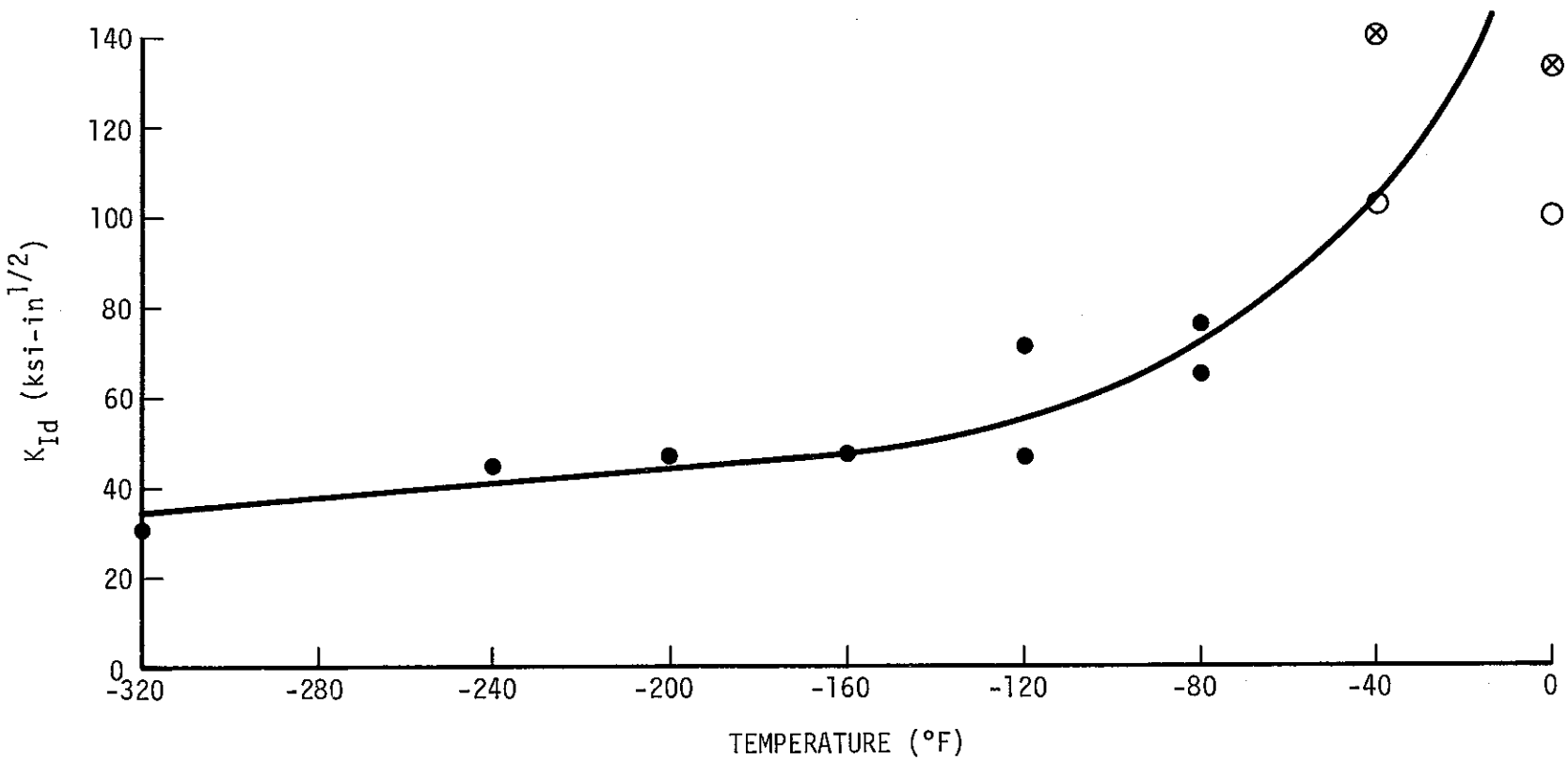

Figure 22. K_{Id} as a Function of Temperature for Plate M

ClibPDF - www.fastio.com

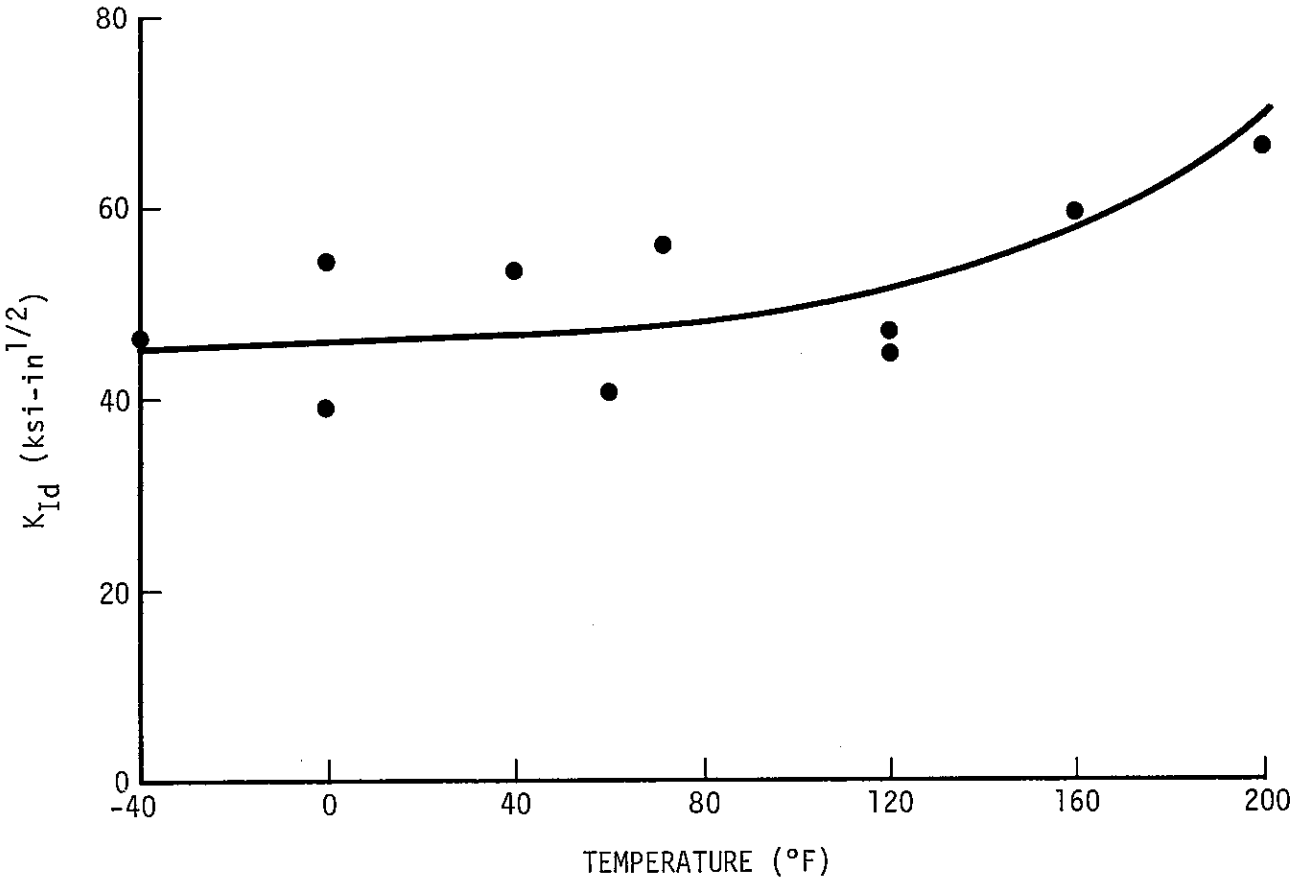

Figure 23. K_{Id} as a Function of Temperature for Plate Q

ClibPDF - www.fastio.com

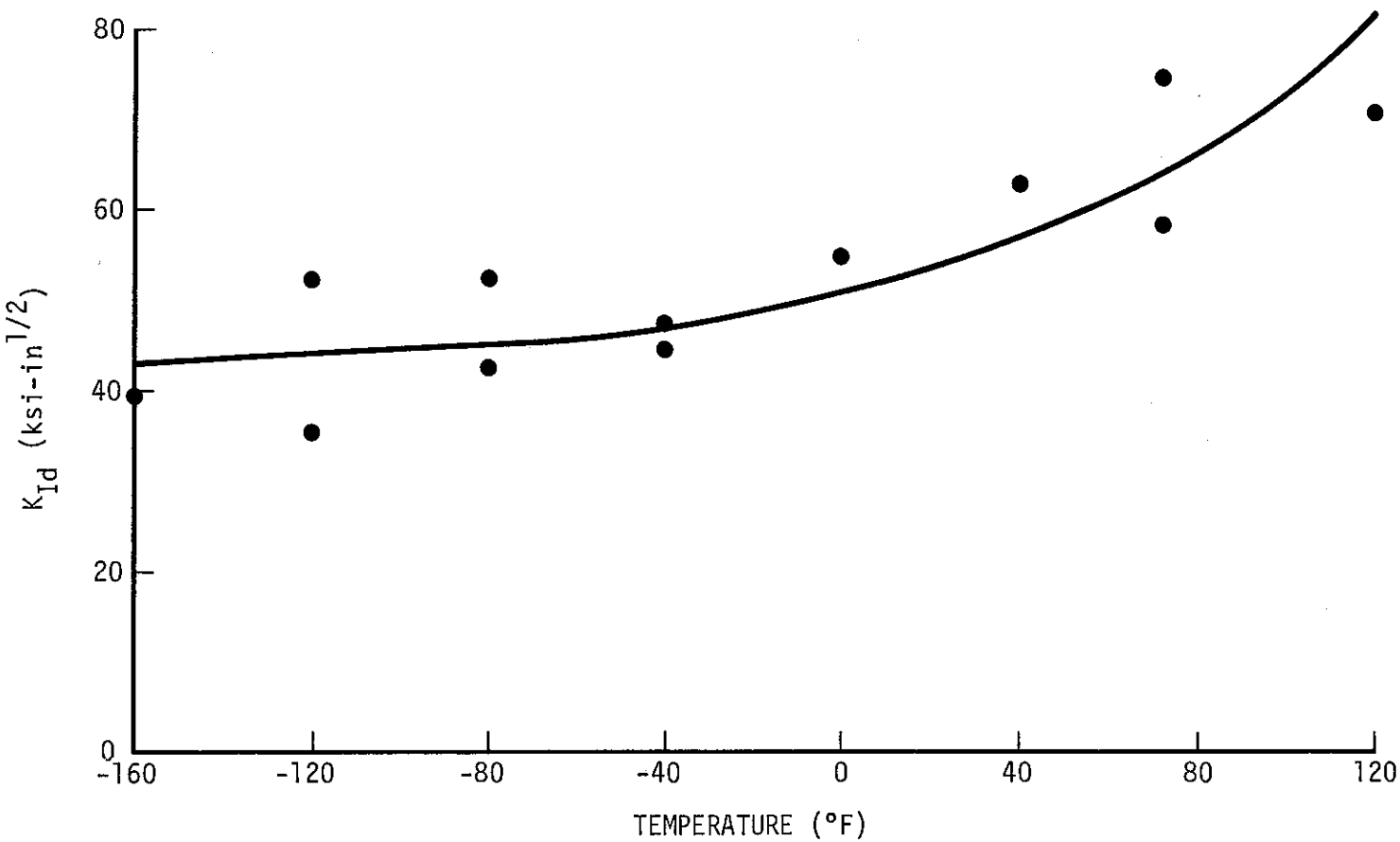

Figure 24. K_{Id} as a Function of Temperature for Plate R

ClibPDF - www.fastio.com

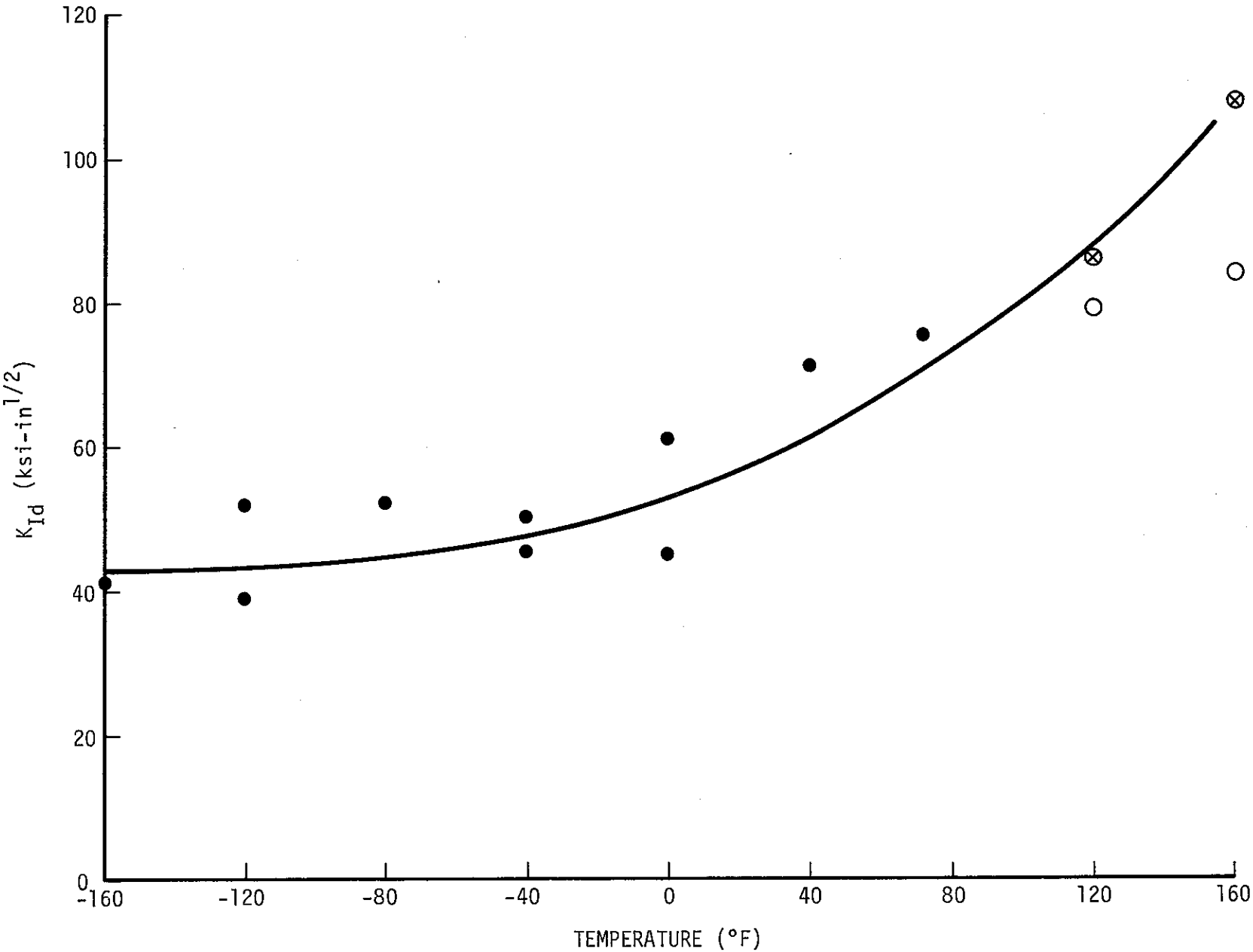

Figure 25. K_{Id} as a Function of Temperature for Plate Z

ClibPDF - www.fastio.com

ClibPDF - www.fastio.com

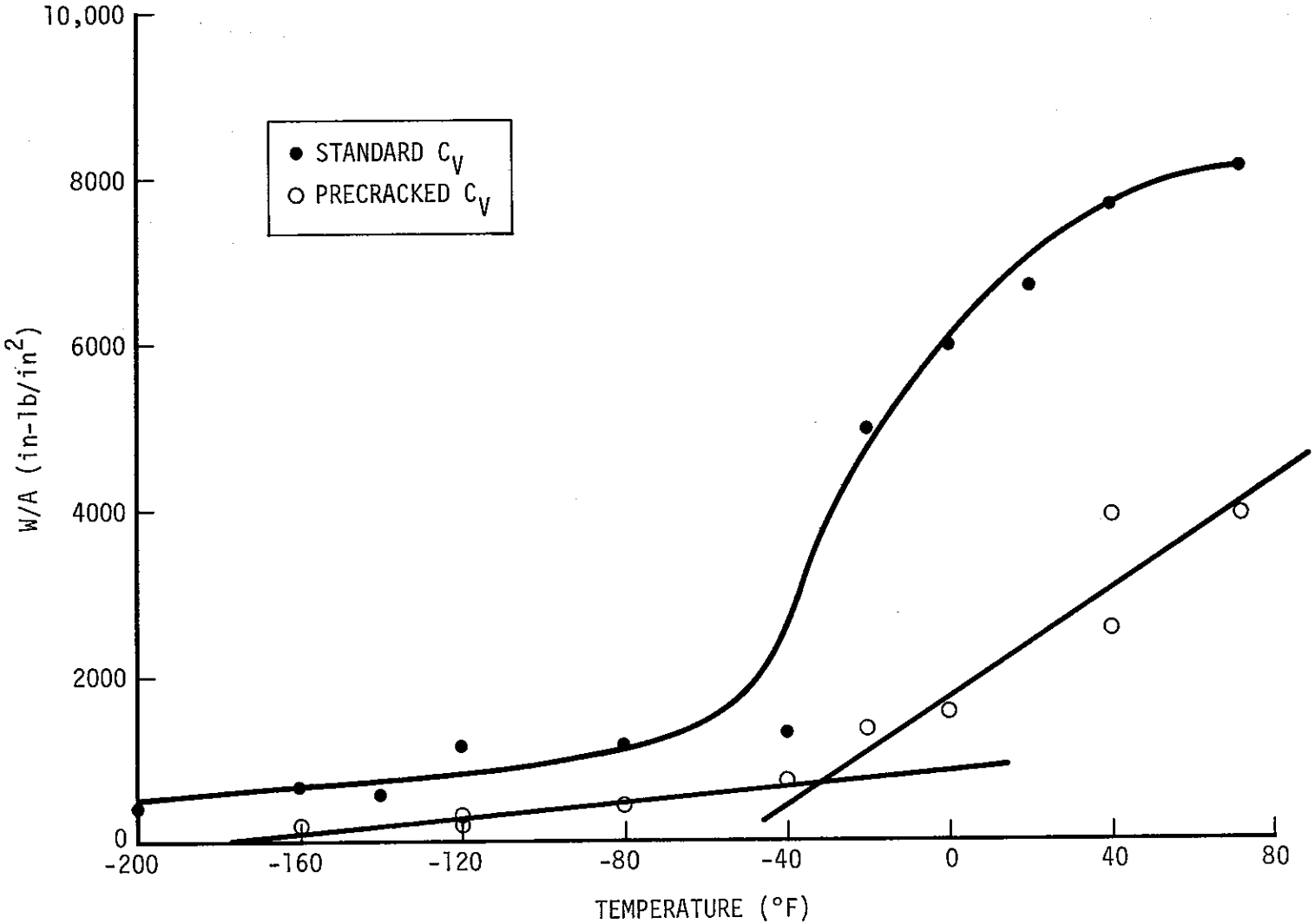

Figure 26. Charpy V-Notch Energy as W/A for Plate L

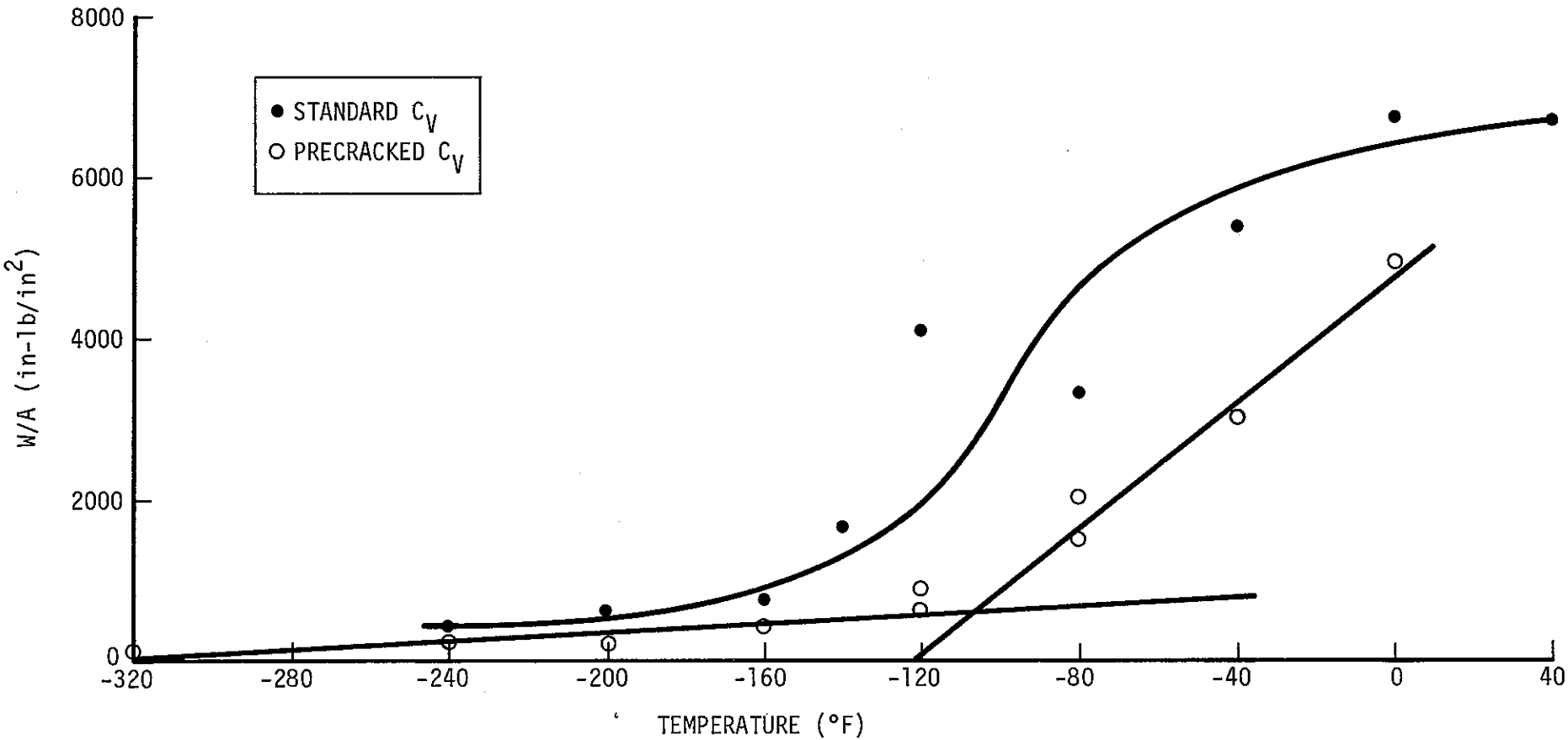

Figure 27. Charpy V-Notch Energy as W/A for Plate M

ClibPDF - www.fastio.com

ClibPDF - www.fastio.com

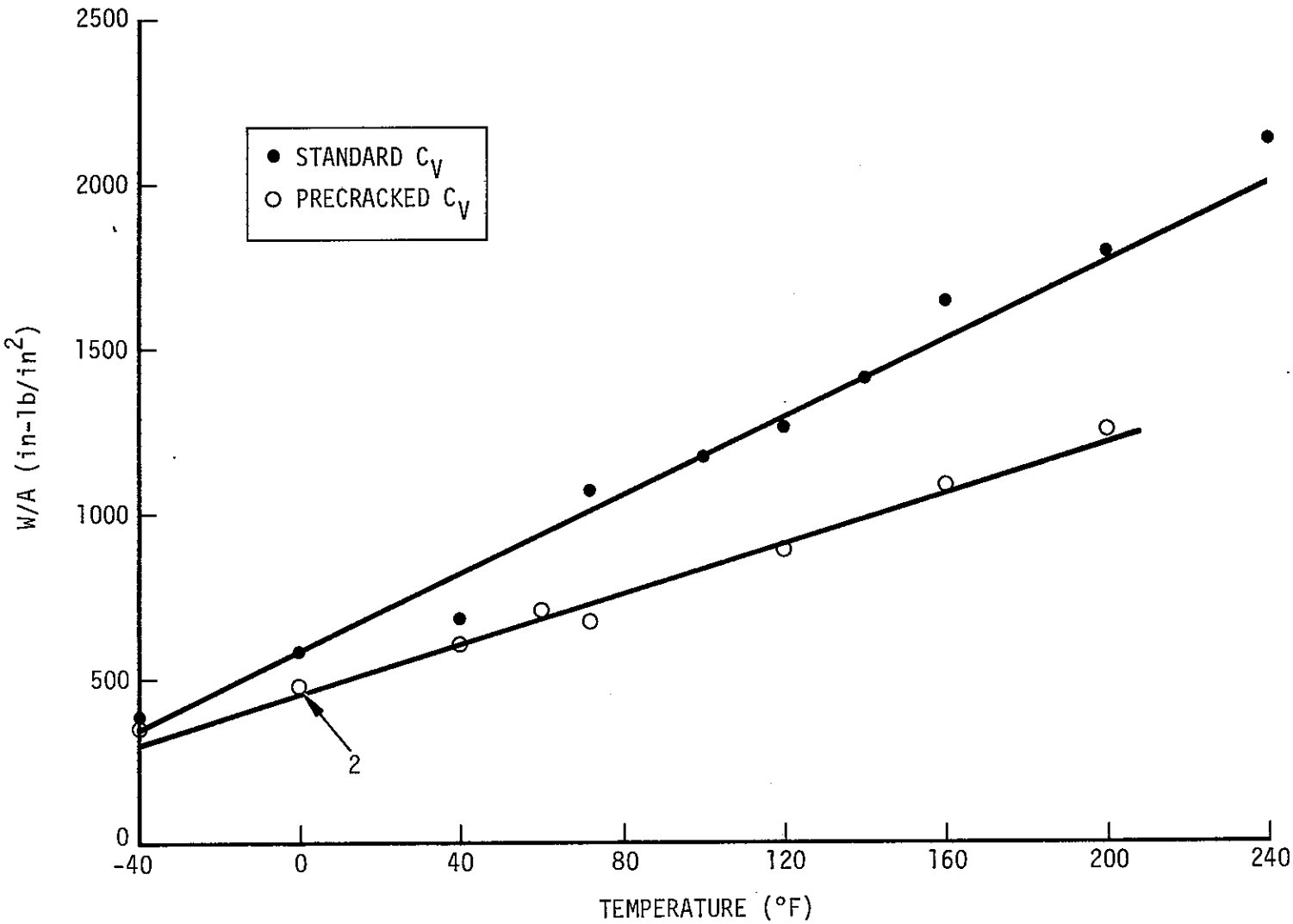

Figure 28. Charpy V-Notch Energy as W/A for Plate Q

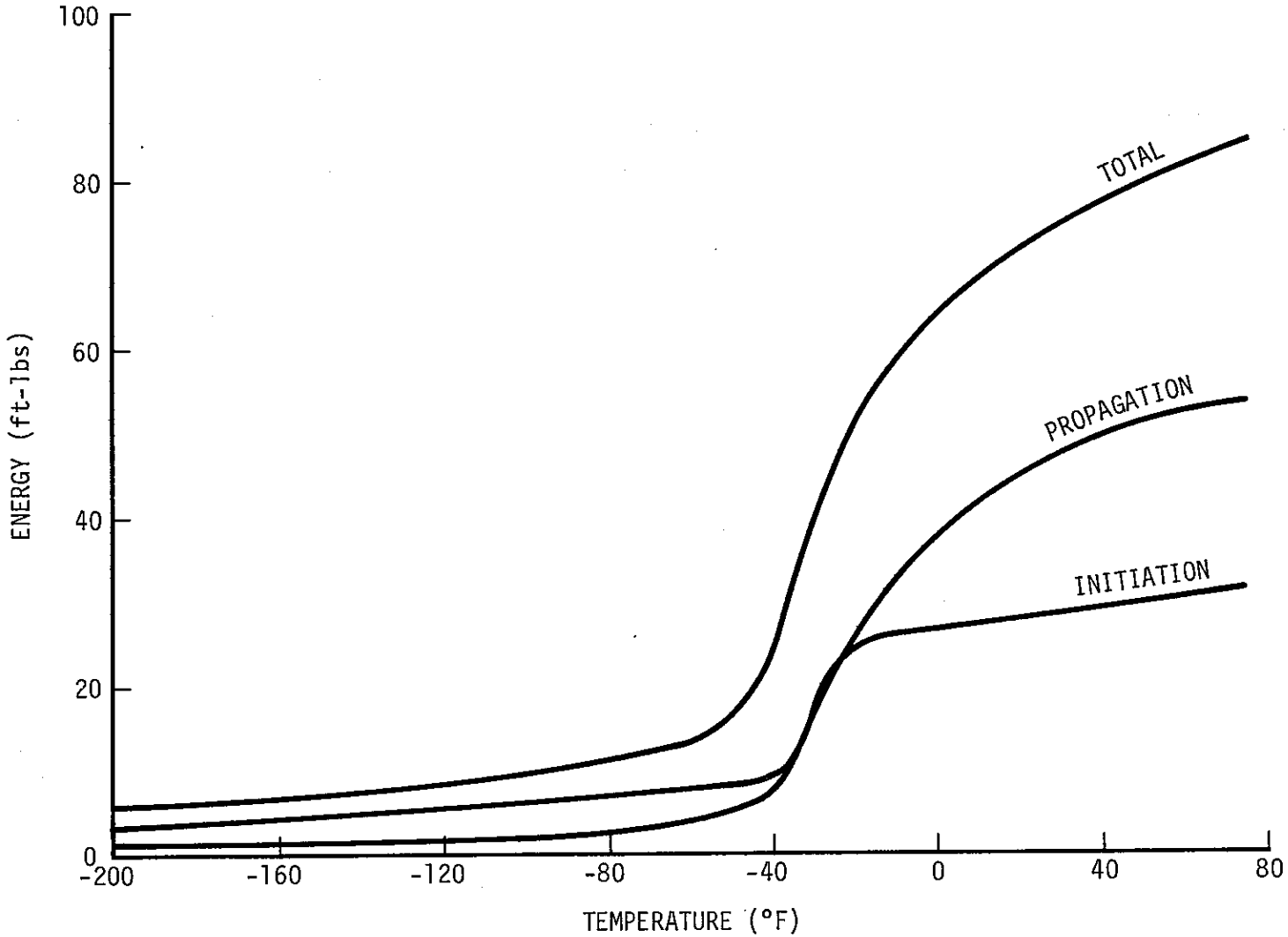

Figure 29. Components of Charpy V-Notch Energy for Plate L

ClibPDF - www.fastio.com

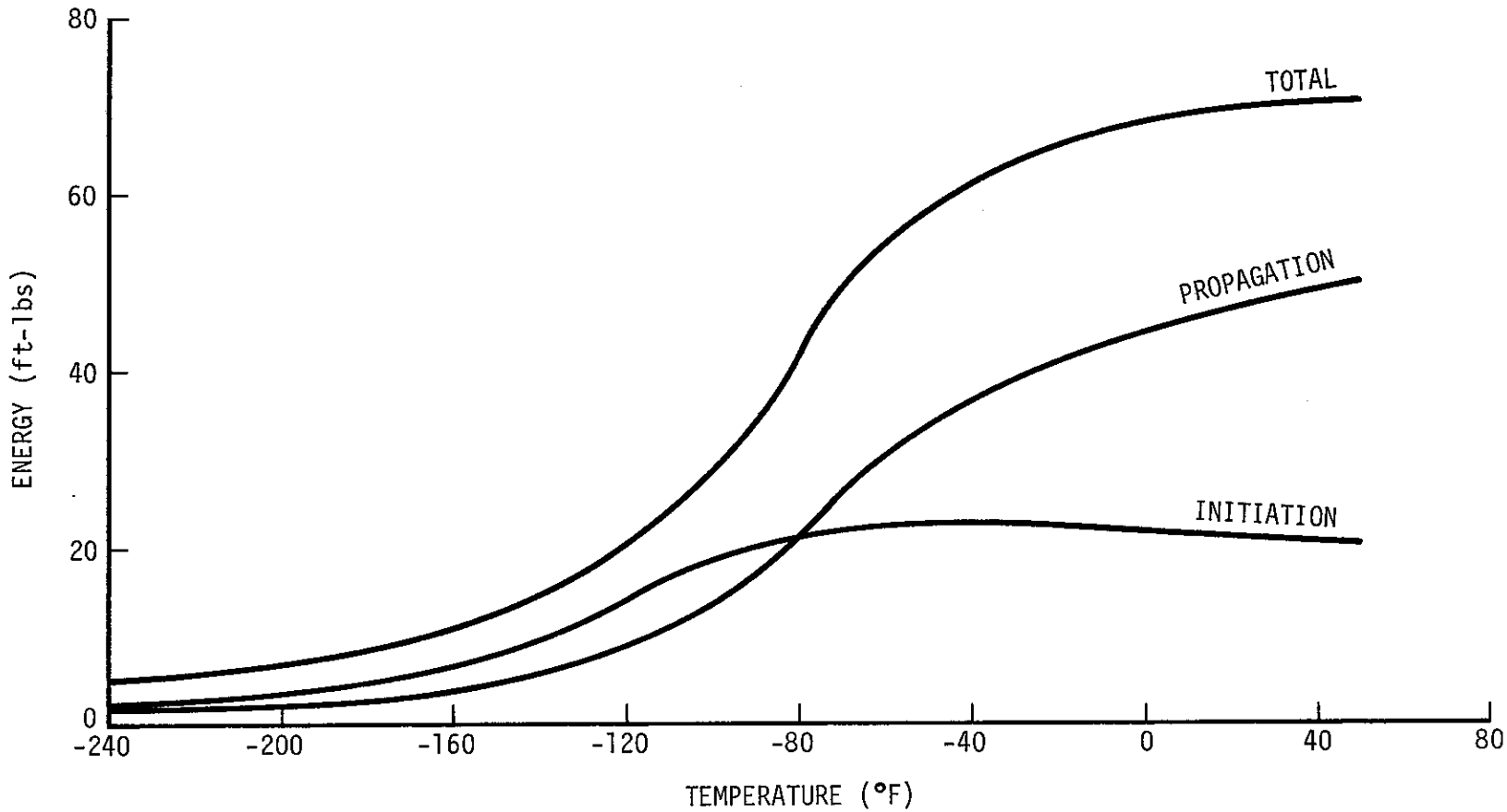

Figure 30. Components of Charpy V-Notch Energy for Plate M

ClibPDF - www.fastio.com

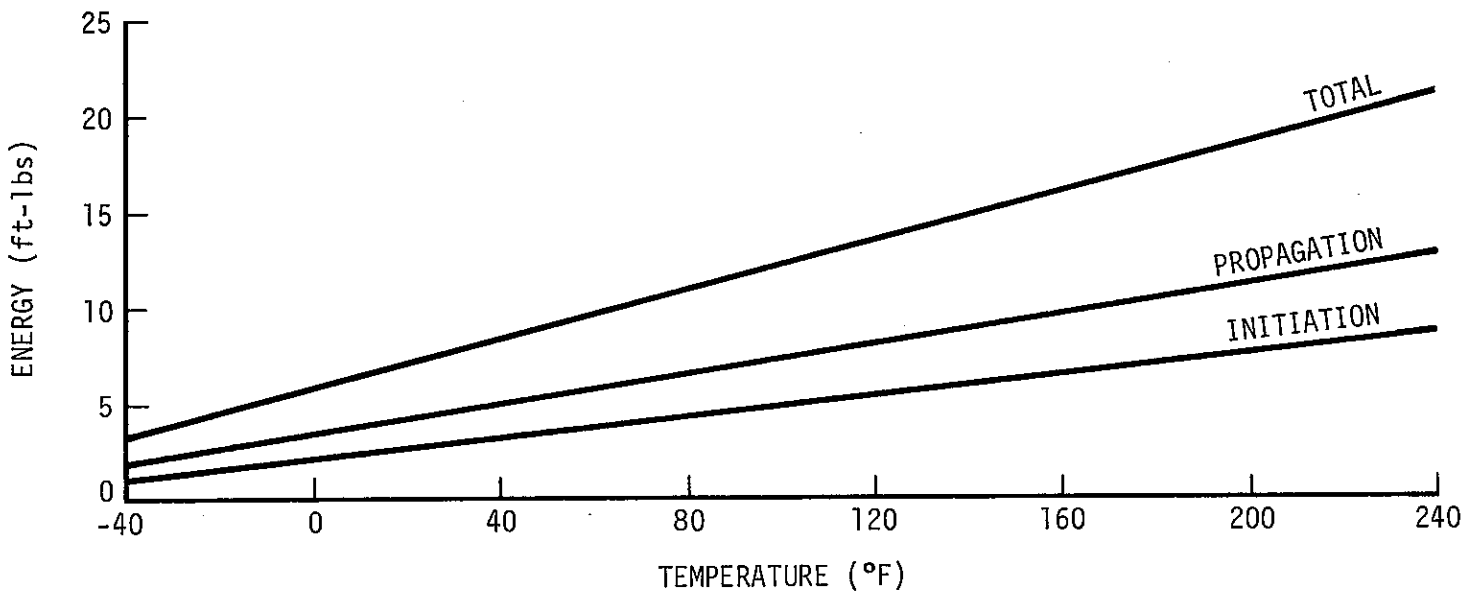

Figure 31. Components of Charpy V-Notch Energy for Plate Q

ClibPDF - www.fastio.com

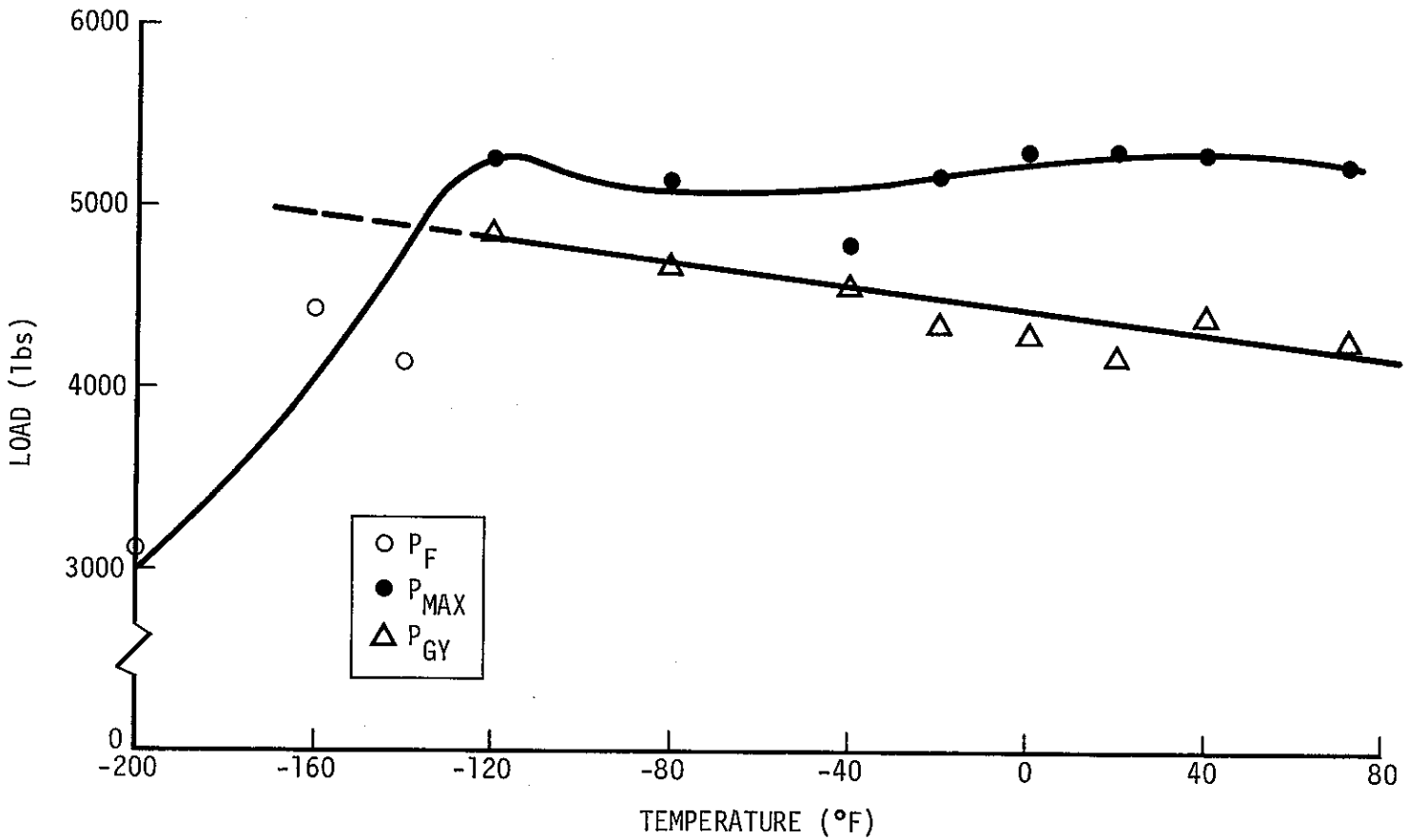

Figure 32. Charpy V-Notch Load-Temperature Diagram for Plate L

ClibPDF - www.fastio.com

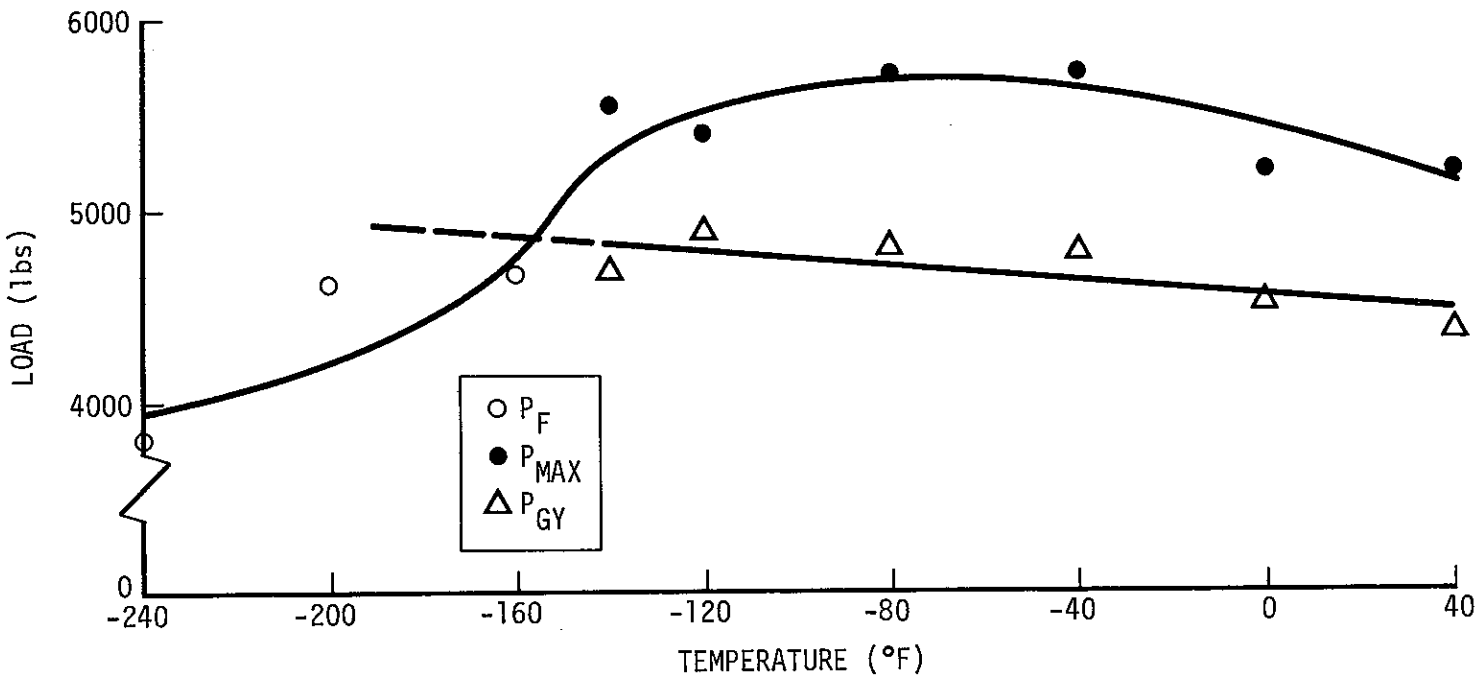

Figure 33. Charpy V-Notch Load-Temperature Diagram for Plate M

ClibPDF - www.fastio.com

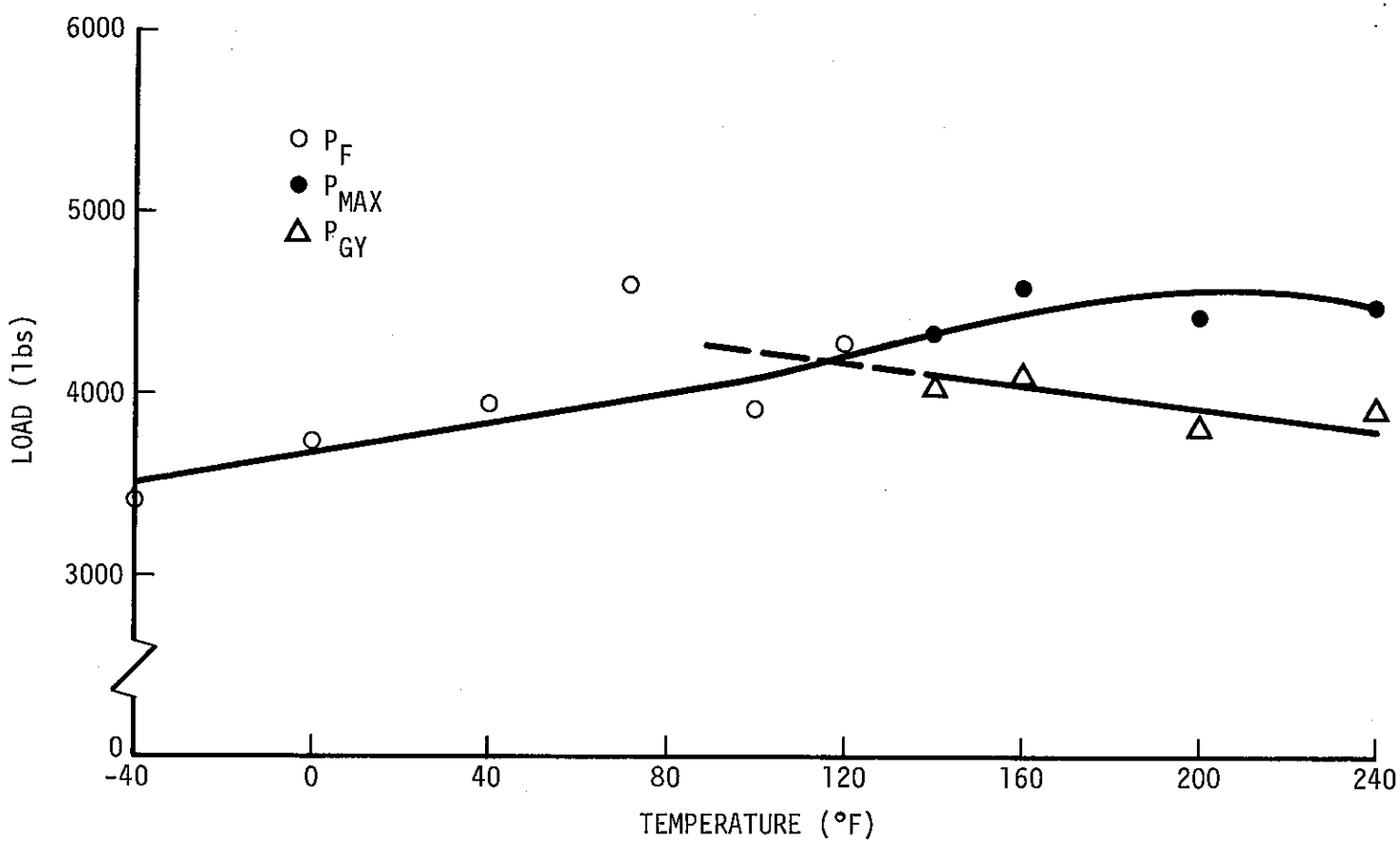

Figure 34. Charpy V-Notch Load-Temperature Diagram for Plate Q

ClibPDF - www.fastio.com

ClibPDF - www.fastio.com

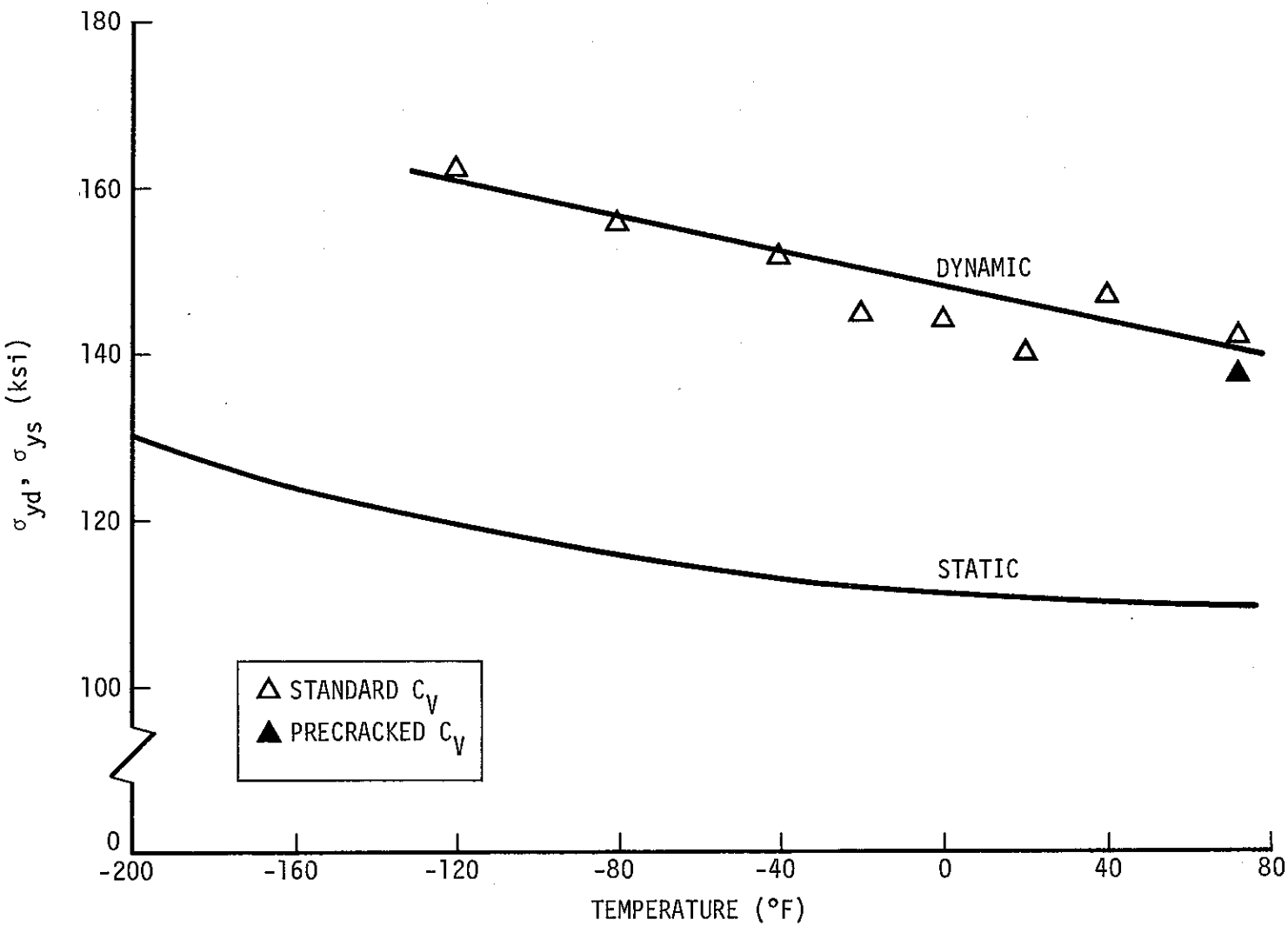

Figure 35. Static and Dynamic Yield Strengths for Plate L

ClibPDF - www.fastio.com

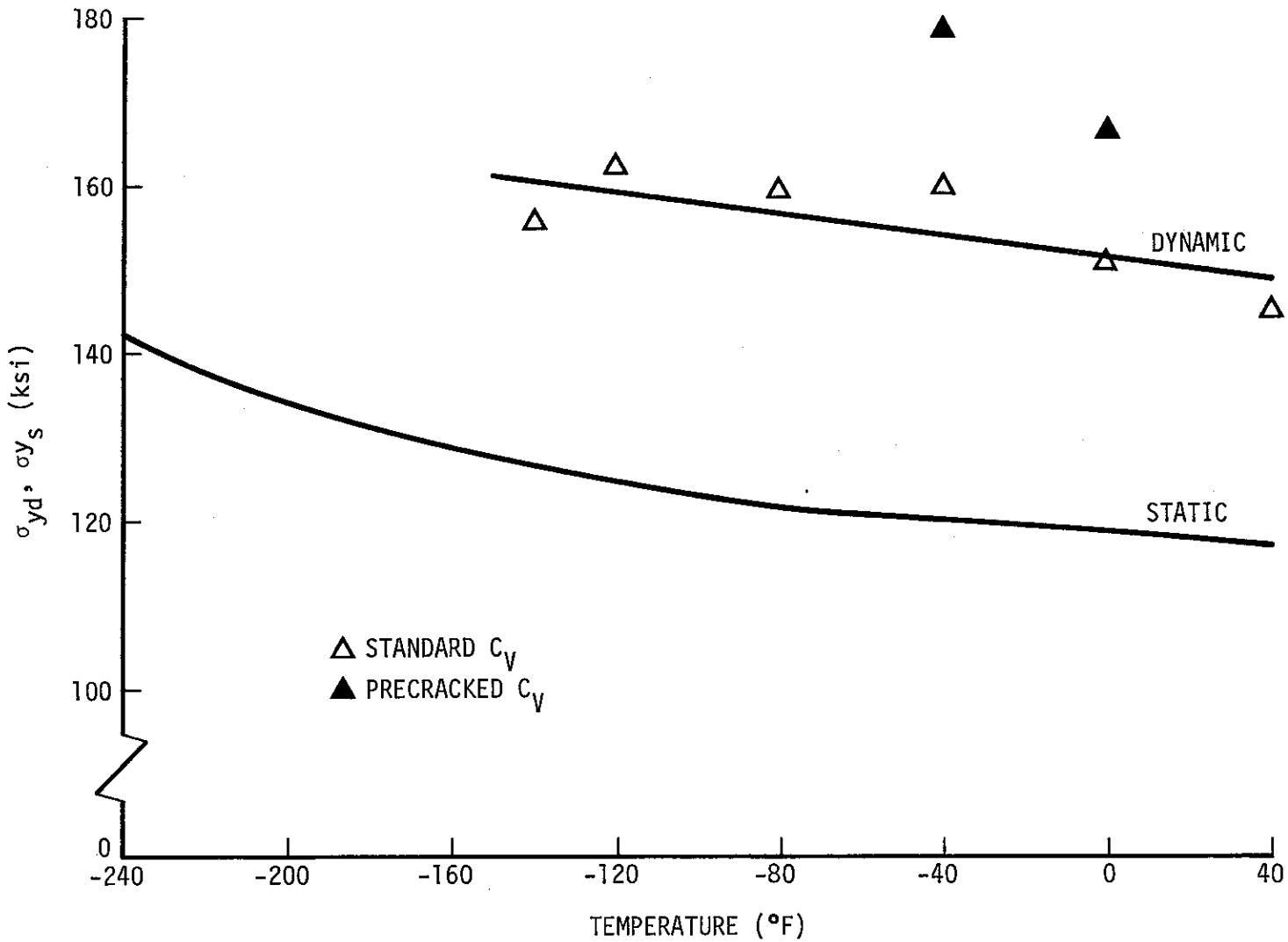

Figure 36. Static and Dynamic Yield Strengths for Plate M

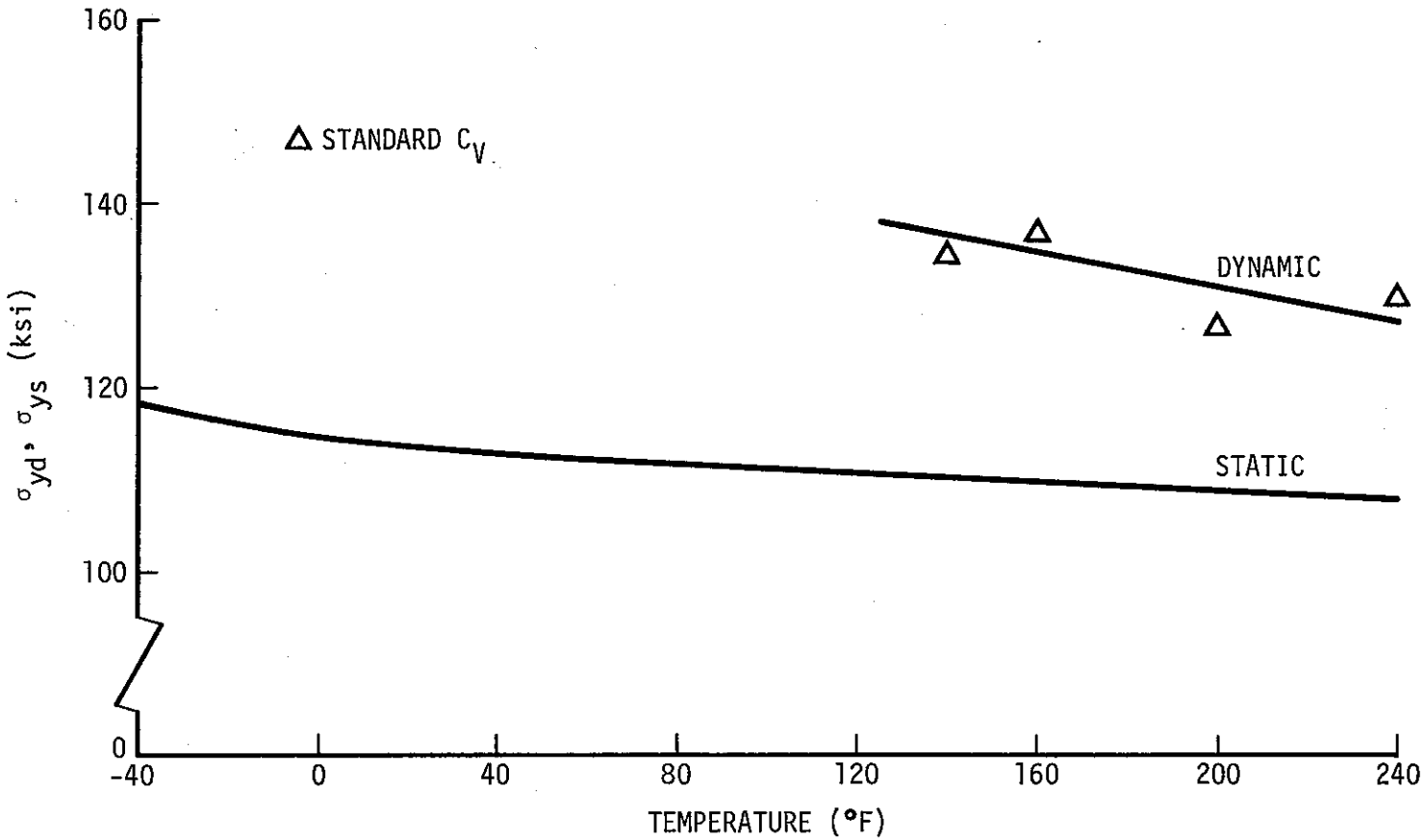

Figure 37. Static and Dynamic Yield Strengths for Plate Q

ClibPDF - www.fastio.com

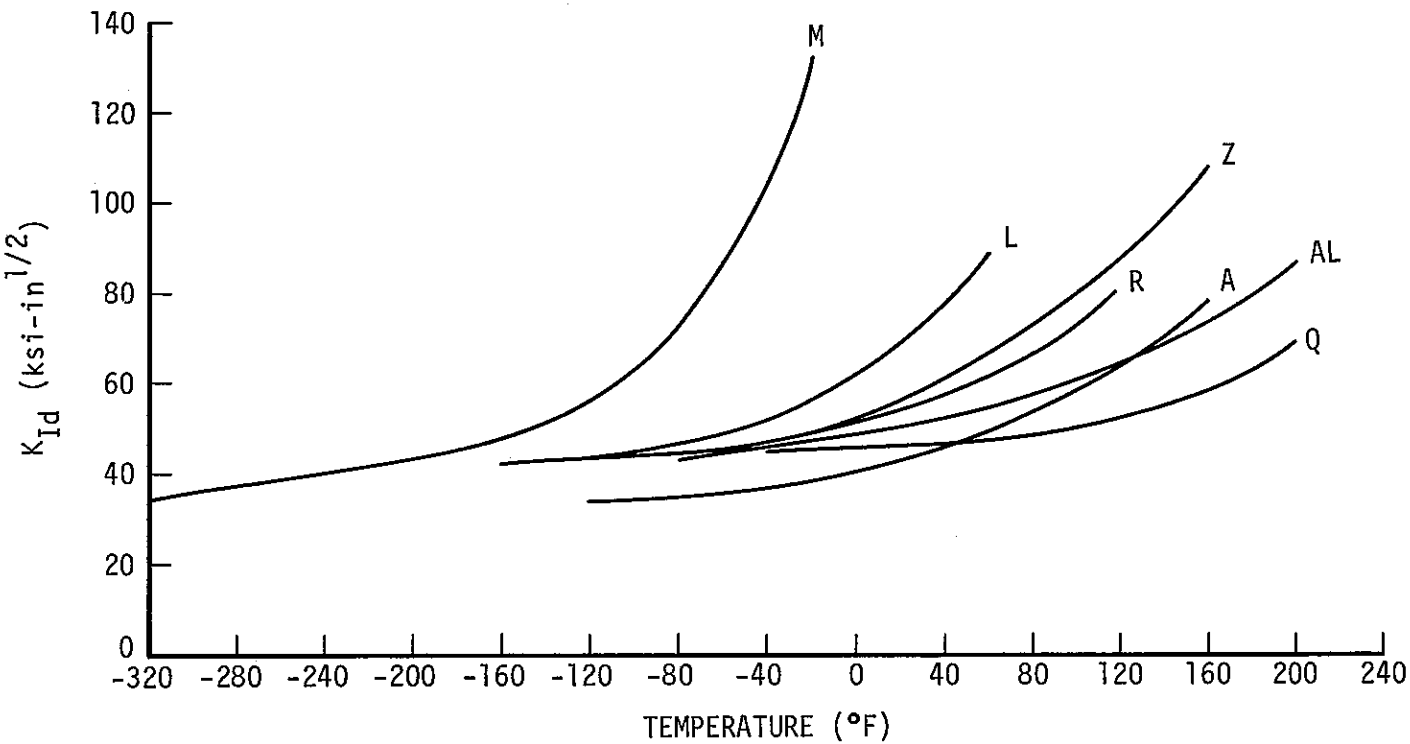

Figure 38. Dynamic Fracture Toughness Comparison for all Seven Heats of Steel

ClibPDF - www.fastio.com

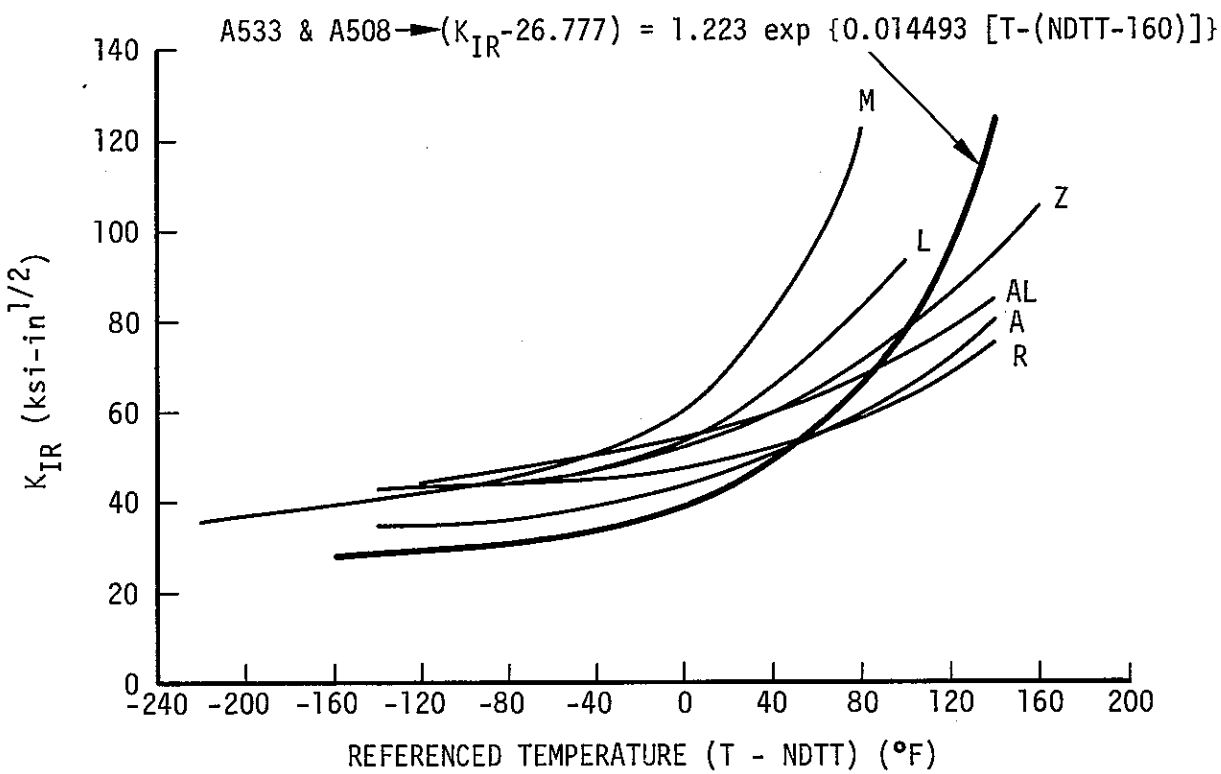

Figure 39. Referenced Toughness

ClibPDF - www.fastio.com

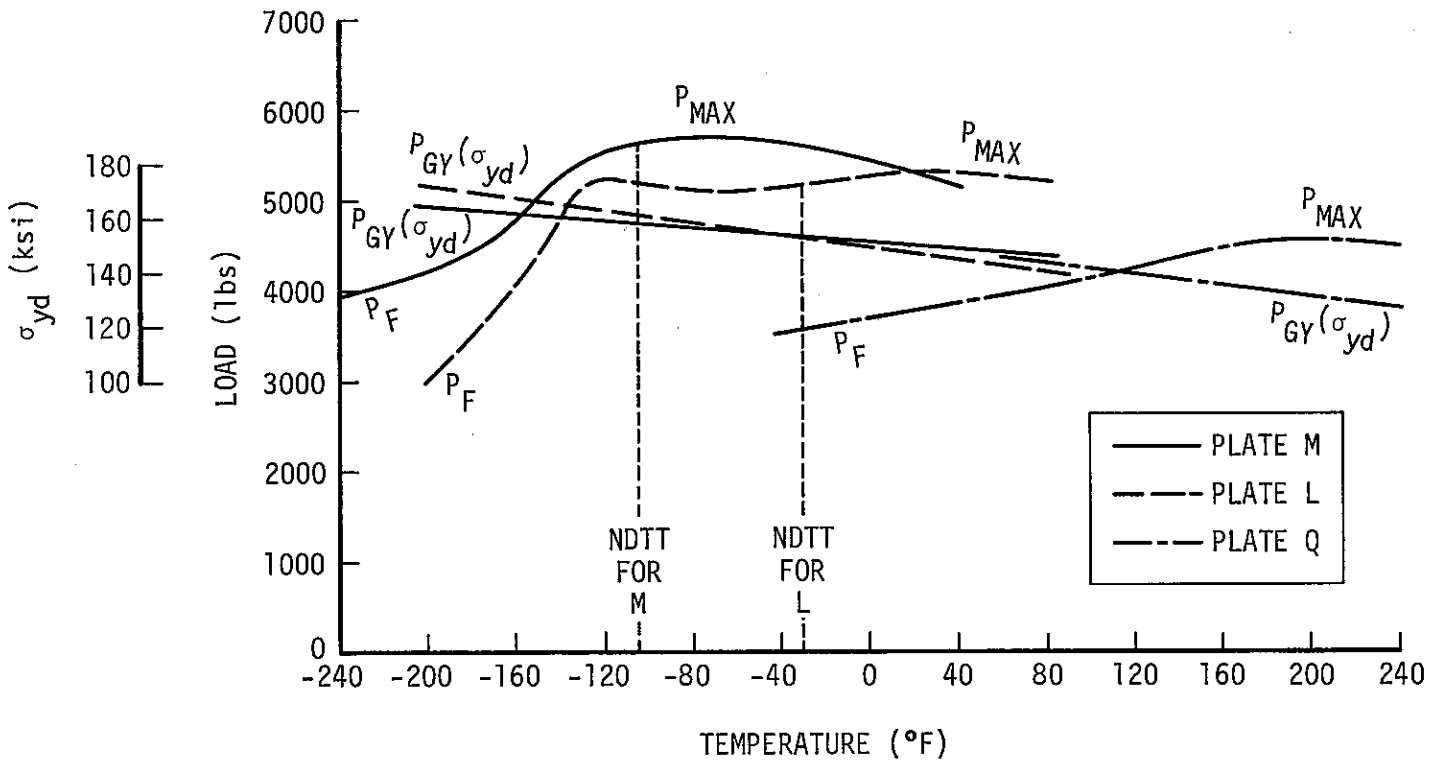

Figure 40. Charpy V-Notch Load Diagrams for Plates L, M, and Q

ClibPDF - www.fastio.com

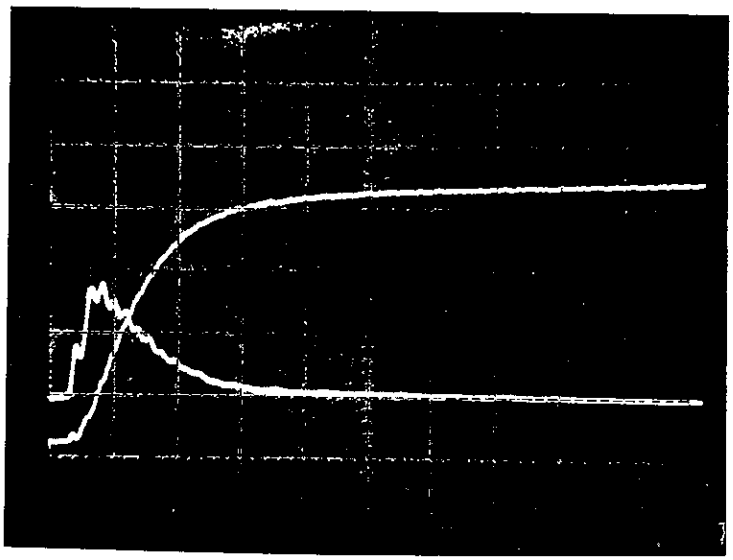

FIGURE 41. Oscillograph from a Plate Q Test Performed at +120°F

ClibPDF - www.fastio.com

ClibPDF - www.fastio.com